Muscle Stimulation via Whole Body Vibration for Postural Control Applications

ISOTTA RIGONI

Doctor of Philosophy

ASTON UNIVERSITY

February 2021

Thesis summary

Aston University

Muscle Stimulation via Whole Body Vibration for Postural Control Applications

Isotta Rigoni

Doctor of Philosophy

2021

Although the ability to balance might feel effortless to the most, it should not be given for granted as even the normal process of ageing can compromise it, jeopardising people physical independence. It is therefore important to implement safe training routines that ultimately improve postural control strategies.

We evaluated the suitability of whole body vibration (WBV) training –which induces muscle contraction via the stimulation of muscle spindles - for postural control applications. First, we tested the efficacy of different combinations of stimulation frequency and subjects' posture in eliciting a response from those muscles that play a key role for the implementation of postural responses. Each combination was evaluated by jointly measuring the resulting muscular activation and soft-tissue displacement. Then, we investigated how the selected WBV stimulation affected the balance of healthy subjects. We evaluated the latter by analysing centre of pressure trajectories, muscle and cortex activation and their respective interplay.

We found that high frequency vibrations, delivered to participants standing on their forefeet, evoked the greatest contraction of the plantarflexors. Undisturbed balance recorded after such stimulation was characterised by an increased sensitivity of muscle spindles. In line with the latter, the communication between the periphery and the central nervous system (CNS) increased after the stimulation and different muscle recruitment patterns were employed to maintain balance. On the posturography side, stability was found to be compromised in the acute term but seemed to have recovered over a longer term.

Together, these findings suggest that, if appropriately delivered, WBV has the potential to stimulate the spindles of the plantarflexors. By doing so, vibration training seems to be able to augment the communication between the proprioceptive organs and the CNS, on which the system relies to detect and react to perturbations, leading to sensorimotor recalibration.

Keywords: muscle spindle stimulation · undisturbed balance · electromyography (EMG) · coherence analyses (CMC/IMC) · posturography

Acknowledgments

In the first place, I would like to thank my supervisors. Antonio, thanks for giving me the opportunity of embarking on what has been the most challenging and revealing adventure of all. Tecla, thanks for never letting me down and for teaching me how to always be critical of my own work.

I would like to thank my reviewers. I am grateful for the time you are dedicating to read my thesis and I am enthusiastic of discussing it with you.

I would of course like to thank Mahmoud, for supporting and believing in me even when no written obligations were in place. Besides the technical advices, you showed me the researchers I one day hope to be.

Thanks to all my friends. It would be easier to divide you according to *where* or *when* we have met, but the reality is that -independently of how long our paths have crossed- each of you has a piece of my heart and always have. I am just so blessed to have shared with you laughs and tears which have shaped the persons we have now become. Thanks for sharing your life with me.

Thanks to my family.

Mum, thanks for always believing in me. Your solidity helped me overcoming the lowest times and to know you are always there, well, it is my anchor.

Dad, thanks for being the amazing person you are. The smile with which you approach everything in life is what has offered me brighter perspectives in dark times. Thanks for always showing me the side you are on, the bright one.

Ani, thanks for always reminding me where I come from. Besides the things for which we differ, those that we have in common are those that constitute the essence of my own person. Thanks for being one of my guides.

And then, thanks to Giulio.

Thanks for being so much more than just a boyfriend. Thanks for being my confident and counsellor but, among all, thanks for being my best friend. Everything is funnier, spicier and way more exciting if it is with you. You are just the most beautiful person I know and, even now that you are sitting in front of me typing on your computer, I cannot realize of how lucky I must have been that time in Via Degli Scrovegni. This thesis would have not been possible without your support (and patience).

And this is why this thesis is dedicated to you.

Table of Contents

List of Abbreviations

ANOVA	Analysis of Variance
AP	Anterior-Posterior
BB	Baseline Balance
BBA	Beta-band Activity
BC	Betweenness Centrality
BF	Biceps Femoris
BMD	Bone Mineral Density
CC	Clustering Coefficient
CI	Complexity Index
CMC	Corticomuscular Coherence
CNS	Central Nervous System
COM	Centre of Mass
COP	Centre of Pressure
DV	Dependent Variable
EEG	Electroencephalography
(s)EMG	(Surface) Electromyography
EPSP	Excitatory Post-Synaptic Potential
FDR	False Discovery Rate
FF	Forefeet
FIR	Finite Impulse Response
GL	Gastrocnemius Lateralis
GRF	Ground Reaction Force
HS	Hack Squat
IAP	Intracellular Action Potential
IMC	Intermuscular Coherence
IPSP	Inhibitory Post-Synaptic Potential

IV	Independent Variable
LLAT	Long Latency
MCP	Multiple Comparison Problem
MD	Mean Distance
ML	Medial-Lateral
MLAT	Medium Latency
MSE	Multiscale Sample Entropy
MU	Motor Unit
MUAP	Motor Unit Action Potential
MUAPT	Motor Unit Action Potential Train
MV	Mean Velocity
NNMF	Non-Negative Matrix Factorization
PC	Participation Coefficient
PSB	Post-Stimulation Balance
PSD	Power Spectral Density
RF	Rectus Femoris
RMS	Root Mean Square
SD	Standard Deviation
SE	Sample Entropy
SLAT	Short Latency
SNR	Signal-To-Noise Ratio
SOL	Soleus
STR	Strength
TA	Tibialis Anterior
TVR	Tonic Vibration Reflex
WBV	whole body vibration

List of Figures

List of Tables

1. General Introduction

The ability to control and move our body is the backbone of a happy existence. Once acquired and if unimpaired, it gives us the opportunity to focus on tasks that are cognitively more demanding and interesting without the need to actively think about how to perform the action required. Even for the accomplishment of the simplest movement, a certain degree of motor control is still required to carry it out neatly and precisely. Luckily, our central nervous system (CNS) is able to autonomously work out the most efficient combination of muscles needed to perform a specific action and to synchronise their recruitment in the most efficient way, which results in what is known as “muscle coordination”.

Although it might feel effortless to the most, even standing requires a certain level of muscle activation and, in most cases, it is carried out without people having to actively decide which muscles to contract. However, in the case of neuromuscular impairments or sensory loss, even balancing on two legs on a stable surface can become extremely challenging. Without going into the details of specific pathologies, it is well established that even normal ageing leads to a general degradation of sensory organs, which include proprioceptive receptors located in the muscles, i.e. the muscle spindles (Miwa et al., 1995; Swash and Fox, 1972). Since these receptors contribute to the perception of our body in space (Gandevia, 1996; G M Goodwin et al., 1972; Proske, 2005), they play a fundamental role in the actuation of postural responses and their degradation is thought to partially explain the decline in standing balance that is usually observed with ageing (Lord et al., 1994, 1991; Swash and Fox, 1972). Therefore, finding a way to improve proprioceptive sensitivity becomes crucial for either training or rehabilitation programme aiming at improving postural control.

Since 1980s, the stimulating effect of mechanical vibrations on muscle spindles is known and has paved the way for vibrations to be included in both rehabilitation and training routines (Burke et al., 1976b, 1976a; Burke and Schiller, 1976; Hagbarth et al., 1976). Due to the enhanced muscle contraction that results from muscle spindle stimulation and for the advantages that come from muscles being able to produce a greater deal of force, practical ways to deliver vibrations have been researched. Among these, whole body vibration (WBV)

consists in the delivery of vibrations via mean of an oscillating platform with which the patient keeps contact, usually by standing on it. When vibrations are transferred from the sole of the feet to different muscles in the body, the change in muscle length is detected by muscle spindles and a proprioceptive response is triggered. The latter is then translated into an action potential travelling down a motor neuron, leading to the contraction of the muscle fibres connected to it. As part of the neuromuscular system, muscle spindles and the CNS are in constant communication with each other. The first provide feedbacks on the status of the periphery and the latter is in charge of processing not only proprioceptive, but also vestibular and visual information to control postural balance (Martin and Park, 1997). Specifically, ascending information coming from the peripheral body allows the detection of an external perturbation or a change in the position of the limbs: once these are processed, the appropriate muscle contraction is initiated to react to the perturbation and regain balance (Forbes et al., 2018). Due to this consolidated knowledge, researchers wondered whether more sensitive muscle receptors would translate into a richer flow of proprioceptive information to the CNS and ultimately improve the ability to maintain an upright stance.

As hypothesised, the addition of WBV to training routines led to improvements of postural control in healthy subjects (Dallas et al., 2017; Ritzmann et al., 2014; Torvinen et al., 2002b) although controversial results were also reported (Torvinen et al., 2002a, 2002c). Similarly, studies performed on older adults and different patients reported positive *but weak* evidence of WBV benefits on balance in such populations (Lam et al., 2012; Osugi et al., 2014; Rogan et al., 2011; Saquetto et al., 2015; Turbanski et al., 2005), which also led to inconclusive results. (Ebersbach et al., 2008; Lam et al., 2012). These discording results might be due not only to the intrinsic differences between the sub-populations being tested, but also to the different WBV protocols being used. When delivering vibrations to the whole body via a vibrating platform, many parameters should in fact be taken into account, such as the stimulation frequency, the static (or dynamic) exercise performed by the subject, the exposure time and so on. These variables do in fact affect the desired outcome of the treatment –the muscle response- and as such should be appropriately tuned.

The main objective of this thesis was therefore to deepen the understanding of WBV stimulation in the context of postural control intervention, addressing the aforementioned issues. Specifically, the first goal was to define a mechanical stimulus that –via the selection of the appropriate vibration frequency and subjects' posture- would target those muscles that are mostly recruited during upright standing. Then, the second goal was to use the defined stimulus for WBV stimulation and to assess its effect on postural control by recording a balance task before and after the treatment. Taken altogether, the findings of this thesis could play an important role in the investigation of the use of WBVs to stimulate muscle spindles and might pave the way for researching the restoration of lost sensitivity in these sensory organs, possibly having practical application in neuromuscular rehabilitation for healthy ageing.

The following five chapters are therefore meant to describe not only the experimental studies conducted to achieve such goals, but also to give a theoretical and methodological background necessary to appreciate the analyses performed on the data and the conclusions drawn from it. The goal of the literature review proposed in Chapter 2 is to offer an overview of the possibilities and limitations linked to WBV as well as providing a description of postural control and the physiological processes involved in it. Chapter 2 is concluded with the presentation of the research questions formulated for this project and a quick description of the studies designed to address and answer such questions. Chapter 3 represents a mathematical description of the recording techniques used in the studies hereby presented. From surface electromyography to static posturography, the techniques are presented along the mathematical background of the analyses utilised to quantitatively investigate the data. Chapter 4 describes the first experimental study of the thesis, which goal was to define a WBV stimulation to target the superficial muscles of the lower leg that are mostly engaged for postural control. Chapter 5 describes the second experimental study, which objective was to assess the effect of the previously-defined WBV stimulation on undisturbed balance. Although a discussion of the findings is provided in each chapter, Chapter 6 offers an overall summary of the key results and their joint interpretation, along with a consideration of the possible future directions of this research.

2. Literature Review

2.1 Whole Body Vibration

Whole body vibration (WBV) is a non-pharmacological mean of intervention whose use has recently grown in the rehabilitation and sport field (Saquetto et al., 2015). This treatment consists in the delivery of mechanical stimuli to the body via a vibrating platform, on which a subject stands performing either static or dynamic exercises. WBV has been proven to be beneficial under several aspects (Rittweger, 2010) among which muscle stimulation is the most credited (Cardinale and Bosco, 2003). It is in fact renowned that vibrations, applied to tendons or muscle bellies, induce a higher muscle spindle activation (De Gail et al., 1966; Marsden et al., 1969) that is measurable as an increase of firing rate of proprioceptive fibres (i.e. *Ia* fibres). However, it is not yet clarified how this enlarged amount of action potentials from the sensory network is then transduced into a higher motor unit (MU) activation rate (McBride et al., 2010; Shinohara, 2005). Nevertheless, the inclusion of WBV in training programs has successfully resulted in increased explosive muscle strength and muscle power in both trained athletes (Bosco et al., 1999; Mahieu et al., 2006) and young nonathletic adults (Torvinen et al., 2002a). The addition of a specific vibration treatment to the ordinary rehabilitation protocol for children with cerebral palsy showed positive outcomes too: both gait speed and gross motor function increased significantly for children who underwent WBV, indicating a possible improvement of motor coordination due to the treatment (Saquetto et al., 2015).

Besides the effects on the neuromuscular system, WBV impact has recently been investigated also on bone mineral density (BMD). Even though controversial results can be found in the literature, two meta-analysis revealed similar outcomes, namely that long exposure to WBV produces small but significant improvements in hip and spine BMD in post-menopausal women (Fratini et al., 2016; Slatkovska et al., 2010). Although these findings suggest the use of WBV as a possible non-pharmacologic supplement to prevention and therapy protocols of osteoporosis (Mahieu et al., 2006; Ruan et al., 2008; S. M. P. Verschueren et al., 2004), controversial results obtained in other studies (Tankisheva et al., 2015; Wysocki et al., 2011) underlie the need of further research before WBV is used in clinical practice.

Furthermore, the effects of WBV have been also investigated for other aspects:

- *Impact on the neuromuscular system*. WBV induces progresses in balance due to neural and neuromuscular adaptation through muscle spindles stimulation. Those neural receptors indeed send information to the central nervous system (CNS) in charge of controlling postural balance (Martin and Park, 1997). For example, the inclusion of WBV in training protocols led to improvements of postural control in both healthy and pathological subjects (Dallas et al., 2017; Ritzmann et al., 2014; Saquetto et al., 2015), suggesting the addition of a WBV treatment to the conventional fall prevention protocols for the elderly population (Osugi et al., 2014). However, Torvinen et al. (2002) reported controversial outcomes on postural control on healthy young adults (Torvinen et al., 2002a, 2002c).

- *Hormonal level.* The growth hormone response, for example, is increased when a regular resistive exercise is combined with vibration (Kvorning et al., 2006).

- *Blood flow*. Changes in blood flow have also been recorded: both skin blood flow (Lohman et al., 2007; Rittweger et al., 2000) and muscle perfusion are enhanced during WBV exercises (Kerschan-Schindl et al., 2001).

- *Intramuscular temperature*. The use of a vibrating platform has also been proven in successfully raising the intramuscular temperature more quickly and more efficiently than any other traditional warm-up forms (e.g., cycling or hot bath (D. J. Cochrane et al., 2008). This suggests the use of WBV as a mean of warming-up in those sports that require high muscle power.

Although the use of WBV seems promising, there are unresolved aspects that still limit its systematic use in sport training and clinical rehabilitation. The first barrier is represented by the lack of a standardised protocol, which prevents clinicians from appropriately delivering the

treatment to patients (Rittweger, 2010). This is mostly due to the many variables that play a role in determining the outcomes of the treatment and to the (still unclear) way in which they affect the results. Examples of WBV determinants are the frequency and amplitude of the vibration, the posture of the subject on the platform and the type of platform itself (Rittweger, 2010). Different combinations of some of the aforementioned variables were tested and their effect was evaluated in terms of the relevant electromyographic (EMG) activity (Lienhard et al., 2014a; Ritzmann et al., 2013), but no definitive conclusions were drawn. This brings the attention to the second big uncertainty, namely the interpretation of the surface EMG (sEMG) signal recorded during WBV. A debate is still ongoing about the meaning of the sharp peaks that appear in the sEMG spectrum at the stimulation frequency and its superior harmonics. While some interpret these as an enhanced muscular activation triggered by the vibrations (Ritzmann et al., 2010; Xu et al., 2015), others believe that motion artefacts -mainly caused by cable swinging and skin stretching- account for most of the peak content and should therefore be removed (Abercromby et al., 2007a; Fratini et al., 2009a). More details on WBV-induced motion artefacts and how to deal with them are given in Chapter 3 (see paragraph 3.1.3).

2.1.1 Mechanisms behind WBV effect on muscles

Although WBV intervention has been proven effective to increase muscle contraction, and in turn, strength and power (Marin and Rhea, 2010a, 2010b; Osawa et al., 2013), the mechanism capable of eliciting such physiological response is still poorly understood. The following sections aim at presenting the two processes hypothesised to be responsible for it, namely tonic vibration reflex (TVR) and muscle tuning.

2.1.1.1 Tonic Vibration Reflex

The mechanism that is mostly accredited for triggering a response from the musculoskeletal system is similar to the one known as TVR (Bongiovanni and Hagbarth, 1990; Burke et al., 1976a; Burke and Schiller, 1976). According to the latter, vibrations applied to foot soles induce changes in muscle length that stimulate the sensorial structures present within the muscles, namely the muscle spindles. The latter are sensory organs located between extrafusal muscle

fibres and are connected to the CNS via primary and secondary endings that carry proprioceptive information. These afferent nervous fibres wrap around the intrafusal muscle fibres that constitute the spindles and detects changes in the length of muscles. When WBV-induced muscle stretch is detected by the spindles, motor neurons are activated via reflex responses and instruct muscle fibres to contract. This increased flow of APs to the muscles translates into an enhanced muscle fibre firing rate that, in turn, is measurable as a greater muscle activation –as observed during WBVs. The hypothesis that the enhanced muscle activity recorded during WBV is triggered by the TVR was well justified by the findings of pioneering studies on the effect that locally applied vibrations had on muscle response.

Important results came from the investigation of vibration-induced soleus response in the decerebrate cat (Homma et al., 1972). These showed that the MU inter-pulse intervals– which are defined as the time between an ending discharge and the adjacent one- were integer multiples of the vibratory cycle, indicating that MU discharge rate was synchronised with the vibratory stimulus. Subsequent results suggested that the same MU synchronisation would be applicable to humans as well (Hirayama et al., 1974) and were soon confirmed.

When vibrations were applied to the Achilles tendon, the triceps surae MU discharge rate was found to synchronise with the vibratory cycle (Burke and Schiller, 1976). However, isolated MUs were not able to synchronise with the stimulus in a one-to-one fashion, but rather dropping sporadic cycles. A similar response was observed in the jaw elevator muscles of participants who were voluntarily contracting them while sustaining vibrations (Hagbarth et al., 1976). Since it became clear that –under vibratory stimulation- even discharges of voluntarily driven MUs were phase-locked to the vibratory cycle, it was proposed that MU discharge timing depends on the level of synchronisation of the *Ia* afferent firing rate (Hagbarth et al., 1976). Further findings suggested that not only primary endings were responsive to a vibratory stimulus, but also *II* afferent fibres and Golgi tendons, indicating that *vibrations trigger the response of the whole proprioceptive apparatus* (Burke et al., 1976b).

While it has been proven that spindle endings responses were phase-locked to the vibratory cycle -with their firing pattern being either at the stimulation frequency or at subharmonics of it (Martin and Park 1997; R. Person and Kozhina 1992; R. S. Person and Kozhina 1989)- the discrepancy between their firing rate and MUs' one has not fully been clarified yet. One obvious response is the difference in the discharge rate of the structures of interest: sensory organs on one side and MUs on the other. While primary and secondary endings have been proven to have high discharge rate upper thresholds, axonal impulses descending motor neurons cannot physiologically propagate at a frequency higher than 50 Hz (Basmajian, 1978). A second possible explanation of the difference between receptor and actuator timing could lie within the pathways through which the afferents communicate with motor neurons. Although the TVR is thought to be primarily generated by the vibration-locked firing pattern of *Ia* fibres through monosynaptic pathways, it cannot be excluded that polysynaptic pathways are employed too to process these proprioceptive signals (Homma et al., 1972; Kanda, 1972). Results obtained by Burke et al. (1976) did in fact show that sustained vibration led to a decrease in motor neuron response, suggesting that afferent signals are processed through an additional pathway other than the monosynaptic one (Burke and Schiller, 1976). In conclusion, it is presumably safe to state that both monosynaptic and polysynaptic pathways are involved in the processing of proprioceptive feedback that arise in response of vibrations.

Although nowadays there is a common agreement on the fact that the TVR arises in response of vibrations applied *directly* to tendons or muscle bellies, evidence for the TVR to be actually triggered by WBV is still limited. However, encouraging results have recently been reported. A study comparing the latencies of stretch reflex responses with those obtained from sEMG activity of muscles undergoing WBV interestingly resulted in recording very similar latencies (Ritzmann et al., 2010). Furthermore, intramuscular recordings during WBV showed that MU firing rate was phase locked to the vibratory cycle, although not in a one-to-one fashion (Pollock et al., 2012), resembling the findings from the pioneering studies reported above.

Despite these findings suggest that a reflex response does occur probably as a consequence of vibration-induced muscle stretch, it is still unclear to what extent it contributes to increase muscle activity during WBV.

2.1.1.2 Muscle tuning

Another way to understand how muscles respond to WBVs is to look at the stress that vibrations represent for the body and the mechanisms the body relies on to control shock transmission. Among these, muscle activity and joint kinematics are those over which the body has a prompt control (Gross and Nelson, 1988; Lafortune et al., 1996). Since subjects are usually asked to keep a static posture during WBV exercises, the energy dissipated through joint kinematics is constant. Therefore, the only process through which harmful vibrations can be dampened during WBV is the regulation –or tuning- of muscle activity.

The idea that muscles reduce resonance by dampening vibrations -especially when the frequency of the latter is close to the natural frequency of soft tissues– has been around for a while (Nigg and Wakeling, 2001). Muscle tuning is a defensive mechanism perpetrated by muscles to minimise soft tissue vibrations that has been proposed to arise in response to ground reaction forces generated during physical activities and that has been proven to occur in several occasions (Wakeling and Nigg, 2001a). When a pendulum apparatus was used to deliver different impact forces to the heels (modulated by the use of different shoe sole materials), diverse muscle activation patters were recorded, suggesting that muscle activity was adjusted to the distinct impact force loading rates (Wakeling et al., 2001). A similar result was then obtained during actual running trials performed with different shoes, which -once again- altered the impact force loading rate (Wakeling et al., 2002b). During a walking trial performed with soft and hard shoe conditions, no changes were recorded in the ground reaction force (GRF) transferred from the ground to the lower limb tissues, although a bigger force transmission was expected for the soft-shoe condition (Wakeling et al., 2003). Since the force transmitted was constant in both conditions and since an enhanced muscle activity was measured during the soft shoe condition recordings, it could be concluded that vibration

dampening must have increased. Moreover, the frequencies of the impact resulting from the soft shoe condition were closer to soft tissue resonance frequency, confirming that muscle activity increased to avoid vibration-induced resonance of soft tissue. As for vibrations delivered artificially to the whole body, in a similar way to what happens during WBVs, muscle activity was measured in response to continuous and pulsed vibrations delivered through a platform (Wakeling et al., 2002a). Results from this study confirmed that when the stimulation frequency is similar to the natural frequency of the soft tissues compound, a greater muscle activity is registered. The increase of muscle activation and force production leads to a dissipation of the vibration power through the cross-bridge cycles that ultimately results in a greater vibration dampening. Furthermore, when muscle activity increases, tissue stiffness increases and their natural frequency shifts toward higher values, avoiding harmful free vibrations of soft tissues, namely “resonance” (Wakeling et al., 2002a). In fact, as it is the mass and the stiffness of a system that define its natural frequency, muscle activity has a direct effect on the natural frequency of soft tissues. In other words, when cross-bridges within the muscle fibre are activated in response to impact forces, the induced mechanical work is dissipated and stiffness is generated, leading to a dampening of tissue vibrations (Cardinale and Wakeling, 2005).

As for the TVR, muscle tuning has been hypothesised to be one of the mechanisms behind muscle response to the mechanical stimulation delivered via WBV and recent results suggest it might be so (Cardinale and Wakeling, 2005). Resonant-like behaviour of quadriceps rectus femoris (RF) were measured in response of WBV application (Fratini et al., 2009b), confirming the above-mentioned hypothesis. Similar results were obtained from the RF, biceps femoris (BF) and gastrocnemius lateralis (GL) when the relevant vibration-induced motion was recorded by an accelerometer placed on each muscle belly (Cesarelli et al., 2010). Interestingly, a different resonant-like motion was measured for each of the three muscles in the two analysed positions, which were hack squat (HS) and on the forefeet (FF). Accelerometers placed on RF and BF bellies showed the biggest displacement in the HS position when a mechanical stimulus of 23 Hz and 18 Hz was provided, respectively. The

displacement recorded in correspondence of the GL, instead, was appreciable only when participants were on FF and was maximum when a 27 Hz stimulus was used. These results show the dependency of the physiological response on the parameters of the mechanical stimulation and are indicative of the complicate way in which vibrations propagate in the body. They show that not only the WBV frequency but also the posture kept by the participants affect muscle response, as on the latter depend muscle tension and stiffness (Wakeling and Liphardt, 2006; Wakeling and Nigg, 2001a).

2.1.2 WBV treatment parameters

As mentioned before, one of the biggest obstacles that prevents WBV from being systematically used in clinical and sport rehabilitation routines is the large number of determinants that play a key role in the treatment and highly affect its outcomes. Some of these parameters and the way in which they affect WBV outcomes are discussed in the following sections.

2.1.2.1 Frequency and Amplitude

The nature of the delivered stimulus is of obvious importance and, therefore, both frequency and amplitude of the applied vibrations have an impact on the relevant muscle response. The relationship between the stimulus characteristics and the muscle outcomes is not completely clarified yet, but some progresses have been made regarding the choice of these parameters.

The range of frequencies that is commonly used in sport and clinical research is between 5 Hz and 60 Hz (Di Giminiani et al., 2015; Fratini et al., 2009b, 2009c; Lienhard et al., 2014a), which interestingly falls in the range of muscles natural frequencies (Wakeling and Nigg, 2001b). Some studies suggest that muscle activation in the lower limbs increases linearly with the vibration frequency and the platform displacement (Lienhard et al., 2014a; Pollock et al., 2010; Ritzmann et al., 2013). Nevertheless, Fratini et al. (2009) recorded a different trend in the electromyographic response of the RF. The average root mean square (RMS) values of sEMG did not increase linearly with the frequency, but peaked at 23.3 Hz and decreased for

bigger frequencies. Interestingly, this behaviour was visible only after filtering the signal with sharp notch filters, but we have to postpone this topic to paragraph 3.1.3, where it is discussed in detail. An absence of linear relation between RMS values of sEMG and frequency was also reported in measurements from the vastus lateralis, where the greatest muscle response was observed in correspondence of a 30 Hz stimulus rather than the maximum frequency used as stimulation (Cardinale and Lim, 2003a). Similar results were also obtained when the outcomes evaluated were different from electromyographic measurements: low frequency WBV (20 Hz) were proven to be more efficient than high frequency WBV (40 Hz) in the enhancement of hamstrings' flexibility and squat jump (Cardinale and Lim, 2003b). Altogether, these findings indicate that muscle response might not be linked to the stimulation frequency in a linear fashion, but rather that specific frequencies trigger the greatest muscle activation, which is in line with the muscle tuning paradigm.

To the best of the author's knowledge, the effect of the stimulus amplitude has instead been less investigated, but it has been proven to affect muscle activation as well. The latter is the vertical displacement undergone by the platform during a vibratory cycle and greater muscle responses were registered in correspondence of bigger stimulus amplitudes (Lienhard et al., 2014a; Pollock et al., 2010).

2.1.2.2 Subject's posture

If the specifics of the stimuli are of obvious importance, the posture of the subject is relevant as well. Since tension and muscle stiffness affect the way in which vibrations are transferred along the kinematic chain (Wakeling and Liphardt, 2006; Wakeling and Nigg, 2001a), the posture kept by a subject on the platform is essential to facilitate the propagation of the stimulus towards specific muscles.

Burke et al. (1976) observed that voluntary isometric contraction of muscles can enhance the response of muscle spindles to vibrations. This finding suggests that, when muscles are isometrically contracted, the vibration-induced firing rate of primary and secondary

endings is increased, indicating that WBV outcomes are maximised if the stimulus is delivered to voluntarily contracted muscles. A simple way to deliver WBV to contracted muscles in the lower limbs is to instruct the subject to maintain a specific posture. This will ensure a contraction of the target muscles throughout the duration of the treatment.

In literature it is common to find that subjects are asked to keep a hack squat position, although examples of single leg squat equally resulted in improvements of muscle power and strength (Bosco et al., 1999; Fagnani et al., 2006). According to the type of intervention, athletes were sometimes instructed to hold positions that resembled sport specific gestures (Wyon et al., 2010) or to perform training exercises on the platform (Delecluse et al., 2005; Mahieu et al., 2006). Encouraging results were also obtained in improving postural control when subjects maintained a forefeet stance on the vibrating platform (Ritzmann et al., 2014). Nevertheless, a direct comparison of static and dynamic WBV exercises showed that a greater electromyographic activity is evoked from muscles in isometric contraction conditions, rather than from muscles contracting in an eccentric and concentric fashion (Abercromby et al., 2007a). However, no actual physiological justification has been provided on the reason why static WBV exercises might be more efficacious than dynamic ones.

An insight on how muscle response can be affected by the position acquired during WBVs was offered by analysing the local muscle motion induced by the vibrations recorded by accelerometers placed on the skin in correspondence of the muscle belly (Cesarelli et al., 2010). The results showed that while the local motion of thigh muscles (RF and BF) is more pronounced in a HS posture, the motion of a lower leg muscle (GL) is larger when a subject is standing on FF. Similar findings on sEMG signals gave credit to the hypothesis that contracted muscles are more responsive to WBVs, and that this response can be tuned not only by adjusting the frequency of the stimuli but also the posture held by the subject (Ritzmann et al., 2013). Testing different combinations of frequencies, postures, platform type and external loads, two major conclusions were drawn. In the first place, it was found that increased knee flexion angles generated an increased activation of the knee extensor muscles (RF and tibialis

anterior), and a decreased response of the plantar flexor ones (gastrocnemius medialis and soleus). In the second place, it was concluded that a FF stance significantly enhanced muscle activity in the plantar flexors and diminished the response of knee extensors. On one side, these results suggest that different kinematic chains allow for the transmission of vibrations to different muscles. On the other side, they indicate that the acquisition of different postures lead the same muscles to different level of stiffness, changing their natural frequency and therefore altering their response to the same vibratory stimulus, which is once again in line with the muscle tuning paradigm.

2.1.2.3 Other WBV determinants

Among all WBV variables, the frequency of the stimulation and the posture held by participants are the most widely investigated, possibly because their effect on WBV outcomes has been better justified from both the physiological and mechanical point of view. However, there are also other parameters that should be taken into account when this treatment is used and those are:

- the type of platform used to deliver the stimulus
- the exposure time
- the cumulative dose
- the inclusion of external loads.

The following paragraphs aim at describing the way these affect WBV treatment outcomes, in order to explain the uncertainty linked to each of them and therefore the difficulty of appropriately tuning the treatment.

The type of device used in the treatment has been proven to influence the duration of the outcomes: platforms delivering synchronous vibrations evoke a bigger treatment effect on

muscle power and strength for long-term adaptations compared to side-alternating platforms (Marin and Rhea, 2010a, 2010b). These findings therefore suggest the use of a synchronous stimuli to observe long-term improvements, and the use of a side-alternating one to elicit acute effects in muscles.

As well as the platform used, *the amount of time* subjects are continuously exposed to the mechanical stimuli affects the final WBV outcomes. Exposure times ranging from 30 seconds up to 20 minutes are used for one single session in current protocols (Bosco et al., 1999; Dallas et al., 2017; Ritzmann et al., 2014; Sucuoglu et al., 2015). However, previous findings demonstrated that prolonged periods of vibration causes not only a decrease in EMG activity, but also a reduction in MU discharge rate and contraction force (Bongiovanni et al., 1990). Specifically, 10-20 seconds of vibration seem to be sufficient to increase *Ia* afferent inputs, while sustained vibrations reduce their inflow to alpha motor neurons (Shinohara, 2005).

If long-term outcomes are the objective of the treatment, *the cumulative dose* is another parameter that should be consciously tailored, which is the total amount of vibrations delivered to the participant throughout the duration of the treatment. A significant increase in lower-limb extension strength was recorded after two-month of WBV exercises in young non-athletic adults, which reversed and decreased by the end of the fourth month of intervention. A net improvement was instead registered for the jump height by the end of the treatment (Torvinen et al., 2002a). The effect of the total amount of exposure to vibration undergone by the subjects throughout the treatment is not of simple investigation due to the variability observed in the different studies. Each study, indeed, adopts a different WBV treatment protocol, sometimes changing the stimulus specifics (frequency, amplitude and type of platform used), the exercises and the exposure time along the treatment period (Delecluse et al., 2003).

The inclusion of external loads, for example via the use of a weightlifting bar, can affect the intervention outcomes too. Studies showed that WBV performed with additional loads of 20%, 30% and 40% of the subject's body mass increase not only muscle response, but also

metabolic power and performance (Garatachea et al., 2007; Rittweger et al., 2001; Ritzmann et al., 2013). Although it is suggested that greater loads stimulate greater responses in term of oxygen consumption and heart rate principally in the young population (D.J. Cochrane et al., 2008), conclusive results have not been produced yet.

The differences found in the afore-mentioned studies do not only depend on the variety of protocols used and population tested, but also on the way the results were analysed and interpreted. Chapter 3 presents more details on the preprocessing steps and the analyses employed in the present thesis.

2.2 Undisturbed upright standing

Maintaining an upright stable posture does probably feel effortless to most human beings. However, this easiness does not reflect the complexity of the control mechanisms that are actuated by the nervous system to keep the body in balance. Moreover, it does not matter how trained the postural control mechanisms are: a completely still upright posture is impossible to achieve and maintain, since the body constantly sways. The incapacity of keeping a completely stable upright stance is due to the fact that, differently from other animals, humans are shaped as long bodies that develop in the vertical direction, rather than in the horizontal one, and have a small base on which to balance. In addition, two thirds of the mass of a human body is located above the waist, placing the body centre of mass (COM) in front of the ankle joint (Forbes et al., 2018). Because we live in a gravitational environment, gravity acts on the standing person who would fall forward if no other forces acted in the opposite direction. The forces that prevent a standing person from falling forward are those generated by the plantarflexor muscles in the calf, namely the gastrocnemius and the soleus (SOL). The contraction of the triceps surae muscles pulls the person backward and prevents the body from toppling. However, since it is practically impossible to exert the exact amount of force necessary to fully stabilise the COM, the dorsiflexor muscles -such as the tibialis anterior (TA)- are engaged as well to counterbalance those forces that pull the body backwards. These corrections are continuously

ongoing and are reflected by the constant sway of the body, which makes even quiet standing an actual dynamic effort (Horak et al., 1997).

The COM of a body is where the mass of the latter is balanced and can be calculated by weight-averaging the COM of the segments of which the body is composed. Since the COM can be approximated as the application point of the resultant of the external forces, a force equal and opposite to the gravitational forces must act on the COM for the standing body not to lose equilibrium. Although the centre of pressure (COP) is sometimes wrongly interpreted as the projection of the COM on the base of support, it actually represents the location of the GRF equal and opposite to the resultant of the forces exerted by the muscles to resist gravity and accelerate the COM. In other words, while on one side the COM reveals the actual body sway, on the other side the COP reflects the neuromuscular response actuated to adjust COM imbalances (Winter, 1990). The condition necessary for maintaining an upright stance is that the horizontal projection of the COM does not exceed the base of support (Horak and Macpherson, 1996). In the case of bipedal undisturbed balance, the latter is the surface defined by the area under the feet. Generally, static stability is proportional to the mass of the body and the surface of the base of support. Moreover, the higher is the COM with respect to the base of support, the less stable the body is (Hayes, 1982).

To investigate the biomechanics of human free standing, the standing body has often been described as an “inverted-pendulum”, where the feet are the fixed base and the rest of the body (legs, trunk, neck and head) is free to move around the ankle as a single rigid segment (Winter et al., 1998). According to this model, the COM position is adjusted in the sagittal plane mainly by plantarflexor/dorsiflexor torques that act around the ankle and represent the so-called “ankle strategy” (Horak and Nashner, 1986; Winter, 1995). Oscillations in the frontal plane are instead mostly controlled by the hip abductor/adductor moments -the so-called “hip strategy”- as the ankle invertor/evertor torques are negligible in this plane (Winter, 1990). Although the hip strategy is still adopted to avoid a forward fall, it is the ankle strategy that represent the dominant mechanism during quiet standing (Gatev et al., 1999; Winter, 1990).

However, although the inverted-pendulum is useful for understanding the mechanics of human standing, the ability of balancing on two legs without falling goes beyond the simplification offered by this model. This ability does in fact result from the processing of a huge amount of sensory information that allows the fine tuning of muscle activation to counteract a loss of balance. All together, these mechanisms represent the so-called “postural control”, which is described in the next paragraph.

2.2.1 Postural control

For a long time, postural control was believed to be a simple summation of reflex responses. This view was supported by studies showing that animals were able to maintain balance by tonic reflexes alone (Magnus, 1925), which led to the hypothesis that the same low level mechanisms would apply to humans. However, many were the reasons for which not to pursue such parallelism. Firstly, human balancing is different from that of most animals as its stance is bipedal rather than quadrupedal, making the base of support smaller and making it easier for the COM -which is also at a higher position with respect to the base- to be located outside of it (Loram et al., 2005a). Secondly, the contribution of short latency (SLAT) responses (reflexes) to postural control was shown to be minimal even in animals since cats with spinal transections –but intact SLAT reflexes- were unable to maintain an unsupported stable stance (Fung and Macpherson, 1999). Nevertheless, it was proposed that human beings could maintain an upright stance by the instantaneous activation of muscle activity via stiffness control (Winter et al., 1998). According to this model, the sole role of the CNS was to select the right tonus for the ankle muscles. However, this model was soon challenged by the fact that ankle stiffness alone was proven not to be enough to balance, suggesting that an active mechanisms of stabilisation must be responsible for the ability of humans to stand still (Morasso and Schieppati, 1999). Hence, it is reasonable to state that standing balance is achieved by both passive torques –generated by reflexes triggered by muscle lengthening and shortening- and active ones –controlled by cortial drive (Peterka, 2002). Since these active torques are activated through a feedback control system, it became clear that sensorimotor integration played a big role for postural control.

Postural control is therefore nowadays no longer believed to be the result of equilibrium reflexes, but rather the product of fine motor control achieved via complicated neural integrations (Horak and Macpherson, 1996; Ivanenko and Gurfinkel, 2018). It is enough to look at an infant attempting to stand to realise that balancing on two legs is a motor skill itself and requires a certain degree of learning and maturity of the senses to be effectively carried out (Hayes, 1982). The ability to maintain balance does in fact depend on the ability to *detect* internal and external perturbations, *react to* the latter and *generate the appropriate corrective torques* to keep the COM within the base of support. In order to detect internal perturbations (such as excessive muscle lengthening due to losses of balance) or external ones (such as a sudden change in the lightening of the surrounding environment or a displacement of the base of support) humans rely on sensory information of different nature. Proprioceptive, vestibular and visual feedbacks play a fundamental role for postural control, as several studies demonstrated that balance is compromised when these systems are stimulated or challenged (Peterka, 2002). Sensory information are carried from the periphery to the CNS via afferent nerves and processed either at the spinal (SLAT), brainstem (medium latency responses, MLAT) or brain level (long latency responses, LLAT), producing an internal representation of the position of the body (kinaesthesia) (Horak and Jacobs, 2007). Finally, to counteract the loss of balance, muscles are recruited in the appropriate proportion to generate a force that, applied against the base of support, accelerates the COM in the desired direction.

As it is believed to happen in most of the movements performed on a daily basis, muscles are not activated in a single fashion, but rather by common neural signals that are input to muscles located in different part of the body, forming the so-called “muscle synergies” (Bernstein, 1967; Farmer, 1998; Turvey, 1990). These are thought to play a fundamental role even for postural control, further supporting the idea that balancing requires fine motor control and a certain degree of training (Loram et al., 2005a; Morasso and Schieppati, 1999).

2.2.2 Sensory feedbacks

As previously mentioned, sensory feedbacks are fundamental for human postural control and are provided by the vestibular, visual and proprioceptive systems.

The vestibular system is composed of three semicircular canals and the otolith organs –saccule and utricle- to which the canals are connected. The first ones detect angular head velocity sensing its direction. Since their gain is smaller for frequencies below 0.1 Hz, the semicircular canals are thought to encode information about unexpected impulses to the head (above 0.5-1 Hz) rather than slow postural oscillations that characterise undisturbed upright standing. The second ones are sensitive to linear accelerations that occur in every direction, signalling the CNS about the position of the head (tilts). Because their gain is high even at low frequencies (below 0.5 Hz), otolith organs are thought to play an important role in detecting natural slow head oscillations that are characteristic of undisturbed balance. Summarising, the vestibular system -located in the inner ear- detects rotational and linear motion of the head with respect to the vertical (gravity), allowing us to perceive our postural verticality (Forbes et al., 2018). Galvanic vestibular stimulation has been proven to evoke both body sway and body tilt (Day et al., 1997; Hlavacka and Njiokiktjien, 1985), but the application of this stimulation does not fall within the scope of this thesis.

Afferent information from the visual system originate from photoreceptors in the retina that detect changes in contrast and motion of brightness. When signals from the direction-sensitive ganglion cells of both eyes are processed in the brain, the perception of translation and rotation arises. In the context of upright standing, visual information allow for the detection of head orientation with respect to the real visual world, contributing to the perception of self-motion (Forbes et al., 2018). Visual cues permit also the prediction of oncoming obstacles or perturbations, allowing the system to preventively tune the postural reaction. Several studies investigated changes in stability that occurred in response to the closure of the eyes, alterations of the visual field or the motion of the visual surrounds and confirmed the important role they play in balance control (Bronstein, 1986; Dijkstra et al., 1994).

The term somatosensory feedback includes all those sensory information produced by the mechanoreceptors and proprioceptors that allow the detection of the body position. The first ones include receptors that respond to pressure, touch and vibrations and are located in the skin. In the context of postural control, they play an important role in detecting a slip or an alteration of the weight distribution under the foot soles. Specifically, Merkel cells and Ruffini endings respond to low-frequency variations of pressure and skin stretch, while Meissner and Pacinian corpuscles are sensitive to high-frequency deformations and vibration of the skin (Forbes et al., 2018). The second ones instead include receptors that contribute to the perception of body position. Among the proprioceptors, muscle spindles are located within the muscles and are sensitive to changes of muscle length, while Golgi tendon organs are placed within tendons and sense stretch encoding active muscle force production (Forbes et al., 2018).

Among all, somatosensory inputs from the lower limbs appear to be those on which postural responses mostly depend and the reason is twofold (Horak et al., 1994; Inglis et al., 1994). First, proprioceptive thresholds are the lowest in detecting COP velocity, and so lower-limb proprioceptors are the first one to be triggered by a perturbation (Fitzpatrick and Mccloskey, 1994; Peterka, 2002; Sturnieks et al., 2008). Second, somatosensory feedbacks drive postural responses of different latencies: not only SLAT responses, such as the monosynaptic stretch reflex, but also LLAT ones, which originate from higher-level processing of sensory feedbacks and produce postural synergies (Horak and Jacobs, 2007).

2.2.3 Muscle activation

As previously mentioned, contractions of muscle via reflex responses were proven not to be sufficient for stabilising balance and for counteracting postural perturbations (Fung and Macpherson, 1999; Morasso and Schieppati, 1999). Although SLAT responses originated in the spinal cord are thought to be employed in the most automatic early phases of postural responses, more complex muscle activations, which originate from high-level processing in the brain, are engaged in the later phases of these responses (Horak and Jacobs, 2007).

The CNS is indeed thought to deal with the many degrees of freedom that characterise the musculoskeletal system by recruiting muscles in fixed groups, or synergies, ultimately simplifying the problem of motor control (Bernstein, 1967). In other words, synergies are used as an ensemble of heuristic solutions that convert task-oriented goals into “detailed spatiotemporal patterns of muscle activation” (Ting and McKay, 2007). The term “synergy” refers to a set of muscles that are activated by the same neural signal, allowing both a simpler control of movements and flexibility of the final outcome (Torres-Oviedo et al., 2006). It is believed that the wide range of motor behaviours that humans are able to accomplish originates in fact by the activation of just a few muscle synergies, which are recruited in varying combinations according to the task to be accomplished (Ting and McKay, 2007). Although it was proposed that some muscle synergies might be innate to some extent –as those shaping the postural responses of a new-born (Massion, 1998)– there is more evidence is support of the fact that muscle synergies result from adaptive processes, such as the intersubject variations in both the number and muscle synergy patterns (Thoroughman et al., 2007). A synergy control structure was confirmed to be behind human movements like pedalling and walking since outcomes such as the kinematics and whole limb force well correlated with muscle groupings (Barroso et al., 2014; Ting et al., 1999). As for postural responses, a study showed that 95% of the automatic postural response to surface translation was explained by as little as four synergies in cats and that these were similar across the animals (Ting and Macpherson, 2005). Since each synergy was recruited in response of a specific set of directions and it was also correlated with a single force vector, it was suggested that the neural commands (in charge of activating synergies) do in fact signal the endpoint force that should be exerted by the limbs to resist the translation of the surface in that specific direction. Similarly, later analyses of muscle synergies recruited in response of different postural tasks (multidirectional rotation and translation of the base of support at different stances) confirmed the robustness of such synergies (Torres-Oviedo et al., 2006). Indeed, the fact that five synergies were able to reconstruct 80% of the total variability -across cats and tasks- suggested that the generation of functional synergies is at the base of robust task-variables control. Specifically, when the postural task was slightly altered, the differences observed in

the muscular activation were not explained by a change in the recruited synergies, but rather by a different modulation of the activation levels of the synergies belonging to the same set. Even in humans, six synergies were sufficient to reconstruct the postural responses across subjects and tasks, resembling the previously mentioned ankle and hip strategies (Torres-Oviedo and Ting, 2007). Altogether, these results suggest that postural responses are shaped by the recruitment of the same synergies in proportions that vary according to the task.

Although it is commonly accepted that a neural control is at the basis of our ability to perform precise and complex movements, the way in which the CNS actually governs the many degrees of freedom that characterise the musculoskeletal system is still an open question. While synergies offer an insight into the coordinated activation of muscles, intramuscular coherence (IMC) and corticomuscular coherence (CMC) are particularly suited to investigate the neural implementation of the control strategies that allowed the synchronised recruitment of such muscles (Boonstra, 2013). While IMC reflects the common oscillatory input to different muscles, CMC represents the interplay between the periphery and the CNS, or, in other words, both afferent and efferent signals (J. Liu et al., 2019). More details on these powerful measures are given in Chapter 3 (see paragraph 3.3).

2.2.4 Neural markers of Postural control

As previously mentioned, postural control is actuated via the activation of short, medium and long latency responses. The term SLAT includes those stretch reflexes triggered by proprioceptive signals that are processed at the spinal level and lead to the contraction of muscles to counterbalance the detected stretches. Those processed at the brainstem level are instead referred to as MLAT responses and are not always distinguishable from the LLAT ones, which are preprocessed in the cortex, all the way up the neural axis. Because SLAT responses are not enough to stabilise balance, all of them play a role in shaping the postural response to perturbations. Specifically, it is suggested that SLAT and MLAT responses play a big role in the first phase of the response –the most automatic one- where input from the periphery trigger pre-set synergies in the brainstem. The later phases are instead less

automatic and involve responses processed at the cortical level. More in detail, it is suggested that the cortical loop involving the cerebellum is responsible for the human ability of formulating postural responses based on previous experience. Instead, the cortical loop involving the basal ganglia allows the adaptation of postural responses from the current context (Horak and Jacobs, 2007).

The involvement of cognitive-motor processes has been proven to occur during both perturbed and spontaneous upright standing tasks (Maki and McIlroy, 2007; Mierau et al., 2017; Slobounov et al., 2005, 2013; Wittenberg et al., 2017), as the cortical activity was seen to change according to level of attention required. In correspondence of tougher balance tasks, a general increased cognitive load has been observed and quantified as power drops in alpha frequency range or increments of the individual alpha peak frequency (Hülsdünker et al., 2016; Petrofsky and Khowailed, 2014; Slobounov et al., 2009, 2008; Solis-Escalante et al., 2019). In parallel, increased activity in beta (Petrofsky and Khowailed, 2014; Tse et al., 2013), gamma (Chang et al., 2016; Tse et al., 2013) and theta (Hülsdünker et al., 2015; Slobounov et al., 2009) bands were recorded across different studies during more challenging postural conditions. Specifically, beta and gamma frequency bands were proposed as facilitators of sensorimotor integration (Chang et al., 2016), resembling the interpretation proposed by Baker et al (2007). According to the latter, oscillations in beta band (15-30 Hz) might have the potential to recalibrate the sensorimotor system after a movement. More in detail, beta band activity (BBA) is suggested to aid the monitoring of the periphery status, facilitating the processing of inputs from the latter and ultimately maintaining a constant motor output (Baker, 2007). On this note, it was proposed that the role of BBA was to signal the inclination to preserve the *status quo*, promoting the *recalibration* of the sensorimotor system via a more efficient processing of sensory feedback (Engel and Fries, 2010). If interpreted in the context of postural control, since oscillations in beta-band act to stabilise the motor output and minimise diverging movements (Androulidakis et al., 2007, 2006; Gilbertson et al., 2005), an increase in BBA might reflect the attempt of the system to maintain balance, i.e. the status quo. Because BBA might favour a more effective processing of sensory feedbacks, an increase of activity in

this band during a postural task might also reflect a better processing of proprioceptive signals –on which postural control relies- to ultimately recalibrate the sensorimotor set after a disturbance and minimise COP fluctuations.

Activity in beta band have been thoroughly investigated in the context of motor control as oscillations around 20 Hz in the motor and somatosensory cortex were found to be coherent with activity from contralateral muscles (Baker, 2007). The interplay between the CNS and the peripheral muscles was quantified with CMC and was vastly documented to occur during isometric contractions and voluntary movements (Andrykiewicz et al., 2007; Conway et al., 1995; Kilner et al., 2002, 1999; Kristeva et al., 2007, 2002; Omlor et al., 2007; Petersen et al., 2012; Peterson and Ferris, 2019; Roeder et al., 2020; Ushiyama et al., 2017; Watanabe et al., 2020). The same level of evidence is instead not available for motor control involved in postural tasks. Very few studies did in fact evaluate CMC during standing balance (Masakado et al., 2008; Murnaghan et al., 2014) and even less managed to prove the existence of CMC during postural control (Jacobs et al., 2015; Ozdemir et al., 2018; Vecchio et al., 2008). While someone suggest that upright standing does not require cortical control (Masakado et al., 2008; Murnaghan et al., 2014), others highlight that it is possibly due to the fact that CMC depends not only on the task (Kilner et al., 2000, 1999), but also on the functional role and level of specialisation of the chosen muscles (Ushiyama et al., 2012, 2010).

2.3 Thesis' objectives

The main aim of this thesis is to deepen the understanding of Whole Body Vibration stimulation with particular attention to postural control interventions. To this aim, two objectives were define: the following paragraphs describe the research questions and the studies designed to address them.

2.3.1 Customisation of WBV stimulation for calf muscles

The first step undertaken to better understand how WBVs affect postural control mechanisms was to define those stimulation parameters that best targeted the muscles recruited during

such activity. Since the ankle strategy is the one mostly engaged during unrestricted bipedal balance and since the muscles of the lower leg are those needed to put such strategy into play, the first study presented in this thesis is focussed on the selection of those stimulation variables that evoke the biggest response from the TA, the GL and the SOL muscles. Because of the physical limitations posed by the device available in the laboratory and, in order to avoid subject fatigue, the number of variables taken into account was restricted to two: stimulation frequency and subject posture. Soft tissue accelerations and sEMG signals were collected from these muscles and compared across WBV stimulations, during which different vibration frequencies (ranging from 15 to 30 Hz) were utilised and subjects were asked to hold either a HS or FF static posture. The combination of stimulation frequency and subject posture that maximised lower limb muscle response –and therefore boosted the sensitivity of their specific muscle spindles- was used as WBV stimulation in the second study.

2.3.2 Characterisation of WBV effect on postural control

The second objective of this thesis was to understand how the enhancement of the sensitivity of lower limb muscle spindles -obtained via mechanical stimulation- influences postural control. To this aim, both physiological and behavioural outcomes were collected during four minutes of unrestricted balance before and after participants underwent WBV stimulation delivered with the specifics outlined from the first study. COP trajectories were collected and analysed to investigate how the stability of the participants changed after the WBVs. Moreover, in order to understand how WBVs affected the underlying mechanisms that are responsible for such outcome, sEMG and electroencephalographic (EEG) signals were collected from the lower leg muscles and the scalp, respectively.

3. Methodologies

The purpose of this chapter is to provide a comprehensive overview on the recording techniques presented in the following chapters and to offer a technical and mathematical background on the analysis used to quantify physiological effects. Additional and in more depths details can be found in the relative sections of Chapters 4 and 5.

3.1 EMG

Electromyography (EMG) is the recording technique used to quantify muscle activation. Although the electrodes can be of different type and size -intramuscular or surface, bipolar or multichannel, with areas ranging from few mm^2 to hundreds of mm^2- they all record the electrical activity associated with the underlying action potentials (APs) that propagate along the muscle fibres (Merletti and Farina, 2016).

3.1.1 Origin of the EMG signal

Contractions produce electrical activity within the relative muscles, which is generated in a process that involves the central nervous system and the muscle fibres organised in functional units that are generally referred to as *motor units* (MUs). A MU comprises a motor-neuron descending from the spinal cord (or brain stem) to the periphery and all the muscle fibres that are physically connected to it. Muscle contraction is initiated by an AP that propagates along the motor-neuron and terminates in the neuromuscular junction, leading to the activation (firing) of the innervated fibres, the electrical activity of which forms what is known as “motor unit action potential” (MUAP). The repetitive stimulations of a MU produce sequences of MUAPs which are generally referred as motor unit action potential trains (MUAPTs). Specifically, when the AP reaches the neuromuscular junction, acetylcholine –a neurotransmitter- is released and disrupts the membrane resting potential. The excitation of the sarcolemma (membrane of the muscle fibre) leads to a propagation of the depolarisation zone from the neuromuscular junction in both directions to the end of the tendons, generating an intracellular action potential (IAP). In parallel to the electrical phenomenon, the physical muscle contraction occurs. As the IAP propagates, it causes the release of calcium (Ca^{2+}) from the sarcoplasmic reticulum; Ca^{2+} binds with troponin molecules on actin filaments, whose

configuration changes and results in myosin-binding sites being suddenly available. Myosin heads (on thick myosin filament) bind with the now free myosin-binding sites (on thin actin filament) in a bond known as “cross-bridge”. When the myosin head tilts down, the actin filament is dragged in the opposite direction and the muscle fibre shortens. The repetition of this cycle is also referred to as “contractile activity” which leads to the production of the muscle force necessary to perform movements (Merletti and Farina, 2016). Every muscle contraction therefore generates multiple MUAPTs on the same MU and multiple MUAPTs on different MUs. The resultant electrical activity measured internally or on the surface of the muscle is a spatiotemporal summation of all these signals at the measurement sites (electrodes).

The EMG signal represents the recording of this electrical activity and, as well as reflecting the extent of MU activation and their firing rate, reflects the amount of motor neuron firing in the spinal cord or brain stem (Merletti and Farina, 2016).

3.1.2 Preprocessing and analysis of sEMG

In our study we used surface EMG (sEMG) recordings, which are performed using surface electrodes. Since the positioning of the latter is crucial for sEMG recordings to ensure result consistency, electrodes were placed according to the SENIAM guidelines (Hermens et al., 2000, 1999). Before electrode placement, the area was shaved to minimise artefacts induced by body hair and oily substances were removed by rubbing the skin with alcohol (Merletti and Farina, 2016).

Before analysing and quantifying the muscular activation, the sEMG data were band-pass filtered and, as details on the frequency range are specific to the study design, they can be found in the relative sections of Chapter 4 and 5. Generally, the low frequency content was removed as the skin and fat tissues, which separate the signal source from the recording site (altogether constituting the volume conductor), act as a low-pass filter (Merletti and Farina, 2016). To quantify the overall muscular activation, the root mean square (RMS) of the sEMG recordings was used. For a time-series x of N points, its RMS is calculated as follows:

$$RMS = \sqrt{\frac{1}{N}\sum_{i=1}^{N}|x_i|^2}$$

The RMS is an estimation of the amplitude of the sEMG signal, which changes accordingly to the amount of firing MUs and the rate at which APs are discharged and therefore provides a measure of the "strength" of muscle contraction (Merletti and Farina, 2016). EMG recordings are usually normalised by the maximum voluntary contraction and expressed as a percentage of the latter. However, because in this thesis the sEMG RMS values are compared in a paired fashion and electrodes were not replaced between trials, the baseline value was either used as normalisation factor when more than two conditions were tested (study 1) or simply analysed against the one obtained under the other condition (study 2) (Burden, 2010).

The frequency content of sEMG signals was instead analysed via mean of corticomuscular and intermuscular coherence (CMC and IMC, respectively) analyses. The first measure reflects the frequency similarities between the cortical activations and the MUs of a specific muscle (J. Liu et al., 2019; Mima and Hallet, 1999) and the second one represents the common neural input shared between MUs of different muscles (Farmer, 1998). Since the volume conductor causes the attenuation of the spectral content at the low frequencies, all sEMG time-series were full-wave rectified before CMC and IMC were estimated. sEMG rectification has been largely debated (Merletti and Farina, 2016), but it is strongly recommended for coherence analyses as it is thought to be crucial for the demodulation of the neural component from sEMG (Boonstra and Breakspear, 2012; Halliday and Farmer, 2010; Myers et al., 2003; Yao et al., 2007). The synchronisation of muscle activation (IMC) was investigated with state-of-the-art complex network analyses (Boonstra et al., 2015; Kerkman et al., 2020): details on coherence estimation and graph theory are given in paragraph 3.3.

3.1.3 Motion artefacts on sEMG during WBV

Power spectrum of sEMG signals recorded during WBVs present sharp peaks at the stimulation frequency and its superior harmonics (Figure 3.1, a), and their physiological

meaning is still under debate. Similar spikes were addressed for the first time at the beginning of 1990. Since the capacity of individual MU to synchronise their firing pattern to a vibratory stimulus was already demonstrated (Burke and Schiller, 1976; Lebedev and Polyakov, 1992; Person and Kozhina, 1992, 1989), these spikes were explained as a result of the summation of action potentials of several MU phase-locked to the vibratory cycle (Lebedev and Polyakov, 1992, 1991). Based on this interpretation, authors have either ignored or interpreted these spikes in power occurring during WBSs as a demonstration of an increased synchronisation of MU firing rate to the stimulation frequency (Cardinale and Bosco, 2003; Ritzmann et al., 2010; Xu et al., 2015). Only in 2007, Abercromby et al. suggested that such sharp peaks might mostly represent motion artefacts (caused by relative movements between electrodes and the skin and the stretching of the skin itself) and proposed to remove them with band-stop filters (Abercromby et al., 2007a). More formal demonstrations were later proposed and further suggested that motion artefacts accounted for the majority of the variability of spectral peaks (Fratini et al., 2009a; Sebik et al., 2013). Nevertheless, this issue is still debated and there is no definitive agreement on whether the spikes are caused by the tonic vibration reflexes or motion artefacts (Ritzmann et al., 2010; Xu et al., 2015). Although differences and limitations within study set-ups might have generated different outcomes (Bifulco et al., 2013), it is likely that sEMG spectrum contains both reflex activity and motion artefacts (Lienhard et al., 2014b).

While motion artefacts are limited to sEMG spectral peaks, the reflex activity extends to a broader range of frequencies (Ritzmann et al., 2010). It could be therefore concluded that the removal of the spikes in the sEMG spectrum does not affect the deductions that can be drawn on WBV effect on the neuromuscular system. For this reason, and for continuation with previous studies (Cesarelli et al., 2010; Fratini et al., 2009a, 2009b), the spectral spikes were removed via mean of narrow stop band filters. Details on the latter are provided on the relative section of the Chapter 4 and an example of the artefact removal is given in Figure 3.1.

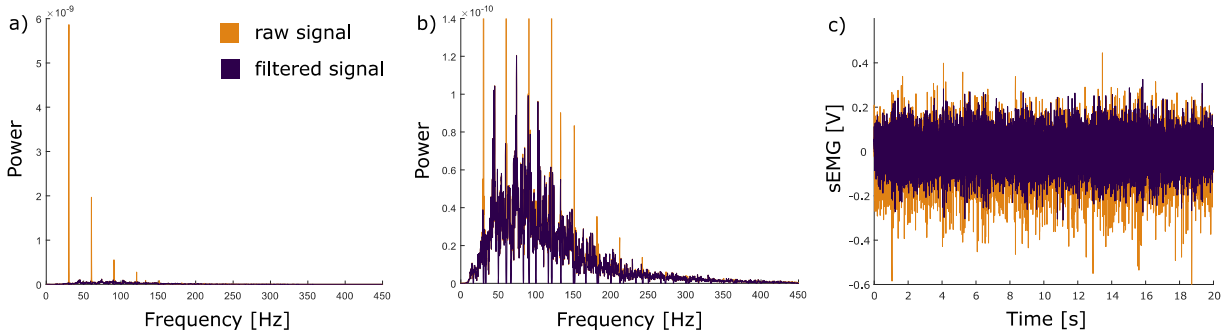

Figure 3. 1: Motion artefacts removal via spectral filtering

Preprocessing of the sEMG signal recorded from the gastrocnemius lateralis during WBV stimulation at 30 Hz. a) Power spectrum of the raw signal (orange) and the filtered one (purple); b) magnification of the power spectrum of the filtered signal, from which the peaks were removed via mean of narrow stop-band filters; c) raw (orange) and filtered (purple) sEMG signal.

3.2 EEG

Richard Caton is usually cited for being the first one to record electrical activity from the brain of animals such as cats, monkey and rabbits (Caton, 1875). However, the activity of the human brain was visualised and quantified in the form of voltage oscillations for the first time by Hans Berger (Berger and Gloor, 1969), who paved the way for neuroimaging research via electroencephalogram recordings. Electroencephalography (EEG) is not the only brain imaging technique, nevertheless, it is one of the few techniques capable of non-invasively measuring the direct neural activation and of having excellent temporal resolution. In addition, the advance of technology has seen the latest models of EEG recording devices become portable and therefore offer freedom of movement, making EEG a suitable technique also for studies involving motor and postural tasks.

3.2.1 Origin of the EEG signal

Electroencephalography records the electrical activity of the brain by measuring the difference in voltage between two recording sites. Since electrodes are placed on the scalp, what EEG records is the summation of excitatory and inhibitory post-synaptic potentials (EPSPs and IPSPs), rather than the individual potentials themselves. The binding of specific messengers

(glutamate for EPSPs and gamma-aminobutyric acid for IPSPs) to the postsynaptic membrane causes ion channels to open, leading to a change in the permeability of the membrane. According to the nature of the ions moving through the membrane (Na^+ and K^+ for EPSPs and Cl^- for IPSPs), the post-synaptic potential is called excitatory or inhibitory, depending on whether it leads to depolarisation (EPSP) or hyperpolarisation (IPSP) of the neuron, respectively stimulating or inhibiting the transmission of an action potential along the axon of the neuron. Among all, pyramidal neurons are those that mostly contribute to the generation of the EEG signal. These are nervous cells placed perpendicularly to the surface of the cortex and, as the cortex folds on itself, they are radiant -oriented along the radius from the centre of the head to the cortex- or tangential to the scalp -placed perpendicularly to the radius that from the centre of the head is projected toward the cortex- (Figure 3. 2 3.2). When triggered at the synaptic site, an EPSP (or IPSP) is generated and an intracellular current -perpendicular to the cortical surface itself- is then associated to the apical dendrite of the neuron and becomes detectable via EEG recordings (Hari and Puce, 2017). This microscopic current is generated by the movement of ions through the membrane of the neuron and is also referred to as “current dipole”. EEG is more sensitive to radial dipoles, although also tangential ones contribute to the overall recorded electrical activity, providing they are not similar in strength and are not placed on the opposite sides of a sulcus (Cohen, 2014). Due to of their orientation and duration, EEG signals are mostly made of post-synaptic potentials rather than action potentials (Hari and Puce, 2017).

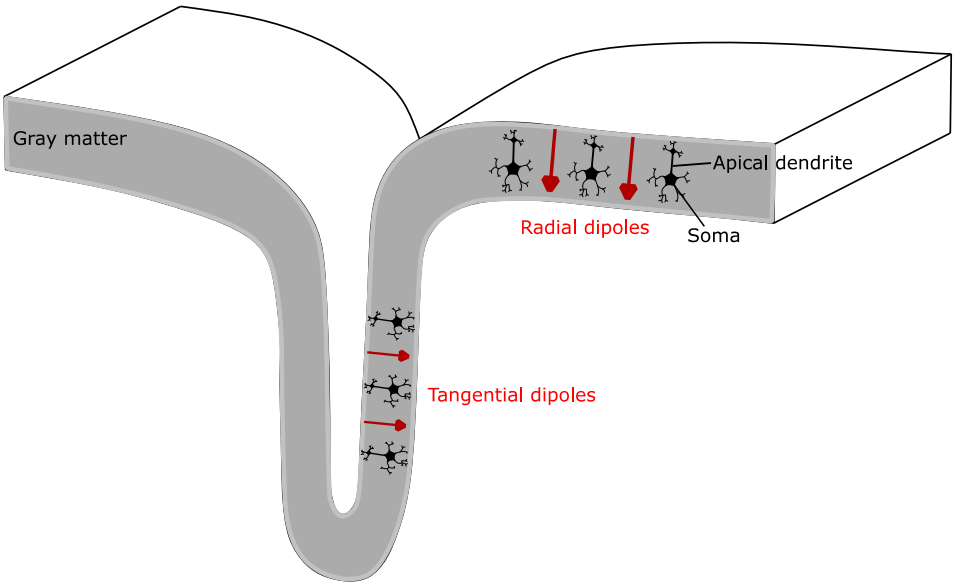

Figure 3. 2: Current dipoles and pyramidal neurons

Schematic illustration of pyramidal neurons (black), which are perpendicular to the cortex, despite of its folding. The excitation of the apical dendrite generates a current flow that is modelled with radial and tangential current dipoles (red), depending on their orientation with respect to the radius that from the centre of the brain projects to the scalp.

3.2.2 Preprocessing and analysis of EEG signals

Since the goal of EEG recordings is to quantify the physiological electrical activation of the brain, any other source of noise that is not related to the relevant phenomena is to be discarded. These artefacts can be of different nature and are usually generated by muscular activations, head or sensor movements, or other electrical sources such as devices present in the recording environment (Hari and Puce, 2017). To discern genuine brain activation from artefacts, a semi-automatic preprocessing pipeline was adapted from previously proposed research (Brunet et al., 2011):

- The raw EEG data were cropped at the time window of interest and successfully de-trended. The obtained signals were mirrored at both ends before filtering to avoid edge artefacts (Cohen, 2014). Then, a zero-phase FIR filter (band pass filter

between 13 and 32 Hz) was applied to extract the content of the signals situated in the beta frequency range. Trials were then cropped to remove the padding and de-trended again.

- To remove extraocular muscle (eye-blink) artefacts, a regression method was preferred to the more commonly used independent component analyses. While in the first one the bias is limited to the selection of regression channels to be used consistently across participants, in the second one the bias extends to the selection of components to be removed for each participant.. According to this method, a channel containing clear eye-blink artefacts is subtracted from the rest of the signals in proportion to their similarity. Since extraocular muscle artefacts are predominant in those channels that are physically close to the eyes, frontal sensors are usually removed from the dataset and used as "reference artefact" channels (Croft and Barry, 2000; Parra et al., 2005; Pedroni et al., 2019). In this thesis, the signals recorded at FP1, Fz and FP2 sites were subtracted from the other channels, proportionally to their contribution to each channel. Therefore, for example, for a trial of N samples acquired with m electrodes, being EOG $[N \times 3]$ the matrix of reference artefact channels and EEG_r $[N \times ch_r]$ the matrix of the remaining channels ($ch_r = m - 3$), the artefact-free EEG_{clean} matrix $[N \times ch_r]$ was obtained as:

$$EEG_{clean} = EEG_r - EOG * (\frac{EOG}{EEG_r})$$

- Noisy channels were identified in a semi-automatic fashion as well: channels whose standard deviation (SD) exceeded the average SD (calculated across all ch_r) by a factor of 1.7 were interpolated. Specifically, the identified noisy channels were replaced by the average of the EEG signals from the neighbouring channels - defined as those sensors that distanced less than 5 cm- (Hassan and Wendling, 2018). This thresholding value was selected after visual inspection of the trials

confirmed that it led to the rejection of those channels exceeding the physiological range of ±80 μV (Hassan and Wendling, 2018).

- The remaining ch_r channels were then re-referenced to the common average, to further increase the signal-to-noise ratio (SNR) for coherence analyses (Mima and Hallett, 1999; Snyder et al., 2015).

The frequency content of the preprocessed EEG signals was then analysed in Matlab ®R2019a (The Mathworks, Inc., Natick, MA). The power spectral density (PSD) was estimated with Welch's averaged periodogram (Welch, 1967), using Hamming windows of one second overlapping by 75%. According to this method, the PSD is estimated for every window and the final PSD is obtained by averaging across windows

3.3 Spectral Analyses, Coherence and Graph Theory

At the basis of EEG and EMG signal processing is the analysis of their frequency content, which can be referred to as "spectral analysis". This procedure corresponds to decompose the original time-series into different sine waves that, if summed together, can reconstruct it (Figure 3.3 d.1 and Figure 3.3 d.2). The extrapolation of these waves –which differ in frequency, amplitude and phase- coincide with the calculation of the Fourier transform of the time-series. In detail, the dot product is calculated between the signal and the sine waves of different frequencies and reflects the similarity between the signal and the sine wave, for every frequency. To calculate the dot product of two vectors a and b of length N each element of a is multiplied by the corresponding element of b and then all points are summed:

$$dot\_product = \sum_{i=1}^{N} a_i b_i$$

Let us consider a time-series x; the Fourier coefficient (X_f) of x for a specific frequency f is given by the dot product of x and the sine wave $e^{\frac{-i2\pi f(k-1)}{N}}$:

$$X_f = \sum_{k=1}^{N} x_k e^{\frac{-i2\pi f(k-1)}{N}}$$

where N are the data points of x. If x was acquired with a sampling frequency Fs, the spectrum can be computed for a maximum of $\frac{Fs}{2}$ frequencies, according to the Nyquist theorem. Once X_f are calculated, the "power spectrum" or "power spectral density" of the signal is obtained by plotting the power (squared value of the modulus of the Fourier coefficient) versus the frequency components (Figure 3.3), and reflects the extent to which the specific sine wave contributes to the original signal (Cohen, 2014).

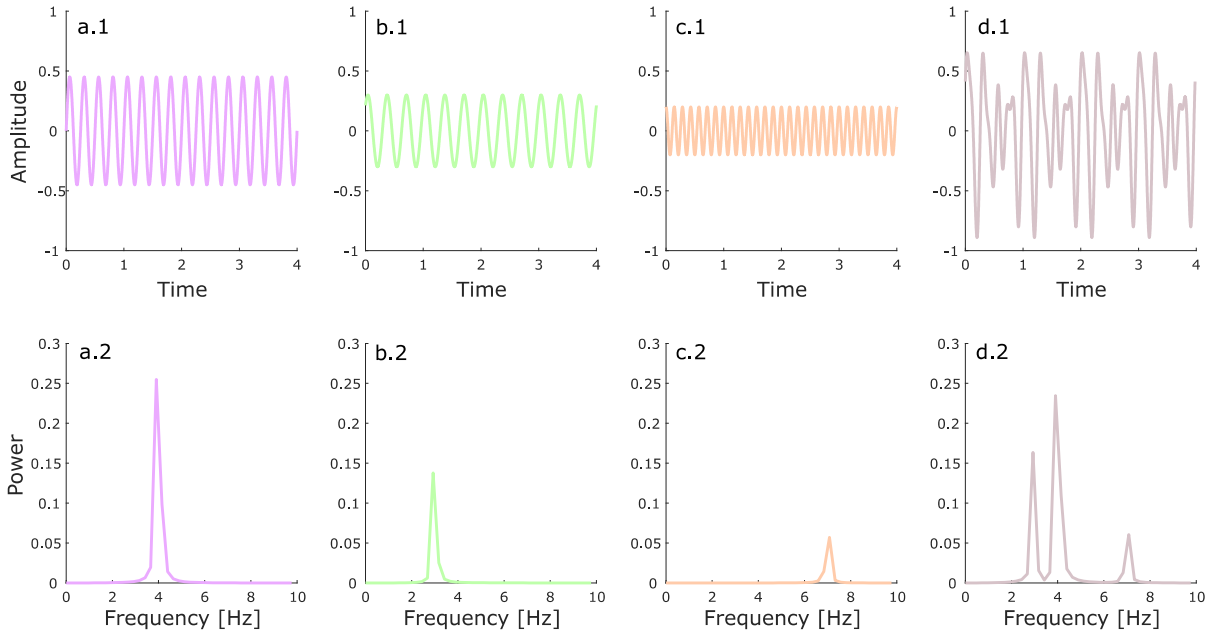

Figure 3. 3: Power spectra of sine waves

Plots of sine waves (top row) and their power spectra (bottom row). a), b) and c) are sine waves characterised by different frequencies and amplitudes; d) is the sine wave given by the sum of the others.

Spectral analyses were performed in this thesis to investigate the extent to which the frequency and phase contents of two signals were similar to each other. *Magnitude-squared coherence* was then selected as a measure of similarity between two time-series x and y and was obtained as following:

$$C_{xy}(f) = \frac{|P_{xy}(f)|^2}{P_{xx}(f)P_{yy}(f)}$$

where P_{xx} is the auto-spectrum of x and P_{xy} is the cross-spectrum obtained by Fourier transforming the cross-correlation of x with y. Practically, while the numerator depends on the phase difference between the two signals –modulated by the amplitude of the signals themselves and averaged over time- the denominator serves as a normalisation factor. The latter results in magnitude-squared coherence values ranging between 0 and 1, indicating *absence of* or *complete correlation* between the two signals, respectively (Cohen, 2014). In this thesis, CMC was calculated between sEMG and EEG signals to quantify the frequency association between neural and muscular signals: details on the permutation test used to assess the statistical significance of the results are given in paragraph 3.5.1 (J. Liu et al., 2019; Mima and Hallet, 1999). Intermuscular coherence (IMC) was instead calculated between sEMG signals recorded from different muscles to assess the common neural drive that is believe to play an important role in motor control facilitation via synergies formation (Bernstein, 1967; Farmer, 1998; Turvey, 1990). State-of-the-art connectivity analyses were used to investigate muscle synchronisation. IMC series were used as the connectivity measure between two muscles and the significance of the network metrics yielded from the analyses were assessed via mean of non-parametric statistics (Cohen, 2014).

In the past decades, network science has been widely used to reflect how different brain regions interact with each other. In order to define and analyse the organisational properties of a network, graph theory turned out to be a powerful framework since 1999 (Biggs and Lloyd, 1999). A graph simply is the mathematical representation of a network as it is made of nodes (vertices) interconnected with each other by edges. Similarly, a network can be represented by a connectivity matrix $[N \times N]$, where the N rows (and columns) represent the nodes and the $N \times N$ matrix elements represent the edges (Cohen, 2014). While matrixes better represent large networks, graphs contain information about the relative location of the nodes and are usually easier to interpret: in this thesis, both visualisation methods are provided

for completeness. Networks can be weighted or binary and directed or undirected. In weighted networks, the coupling strength (edges) between the N nodes are on a continuous range from the strongest connection (highest edge value) to the weakest one (lowest edge value). In a binary network, edges can be either 1 –existent connection- or 0 –inexistent connection. In directed networks, edges yield information about not only how strong the connection is between two nodes, but also in which direction the interaction evolves. For undirected networks instead, this information is not available and the connectivity matrixes are therefore symmetric. In regard of the connectivity measures usually used on neural data, both phase-based (i.e. phase-locking value) and amplitude-based (i.e. linear correlation coefficient) measures, as well as spectral coherence are used to reflect a statistical dependency between brain regions. On EMG dataset instead, intermuscular coherence is the one used to reflect the common neural input to different muscles (Boonstra et al., 2015). In EMG analyses, vertices corresponds to the muscles (the electrodes recording the activity of specific muscles) and edges corresponds to the intermuscular coherence estimated between them.

Weighted undirected connectivity matrixes were obtained for different frequency bands via non-negative matrix factorization (NNMF). Generically, NNMF is used to decompose a matrix V $[n \times m]$ into two matrixes W $[n \times k]$ and H $[k \times m]$ yielding the k basis components and their corresponding weights, respectively:

$$V \sim WH$$

To put it simply, let us assume that V is a matrix of dimensions $n \times m$ where the m columns of V represent the features of the dataset (coherence spectra) and n represents the sample length (frequency bin). Each column v (coherence spectra) can then be approximated by the linear combination of the columns of W (frequency components) weighted by their corresponding elements of H (coupling strengths) (Lee and Seung, 1999). The latter can be rewritten in the following form, where v and h are the columns of V and H:

$$v = Wh$$

For the purpose of this thesis, the IMC spectra of every participants under every condition (totalling m spectra) were gathered in the same matrix V and decomposed into k frequency components (columns of W) and their corresponding coupling strengths (elements of H). For every frequency component, H represented the weighted undirected connectivity matrix reflecting the similarity between the frequency content of two firing muscles. Although connectivity matrixes are usually thresholded for neural data, no threshold was applied in this thesis –other than for visualisation purposes- because of the small size (10x10) of the connectivity matrixes themselves (Boonstra et al., 2015).

To quantify the organisation of the network, different network metrics were employed: strength (STR), clustering coefficient (CC), betweenness centrality (BC) and participation coefficient (PC). These were chosen as they reflect both the segregation and the integration of the network (see Figure 3.4).

- The strength of a node A is calculated by adding the weights of the connections (edges) directly linked to A. It reflects the importance of A with respect to the other nodes (Barrat et al., 2004).

- The clustering coefficient of a node A is given by the ratio of the number of nodes that are connected to A that are also connected to each other and the number of nodes that are connected to A. It reflects the segregation of the network and the level of local specialisation as it depends on the density of the connections created by A's neighbours (Bullmore and Sporns, 2009; Watts and Strogatz, 1998).

- The participation coefficient of A reflects how much A is connected to nodes belonging to other modules. In other words, it provides information about how much information are shared and distributed across modules. Modules are community of nodes with high local specialisation (internal connectivity) but low integration (external connectivity) (Guimerà and Nunes Amaral, 2005).

- The betweenness centrality of A is given by the proportion of all the shortest paths that contain A. A high value of BC indicates that the node is well integrated in the network (Sporns et al., 2007; Zuo et al., 2012).

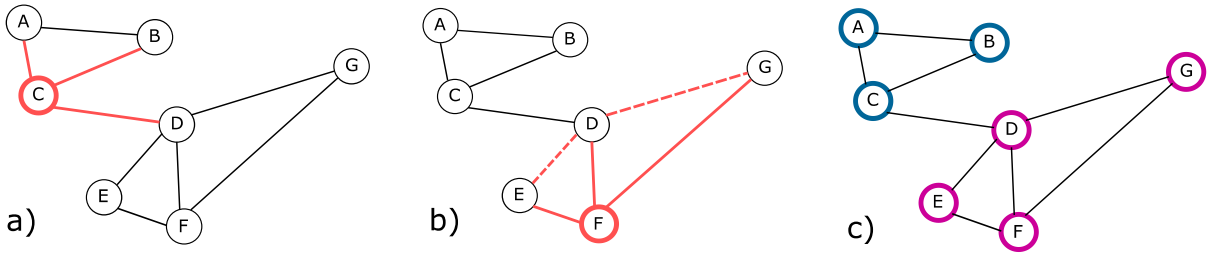

Figure 3. 4: Graph metrics

A network made of seven nodes is displayed. a) The connection of node C with other nodes are highlighted and its STR is 3. b) The CC of node F is 2/3: the denominator is the number of nodes connected to F (continuous line) and the numerator is the number of those nodes connected to F (E, D and G) that are also connected to each other (dashed line). c) Different colours are given to nodes belonging to different modules: C and D (connector hubs) have high PC as they are connected to nodes of different modules; F and A (provincial hubs) have low PC as they are connected only to nodes of their own module.

3.4 COP

To evaluate the ability of a person to balance, dynamic and static posturography is employed as a non-invasive recording technique. The first one consists of assessing balance in response to a perturbation, while the latter characterises the balance performance during quiet standing. For the purpose of this thesis, static posturography was carried out by asking the participants to stand on a force platform that, via mean of force and movement transducers, detects the oscillations of the body and digitise them in what is known as “centre of pressure (COP) trajectories”. The COP motion reflects the motion of the vertical reaction force vector and is usually analysed in the anterior-posterior (AP)–or sagittal- plane and in the medial-lateral (ML) –or frontal- one. To characterise postural steadiness, two metrics were obtained from the COP time-series: the COP mean displacement (MD) and the COP mean velocity (MV). The first one was chosen as it reflects the effectiveness of postural control; the second one was chosen

because of its association with the regulatory activity put into place during postural control (Kim et al., 2012; Prieto et al., 1996). The COP time-series were first de-meaned and low pass filtered at 12.5 Hz (Donker et al., 2007) as 95% of the power of the time-series is below 5 Hz (Maurer and Peterka, 2005). Then, the COP metrics were obtained for both the AP and ML direction. The formula shows how to calculate the mean COP displacement in the ML direction, where N is the number of time points in COP time-series ML:

$$MD_{ML} = \frac{1}{N}\sum_{n=1}^{N} |ML(n)|$$

The mean COP velocity was calculated as the ratio between the total length of the path –given by adding the distances between consecutive time points- and the duration of the recording in seconds (T); the following formula is the one used to calculate the mean COP velocity in the ML direction:

$$MV_{ML} = \frac{\sum_{n=1}^{N-1} |ML(n+1) - ML(n)|}{T}$$

Since anthropometric factors are correlated with postural outcomes (Bryant et al., 2005), the COP displacement and velocity were normalised by participant's height, weight and age by applying a simultaneous detrending normalisation (Chiari et al., 2002; O'Malley, 1996). The COP parameters were regressed against the participants' height and the mean of the original values was added to the regression residuals (Figure 3.5). The latter were then iteratively regressed against the participants' weight and age and the final normalised residuals were used for statistical analysis.

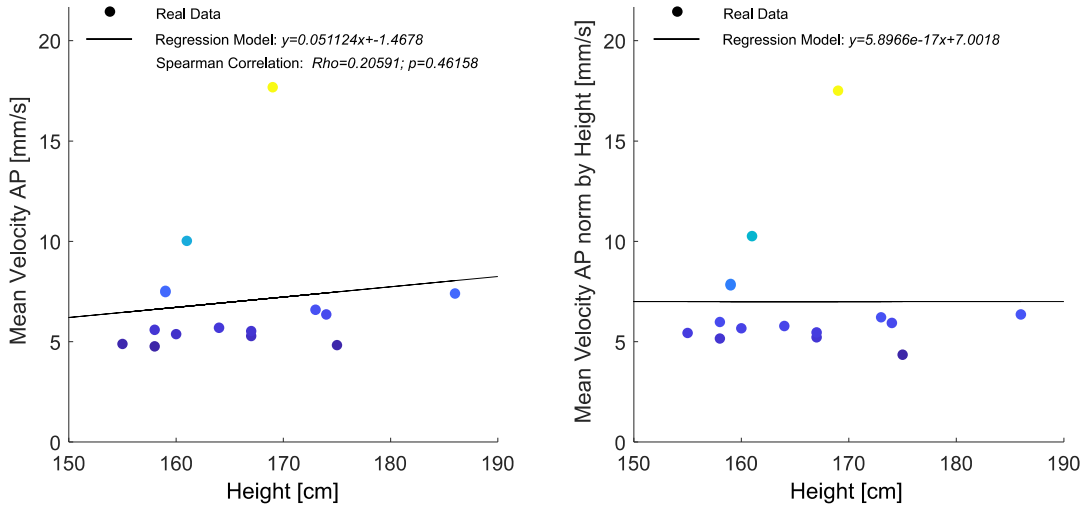

Figure 3. 5: Simultaneous detrending normalisation

Dependency of the AP COP mean velocity on participants' anthropometrics. Left: MV_{AP} collinearity with subjects' height. Right: linear fit of the MV_{AP} after its normalisation vs height. The procedure was repeated iteratively on the normalised MV_{AP} to remove any trend linked to subjects' mass and age.

3.4.1 Sample Entropy and Complexity Index

To gain an insight on the extent of postural control employed by participants after the WBVs, the complexity index (CI) was obtained from the COP time-series as the sum of sample entropy (SE) calculated over different time scale. The SE of a vector provides insights into the regularity of the data in the vector and is calculated as follows:

$$SE(m,r,N) = -ln\frac{\emptyset^{m+1}(r)}{\emptyset^{m}(r)}$$

where N is the vector length, m is the distance between the compared points of the time-series, r is the similarity radius and $\emptyset$ is the probability for two points that are m distance apart to be within the distance r. Computing the SE of a time-series over different time scales yields what is known as "multiscale sample entropy" (MSE) which provides insight not only on the *predictability* of the time series, but also on its *complexity* (Costa et al., 2005). Practically, MSE is obtained by coarse graining the vector with different time windows and computing the SE over the new coarse-grinded time-series. In other words, when a time scale of 2 is selected,

the first 2 data points of the original vector are averaged and the result constitutes the first time point of the new vector; the second 2 data points are averaged and placed in the second position of the new time-series and so on (Figure 3.6). The repetition of this procedure for different windows leads to the formation of new time-series, from which a SE value is calculated. The sum of the SEs over the new coarse-grinded vectors gives the CI, which illuminates about the automaticity of postural control as lower CIs were interpreted as a reflection of less efficient postural control mechanisms. As a minimum number of data points is required to ensure reliable SE probabilities, a sample number of 600 was selected for the longest time scale in the analysis presented in this thesis (Busa and van Emmerik, 2016).

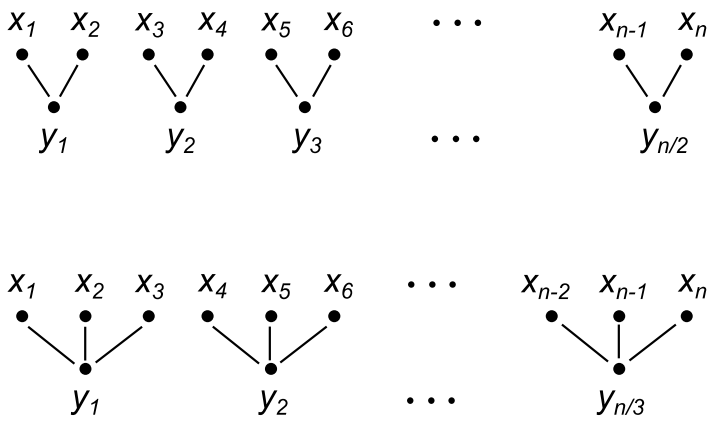

Figure 3. 6: Coarse-graining procedure for MSE calculation

The original time-series x, of length n, is coarse-grinded with a time scale of 2 (top row) and a time scale of 3 (bottom row). The resulting time-series y are of length $n/2$ and $n/3$, respectively and are used for SE calculation.

3.5 Statistical Analysis

When possible, non-parametrical tests were preferred to parametrical ones as no assumptions are needed on the probability distribution of the data and therefore better apply to real physiological data that rarely satisfy the normality assumption. Comparisons of multidimensional data –such as soft tissue accelerations (time domain) and CMC estimates (frequency and channel domain)- were performed with the non-parametric cluster-based

permutation test (Maris and Oostenveld, 2007). Differently, comparisons of summary single values -such as EMG RMS, beta band power averaged across channels and COP measures- between conditions were performed with analyses of variance (ANOVA) (Field, 2013) and the non-parametrical version of the paired-sample Student's t-test, namely the Wilcoxon test. Since a single-group repeated-measures design was used in both studies, dependent-sample permutation test, repeated-measures ANOVAs and Wilcoxon signed-rank tests were specifically selected to test differences between groups (metrics calculated under different conditions) whose samples were obtained from the same participants. Although priority was given to non-parametrical statistics, ANOVAs were employed to assess the significance of the sEMG results of the first study as a corresponding non-parametric test capable of testing for interactions is not available.

3.5.1 Cluster-based permutation test

Cluster analyses were chosen to analyse time and frequency series not only because of their robustness to unknown data probability distributions, but also because they allow the inclusion of physiologically plausible constraints to the data. Moreover, they provide a solution to the multiple comparison problem (MCP) without diminishing the statistical power of the test as much as the Bonferroni correction does. The MCP arises when several tests are run over time points, frequency bins or multiple sensors and the probability of rejecting the null hypothesis (declaring a significant difference between experimental conditions) under the condition of no significant difference increases: in other words, the more statistical tests are run, the bigger the probability of committing a false positive. The cluster-based permutation test does in fact address the MCP by clustering together samples that are adjacent in time (frequency, space), well justified by the neurobiological and physiological assumption that an effect observed at a specific time point (frequency bin, sensor) is likely to persist even at the time point (frequency bin, special location) immediately before and immediately after.

The cluster-based permutation test builds on two key methods which are: 1) the formation of clusters of samples that are continuous along one (or more) dimension of the data,

2) the non-parametric testing of two datasets via mean of permutation tests. In the following paragraphs, the time domain will be considered, but it might as well be the frequency and the spatial one. Therefore, all instances where “time point” occurs could be replaced by “frequency bin” or “sensor”.

The first step is to calculate the so-called *cluster-based test statistic* via the following steps:

1. To test whether two conditions are significantly different from each other at a specific time point, a statistical test (t-test) is run between the two conditions at that specific time point. This procedure is repeated for all time points and results in a statistic (t-statistic) that evolves along time.

2. A threshold (T) is set for the t-statistic obtained for every time point and those t-statistics whose value is above T are clustered together. In this thesis, t-values were thresholded at the 97.5-th quartile as a T=0.05 and a two-sided t-test was chosen to analyse our data.

3. For all the newly formed clusters, the t-statistics are summed together and the cluster with the biggest value is selected as *cluster-based test statistic*, which is used to evaluate the difference between the experimental conditions. We will refer to the cluster-based test statistic of the original groups as t_0.

After the cluster-based statistic is calculated for the original data, its statistical significance is calculated via mean of a non-parametrical *permutation test*:

4. For each subject, randomly draw one of the two trials and place it into subset 1. Place the remaining trials in subset 2, so that the new two subsets have the same number of trials of the original conditions. The outcome of this procedure is the *random partition*.

5. Calculate the cluster-based test statistic on this new subsets as explained in the points above (1-3).

6. Repeat steps 4 and 5 N times (usually N>1000) and use the cluster-based test statistic to build a histogram.

7. Calculate the ration between the random partitions that gave a statistic larger than the observed one (t_0) and the total random partitions: this proportion is called the Monte Carlo estimate and represents the p-value of t_0. In other words, if less than 5% of the random partitions (assuming significance at .05) resulted in a larger cluster-based test statistic than t_0, than the null hypothesis can be rejected and a significant difference between conditions in the cluster can be inferred (Figure 3.7).

A more detailed description of the cluster-based permutation test and its implementation in Fieldtrip can be found in the literature (Maris and Oostenveld, 2007) and (Oostenveld et al., 2011), respectively.

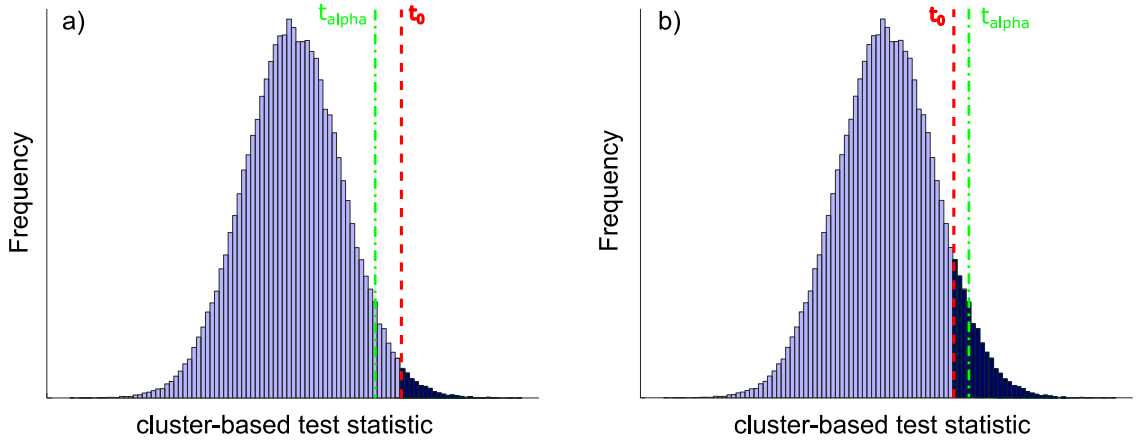

Figure 3. 7: Conditions for H_0 rejection or acceptance

Illustration of the cluster-based test statistic distribution obtained for 1000 permutations. The cluster-based test statistic obtained from the original data (t_0) is depicted by the red vertical dashed line; the cluster-based statistic corresponding to the significance level of 0.05 (t_{alpha}) is depicted by the green vertical dashed line. a) When the proportion of cluster-based test statistics that are larger than t_0 is less than 5%, H_0 is rejected and a statistical difference can be declared. b) If t_0 is smaller than more than 5% of the test statistics, the null hypothesis is instead accepted and no statistical difference is declared.

3.5.2 ANOVA

The term “Analysis of Variance” (ANOVA) refers to those statistical models developed by Ronald Fisher to compare the means of three or more groups. ANOVA represents a generalisation of the Student’s t-test as instead of analysing the differences between two groups, it allows for the comparisons of three or more. However, ANOVA is an omnibus test, which means that it does not provide information on where the differences lie, but only that at least two groups differ significantly from each other. Post hoc tests are to be run afterwards if group differences are to be tested. Although this might seem a redundant procedure –and the debate on whether to skip the ANOVA and jump directly to post hoc tests is currently open (Howell, 2010; Wuensch, 2012)- it is common practice to do so as it well controls the rate of Type I errors, reducing the probability of declaring a significant difference where there is none. A general overview of the simplest version of ANOVAs, one-way ANOVA, will be given and details of the test employed in this thesis, the two-way ANOVA, will be provided.

In order to conduct an analysis of variance, some assumptions are to be met and those that are common to most ANOVA tests are: 1) the dataset should be free from significant outliers; 2) the dependent variable (DV) should be approximately normally distributed for each level of the independent variable (IV) (Field, 2013). Although the assumption of normality is important for ANOVAs, the tests are quite robust and as long as the probability distributions of the data are similarly skewed across levels, the test can be carried out. If this condition is not met, a logarithmic transformation of the data is usually applied to reach a more normal distribution.

If the assumptions are met, the F-statistic is calculated, which is simply a ratio of variances. Specifically, F is calculated as follows:

$$F = \frac{variation\ between\ samples}{variation\ within\ samples}$$

The numerator corresponds to how scattered are the group means from the overall group mean. To put it differently, the further apart are the group means, the more likely it is for the groups to belong to different populations: in fact, the bigger the variability between groups, the bigger F. The denominator corresponds to the variability of the data within each group, or in other words, “how scattered are the samples from the group mean”. If there is low variability within groups, it means that –in each group- data are close to their mean, and F value increases (Figure 3.8).

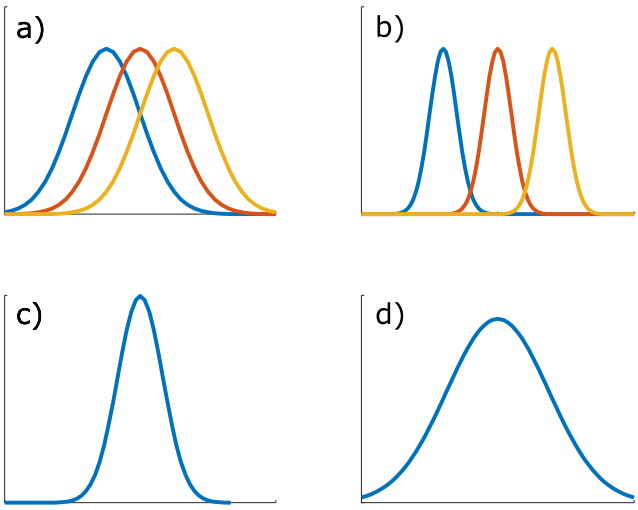

Figure 3. 8: Normal distributions

Normal probability distributions with different mean and standard deviations are here illustrated for the purpose of visualising the following: a) low between-group variability; b) high between group variability; c) low within-group variability; d) high within-group variability.

Once the F-statistic is calculated, its significance is estimated. In order to do that, the F-distribution, which depends on the degree of freedom of the numerator and the denominator, is used to calculate the probability of observing an F-value equal or bigger than the one observed from the data. If this probability –otherwise called p-value- is smaller than 5% (as alpha is usually set to .05), the null hypothesis is rejected and a significant difference between *at least* two of the groups is declared. Post hoc tests can then be run in the form of pairwise comparisons to test where the difference lies.

To test the effect of stimulation frequency and subject's posture (IVs) on sEMG RMS of muscles in the lower leg (DVs) a two-way repeated measures ANOVA was used. Differently from the one-way ANOVA, here the independent variables are two, each of which with its own levels [frequency (4) x posture (2)]. Therefore, it is used to test not only the effect of the IVs – or within-subject factors- but also the interactions between these, as it tests whether the value of one factor affects the effect of the other factor on the DV. For reporting results, the adopted working pipeline was set to be as the following:

- If significant interactions resulted from the two-way ANOVA, post hoc tests were run in the form of paired t-test and one-way ANOVA to analyse the simple main effect of subjects' posture and frequency, respectively (Field, 2013);

- If no significant interaction was found, the main effect of within factors was reported, if significant (Field, 2013).

The MCP was addressed by applying a Bonferroni correction, which is incorporated in SPSS 23.0 (IBM Corp., Armonk, NY, USA): the significance level, alpha, was simply divided by the number of comparisons carried out, including those performed for the analyses of variances and those performed as post hoc tests.

3.5.3 Wilcoxon test

The Wilcoxon signed-rank test was introduced by Frank Wilcoxon (Wilcoxon, 1945). It was selected for this thesis as it represents the non-parametric version of the dependent sample Student's t-test, which is used to compare two groups of variables that are "paired" or, in other words, are obtained from the same subject. While the validity of the t-test depends on the probability distribution of the data –which has to resemble normality- the Wilcoxon signed-rank test does not have such requirement. More simply, the DV should be continuous, the paired values have to be independent from each other and it has to be possible to refer to them as "greater or smaller of" (Lowry, 2015). The steps on which the Wilcoxon signed-rank test builds

on are summarised in the following lines for a comparison run between two groups (condition A and condition B), each of which is made of N observations:

- For every pair, the absolute value of the difference between the groups is calculated: $|x_A - x_B|$.
- For every pair, the sign of the paired difference is calculated: $sign(x_A - x_B)$.
- Those differences that equal zero are removed from the dataset and the dimension is reduced to N_r.
- For every pair, the absolute value of the paired differences are ranked: the smaller absolute value is ranked 1 and those absolute differences that are equal receive the average value of the ranks they span;
- The W-statistic is calculated as the sum of the signed ranks, where R_i is the rank of the ith pair: $W = \sum_{i=1}^{N_r}[sgn(x_A - x_B) * R_i]$.
- The W statistic is compared with a critical value that depends on the sample size: if the absolute value of W results bigger than the critical value, the null hypothesis can be rejected and a significant difference between the two groups declared (Lowry, 2015).

4. Customisation of WBV stimulation for calf muscles

4.1 Introduction

Whole body vibration (WBV) refers to the use of mechanical stimulation, in the form of vibratory oscillations extended to the whole body, to elicit neuromuscular responses in multiple muscle groups. Vibrations are generally delivered through lower limbs via the use of platforms on which subjects stand. Training and rehabilitation programmes utilising this modality often include physical exercise performed on such platforms (Dolny and Reyes, 2008). This approach has become increasingly popular as it evokes a large muscle response and, more importantly, it elicits muscles activity through physiological pathways (Granit and Steg, 1956), improving overall motor performance while enhancing strength and flexibility (Alam et al., 2018; Delecluse et al., 2003; Osawa et al., 2013; Rittweger, 2010; Saquetto et al., 2015; Wyon et al., 2010).

The mechanism believed to be responsible for such outcomes, known as tonic vibration reflex (TVR), has been proven to explain the increased and synchronised motor-unit (MU) firing rates recorded during locally-applied (i.e., focal) vibrations (Burke et al., 1976a; Burke and Schiller, 1976). Indeed, when vibrations are applied directly to tendons or muscle bellies, muscle fibres length changes activating a reflex response from muscle spindles. This translates in an increased MU firing rates phased-locked specifically to the vibratory cycle, i.e. the TVR (Burke and Schiller, 1976; Hagbarth et al., 1976; Hirayama et al., 1974; Homma et al., 1972; Martin and Park, 1997; Person and Kozhina, 1992, 1989).

In WBV, instead, vibrations are not applied locally, but transferred to the target muscles via the kinematic chain determined by the body posture (Cardinale and Lim, 2003a; Pollock et al., 2012; Ritzmann et al., 2010); this provides similar muscular outcomes with respect to focal stimulations as well as additional systemic postural responses, providing better flexibility and applicability to large exercise programmes (Rittweger, 2010). Specifically, when the whole body is exposed to mechanical shocks (such as vibrations), absorption strategies act to dampen oscillations and dissipate energy through modulation of both muscle activity and joint kinematics, over which the body has prompt control (Gross and Nelson, 1988; Lafortune et al.,

1996). Moreover, in WBV, somatosensory feedback pathways are enhanced by reflexes arising from mechanoreceptors in the lower limbs, with significant implications for motor coordination and postural control during quiet stance (Fitzpatrick et al., 1992). Human ability to keep an upright stance, in fact, depends on the integration of somatosensory, vestibular and visual feedbacks (Horak et al., 1997; Peterka, 2002) that translates in specific muscles activation patterns and body sway about the ankle joint (Winter, 1995). The ankle strategy - actuated by modulation of plantar- and dorsi- flexor muscles - is indeed considered the primary approach to reposition the centre of gravity either during quiet stance or in response to external perturbations (Gatev et al., 1999; Winter, 1995). Cross-correlation analyses between muscle activity and centre of pressure further confirm how leg muscles (with particular focus on the Gastrocnemius Lateralis and Soleus) play a central role in postural control dynamics (Fitzpatrick et al., 1992; Gatev et al., 1999). Therefore, it could be inferred that, if selectively targeting lower leg muscles, WBV training may also improve coordination and balance of different subpopulations.

Promising results of WBV training are reported in the literature (Bautmans et al., 2005; Bogaerts et al., 2007; Lam et al., 2012; Mahieu et al., 2006; Ritzmann et al., 2014; Rogan et al., 2011; Torvinen et al., 2002b; Turbanski et al., 2005; van Nes et al., 2004), but a few discording results still jeopardise the systematic use of such approach in training and rehabilitation practices (Torvinen et al., 2003, 2002c; Yang et al., 2015). Conflicting results might be related to the high amount of variability in WBV settings (e.g., stimulation frequency, posture, stimulation amplitude, stimulation duration etc.) used throughout different studies, while still lacking standardised training protocols. Among the most investigated variables, stimulation frequency and subject posture have relevant impact in eliciting an efficient muscle tuning response to WBV (Lienhard et al., 2014a; Pollock et al., 2010; Ritzmann et al., 2013).

Previous findings suggest that muscles contract to reduce the soft-tissue resonance, especially when the stimulation frequency, ω_a, is close to their natural one (Wakeling et al., 2003, 2002a; Wakeling and Nigg, 2001a). This process, known as muscle tuning, is

perpetrated by muscles to minimise the soft-tissue vibrations (Wakeling and Nigg, 2001b)(Wakeling et al., 2001) and has been recently proposed as one of the possible body reactions to WBV (Abercromby et al., 2007a, 2007b). Therefore, a careful selection of stimulation frequency, ω_a, to match the resonant one, ω_0, seems the key element to maximise muscle responses to WBVs (Cesarelli et al., 2010). Generally, the natural frequency of a system depends on its mass, *m*, and stiffness, *k,* according to the equation $\omega_0=\sqrt{k/m}$ (Rittweger, 2010); being the mass of a muscle constant, modulating muscle stiffness via a change in subject posture results in a change in the system's natural frequency. This seems to explain conflicting results in the literature when combined dynamic and static exercises (holding a fixed posture e.g. hack squat) are performed on platforms (Bosco et al., 1999; Fagnani et al., 2006) (Wyon et al., 2010). During dynamic exercises on a vibrating platform the body kinematic chain involved in the transmission of the mechanical stimulus changes continuously, making extremely difficult to define the stimulus delivered at the target muscle group. However, during static exercises on a platform, the energy dissipated through joint kinematics is constant and muscle contraction is the major mechanism tuned to dampen vibration. Indeed, Abercromby et al. confirmed that static exercises during WBV enhance higher muscle response than performing dynamic exercises, during which muscles contract in an eccentric and concentric fashion (Abercromby et al., 2007a).

With the present study, the authors want to provide a comprehensive analysis of the effects of WBV on lower leg muscles. In particular, this chapter reports the findings on muscle activity and soft-tissue mechanical dynamics and their link to both vibration frequency and subject posture, when WBV is delivered via a side alternating platform. Suggestions are presented on the appropriate approach to use for training professionals and practitioners, with consideration given to potential implications for postural control enhancement training.

4.2 Materials and Methods

4.2.1 Subjects and experimental design

Seventeen females and eight males (age: 24.8 ± 3.4 years; height: 172.0 ± 8.6 cm; mass: 64.6 ± 10.5 kg) volunteered in the study after providing written consent. To evaluate muscle activation and displacement during WBV, surface electromyography (sEMG) signals and accelerations were collected from three lower limb muscles during two static exercises performed in static conditions (without WBV – hereafter called baseline activity) and when different vibration frequencies were delivered. The protocol of the study received approval by the Ethics Committee of the School of Life and Health Sciences at Aston University

Pairs of Ag/AgCl surface electrodes (Arbo Solid Gel, KendallTM, CovidienTM 30 mm x 24 mm, centre-to-centre distance 24 mm) were placed over the gastrocnemius lateralis (GL), tibialis anterior (TA) and soleus (SOL) muscles of the dominant leg accordingly to SENIAM guidelines (Hermens et al., 2000) (pink markers in Figure 4.1). The reference electrode was placed on the styloid process of the right ulna. The sEMG data were sampled at 1000 Hz (PocketEMG, BTS Bioengineering, Milano, Italy) and sent wirelessly to a laptop via the Myolab software, version 2.12.129.0 (BTS Bioengineering, Milano, Italy).

Accelerations were measured via tri-axial accelerometers (AX3, Axivity Ltd, Newcastle, United Kingdom; range = ±16g, sampling frequency = 1600 Hz) placed on GL, TA and SOL muscle bellies, next to the EMG electrodes (yellow markers in Figure 4.1). The accelerometers were aligned with the x-axis parallel to the long axis of the leg segment, the z-axis normal to the skin surface and the y-axis perpendicular to the x-z plane. Accelerations were recorded using the open source software OMGUI developed by Newcastle University (“AX3 OMGUI Configuration and Analysis Tool, v38, GitHub,” 2015).

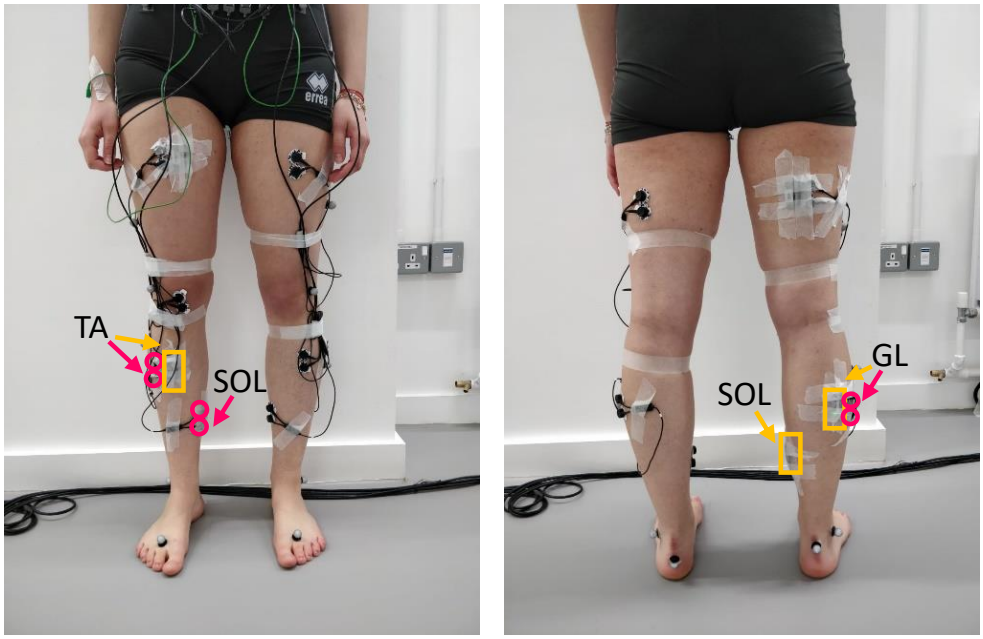

Figure 4. 1: Sensor placement

Pairs of bipolar electrodes were placed in correspondence of TA, GL and SOL muscle bellies, according to SENIAM guidelines (Hermens et al., 2000) and are highlighted with the pink markers. Tri-axial accelerometers were secured next to the sEMG electrodes and are here highlighted with the yellow markers. 4.2.2 Whole Body Vibration stimulation protocol

Subjects underwent the WBVs barefoot. The WBVs were delivered via a side-alternating platform (Galileo® Med, Novotec GmbH, Pforzheim, Germany), as it was shown to evoke bigger neuromuscular activations than synchronous vibrating ones (Ritzmann et al., 2013): a peak-to-peak amplitude of 4 mm was used. For each subject, ten trials were collected to evaluate the effect of different stimulation frequencies -0, 15, 20, 25, 30 Hz- and two subject postures: hack squat (HS) and forefeet (FF). During HS trials, subjects were asked to keep their knees flexed at about 70°, with 0° corresponding to the knee fully extended, and a goniometer was used to check the angle at the beginning of each HS trial (see Figure 4.2, right). During FF trials, subjects were asked to keep their heels in contact with a parallelepiped-shaped foam (30 x 4 x 3 cm) glued on the platform, to ensure their heels were 3 cm off the ground (see Figure 4.2, left).

Trials were administered in a random order with a one-minute break between consecutive trials. Hereafter, trials with vibratory stimulation are referred to as “the WBV trials”

(HS_{15} HS_{20} HS_{25} HS_{30} FF_{15} FF_{20} FF_{25} FF_{30}) and the others as "the baseline trials" (HS_0 and FF_0). WBV trials consisted of 40 seconds: recordings contained 10 seconds with no vibration (WBV_{off} portion), once the subject acquired the prescribed posture, followed by 30 seconds of WBVs at the prescribed frequency (WBV_{on} portion). Baseline trials were used to assess the relevant subject-specific EMG baseline activity (HS_0 and FF_0) over a 30 s period.

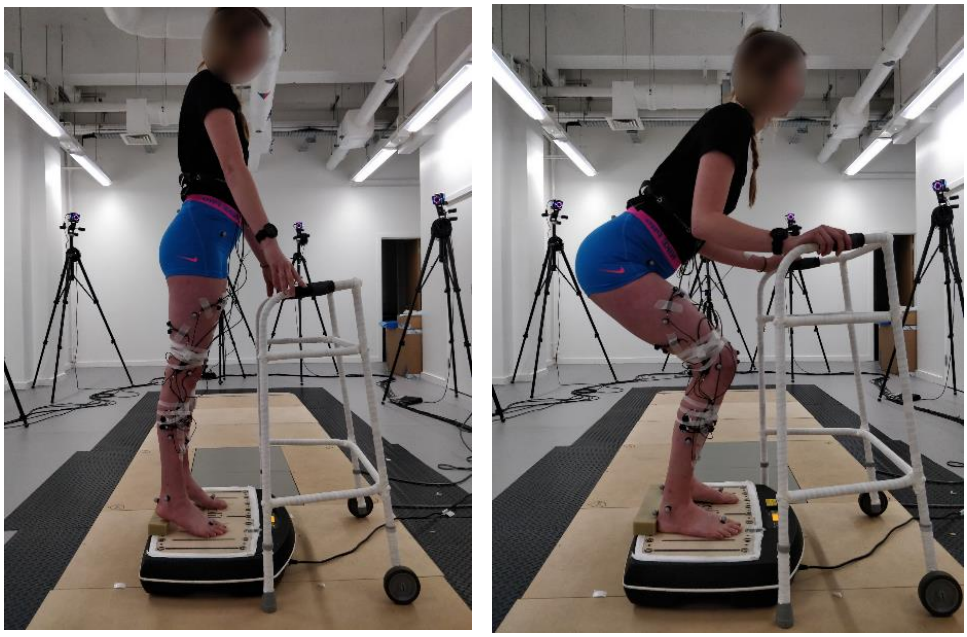

Figure 4. 2: View of study set-up

Participants were asked to hold either a forefeet posture (left) or a hack squat one (right) during the WBV stimulation. The motion capture system is visible in the background as well as the force platform, placed on the left of the WBV one, on which the participant is standing.

Twelve Vicon Vero v2.2 optical cameras (Vicon Nexus, Vicon Motion Systems Limited, Oxford, UK) were used to measure subjects posture and assure consistency throughout the experiment (Abercromby et al., 2007a). Sixteen retroreflective markers were attached to the participant's body, according to the Plug-In-Gait Lower-Limb model. Data were sampled at 100 Hz and knee and ankle angles were obtained by extracting the kinematics in the sagittal plane using the proprietary software. Specifically, the ankle and knee angles were used to check for consistency across conditions and subjects. The first was defined as the angle between the tibia and the normal to the foot (see Figure 4.3, left) and the second one was defined as the angle between the thigh and the extension of the tibia (see Figure 4.3, right).

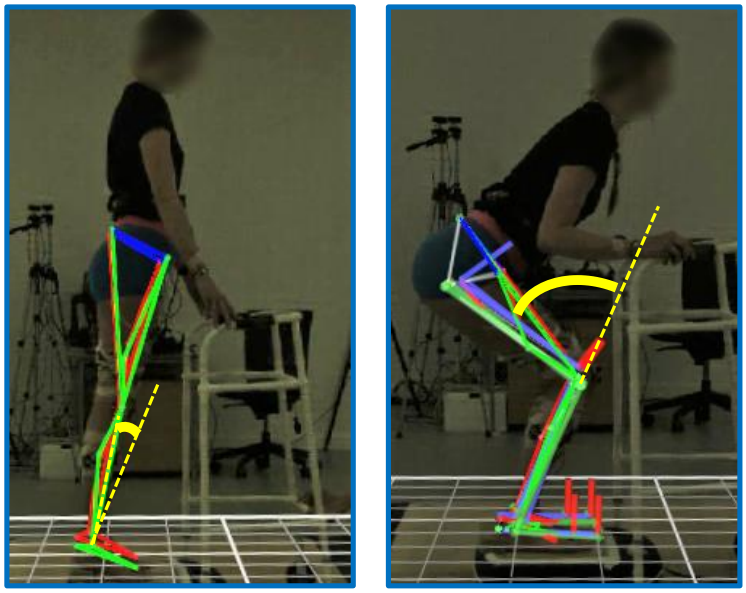

Figure 4. 3: Extraction of participant kinematics

Motion capture outputs are superimposed on the video recording of the participant. The ankle angle (left) and the knee angle (right), that are used to describe participants' posture during the WBV stimulation, are displayed in yellow.4.2.3 Data processing and features extraction

4.2.3.1 sEMG Data

To isolate the muscle activity preceding the stimulation (WBV_{off}) from the one actually induced by the vibrations (WBV_{on}), each WBV trial was split into two epochs: 10 and 30 seconds, respectively. The central portions of these signals (6 and 20 seconds, respectively) were extracted and retained for analyses. Similarly, the central 20 seconds of the baseline trials (HS_0 and FF_0) were extracted and retained for analyses. In total, ten 20 second-long epochs and eight 6 second-long epochs were analysed for each muscle and subject.

All epochs were band-pass filtered between 5 and 450 Hz with a 5th order Butterworth filter (Fratini et al., 2009c) and a mean running root mean square ($rRMS$) value was obtained from both the baseline ($RMS_{baseline}$) and the WBV_{off} epochs (RMS_{WBVoff}).

To remove motion artefacts from WBV_{off} and WBV_{on} epochs (Fratini et al., 2009a), a type II Chebyshev band-stop filter was applied at each stimulation frequency and its harmonics up to 450 Hz on the sEMG spectra. This resulted in 30, 22, 18 ad 15 stop-band filters applied

to epochs derived from WBV trials delivered at 15, 20, 25 and 30 Hz, respectively, following the calculation:

$$\#\text{filters} = round(\frac{frequency\ spectrum\ upper\ limit}{stimulation\ frequency})$$

For each WBV trial, two $rRMS$ vectors were computed on both artefact-free epochs (WBV_{off} and WBV_{on}) (Fratini et al., 2009a) and used to calculate the relevant mean RMS values: $RMS_{WBVoff\sim}$ and RMS_{WBVon}, respectively. To compare the values obtained during the different trials, a factor taking into account the proportion of power removed by the comb-notch filter was calculated (Lienhard et al., 2015):

$$Bias = \frac{RMS_{WBVoff\sim}}{RMS_{WBVoff}}$$

and was used to adjust RMS_{WBVon} values:

$$adjRMS_{WBV} = RMS_{WBVon} * \frac{1}{Bias}$$

To evaluate the WBV-induced increment of muscular activation, $RMS_{baseline}$ were subtracted from the $adjRMS_{WBV}$ obtained for the WBV trials in the respective posture. These resulting values will be hereafter referred to as the $incrementRMS_{WBV}$:

$$incrementRMS_{WBV} = adjRMS_{WBV} - RMS_{baseline}$$

In total, eight values were retained for each subject and used for statistical analysis.

4.2.3.2 Acceleration data

Baseline trials were not included in the following analyses: raw accelerations from WBV trials were analysed in Matlab ®R2019a (The Mathworks, Inc., Natick, MA). Accelerations were

band-pass filtered between 10 and 100 Hz to remove gravity components and accommodation movements, usually confined between 0 and 5 Hz (Nowak et al., 2004; Prieto et al., 1996), and to retain only vibration-induced muscle displacements, located mostly at the stimulation frequency and its superior harmonics (Fratini et al., 2009a). Filtered epochs were then double integrated to estimate local displacement along the different axes ($disp_x, disp_y, disp_z$) and the constant values introduced by each integration were removed with a 5 Hz high-pass filter. The total displacement recorded at each muscle level was estimated as:

$$DISP_{TOT}(\mathrm{t}) = \sqrt{disp_x(t)^2 + disp_y(t)^2 + disp_z(t)^2}$$

where $t = 1,2,\dots,N$, with N being the total number of samples.

To track the low-frequency mechanical muscle response to WBVs, a moving average of $DISP_{TOT}$ ($MovAvgDISP_{TOT}$) was calculated using a 250ms sliding window (Figure 4.4). To compare muscle displacement among different subjects, $MovAvgDISP_{TOT}$ vectors were time-locked to the point where a 0.1 change in the slope was detected, which will be hereafter referred to as the vibration onset. $MovAvgDISP_{TOT}$ from all participants were used for statistical analyses. Acceleration data were analysed in terms of the estimated displacement rather than accelerations themselves as the TVR and muscle tuning mechanisms –known to be those able to increase muscle response (Cardinale and Bosco, 2003; Cardinale and Wakeling, 2005)- are triggered by muscle stretch (namely, change in length) rather than changes in muscle accelerations. Moreover, as the acceleration is used to directly derive the displacement, any significant difference in the first would lead to significant differences in the latter.

To visualise the 3D displacement recorded in correspondence of muscle bellies, Lissajous figures were computed for a representative subject at two time points descriptive of muscle response to vibrations:

- t_P: a peak time-point was selected in correspondence of the maximum value of each $MovAvgDISP_{TOT}$ signal in a 2-second interval after the vibration onset;

- t_A: a common attenuation time-point among the different muscles was chosen to represent the response following the peak phase, where muscle displacement is stabilised and minimised reaching a steady-state. The time-point representing the ending of the peak ($t_{EndPeak}$) was first computed for each muscle and trial: $MovAvgDISP_{TOT}$signals were averaged across subjects and low-pass filtered at 10 Hz. A 0.5 s sliding window search was applied to identify the slope change time point ($t_{EndPeak}$), with a threshold of 0.06. Once a $t_{EndPeak}$ was identified for all muscles and conditions, t_A was defined as:

$$t_A = round(max\ (t_{EndPeak}) + \frac{1}{2} * max\ (t_{EndPeak}))$$

where $max\ (t_{EndPeak})$ is the highest peak duration observed across muscles and conditions.

To quantify the extent of the displacement attenuation at each muscle site, ATT_{DISP} was calculated for each subject as the difference between the maximum displacement recorded at that site and the steady-state one:

$$ATT_{DISP} = MovAvgDISP_{TOT}(t_P) - MovAvgDISP_{TOT}(t_A)$$

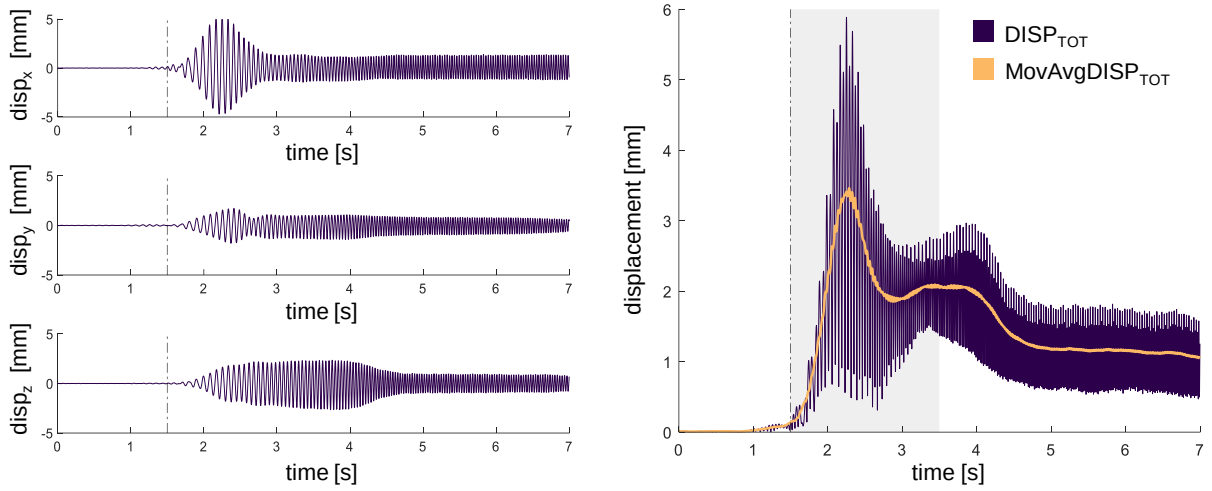

Figure 4. 4: Extraction of muscle dynamics

On the left side, muscle displacement obtained from double integration of the soft-tissue acceleration recorded at the GL site, HS_{30}. Displacement along time is reported for the x, y and z axis. On the right, the GL total displacement obtained from the combination of the signals on the left (in purple): the moving average is depicted in orange. The vibration onset is indicated on the graphs by the vertical dashed line; the two-second interval used for the search of t_P is highlighted with a grey area4.2.4 Statistical Analyses

For each muscle, a cluster-based permutation test was used to compare the mechanical response of muscles over time (Maris, 2012; Maris and Oostenveld, 2007) for:

- $MovAvgDISP_{TOT}$ between the two postures at different frequencies (four tests);
- $MovAvgDISP_{TOT}$ between frequency pairs in HS and FF (twelve tests).

Time series comparisons were performed over the portion of the signals between the vibration onset and t_A to include both the peak and stabilisation phase and because no effect was expected before the WBVs. 5000 permutations were used to build the random distribution against which the test statistic of the actual signal was compared. An alpha level of 0.05 was used to identify the significant clusters for each comparison (Gerber, 2020). To overcome the multiple comparison problem (MCP) introduced by the number of comparisons run for each muscle, the cluster p values were further Bonferroni corrected.

$$corrected\ p_{value} = \frac{0.05}{\#\text{comparisons}} = \frac{0.05}{(4+12)} = 0.003125$$

The same analyses were run on the muscle signals from which the platform one was subtracted. Specifically, for each subject, the $MovAvgDISP_{TOT}$ estimated at the platform site was subtracted from the $MovAvgDISP_{TOT}$ estimated at each muscle level. This additional analysis was run to confirm that the different muscle behaviour observed across frequencies and postures were not caused by differences in the stimulation itself.

To test whether the electromyography activity increased significantly during WBVs, for each muscle, eight Wilcoxon signed rank tests (frequency (4) x posture (2)) compared the $incrementRMS_{WBV}$ to a normal distribution with zero mean and unknown variance. Analyses were performed in Matlab ®R2019a.

For each analysed muscle, a two-way repeated measures Analysis of Variance (ANOVA) was conducted to examine the effect of stimulation frequency and subject posture on $incrementRMS_{WBV}$ [frequency (4) x posture (2)], with Bonferroni corrections. Since muscle responses were investigated per se, outliers were removed from the dataset of the specific muscle after visual inspection of the data. Residuals were inspected and the approximate normal distribution of the data was confirmed by the Anderson-Darling test (Mohd Razali and Bee Wah, 2011). Mauchly's test of sphericity was used to assess the sphericity of the data: when the latter was not met, a Greenhouse-Geisser correction was applied. Analysis were run in SPSS 23.0 (IBM Corp., Armonk, NY, USA) (Field, 2013).

To relate the mechanical response with the physiological one, a Pearson correlation coefficient was calculated between ATT_{DISP} and the outlier-free $incrementRMS_{WBV}$ population, after the subjects that were identified as outliers for ANOVA analyses were removed from the respective ATT_{DISP} population. For each muscle, 15 tests were run to assess the main effect of posture (2), the main effect of frequency (4), interactions (8) and correlation on pooled data (1). To overcome the MCP, the Bonferroni-corrected p value used for declaring statistical significance was p=.0033.

4.3 Results

All subjects were able to undergo WBV stimulations while holding the prescribed postures. The average ankle angles measured in forefeet were -9.35° ± 6.42 where a negative measure indicates a plantar flexion. When participants underwent the WBVs in hack squat, the average knee angle was 70.77° ± 4.43.

The visual inspection of the platform displacement confirms that the amplitude of the stimulation remained constant across participants, postures and frequencies. As expected, the acceleration recorded by the sensor glued to the platform shows that stimuli of increasing frequencies led to increasing platform accelerations (see Figure 4.5).

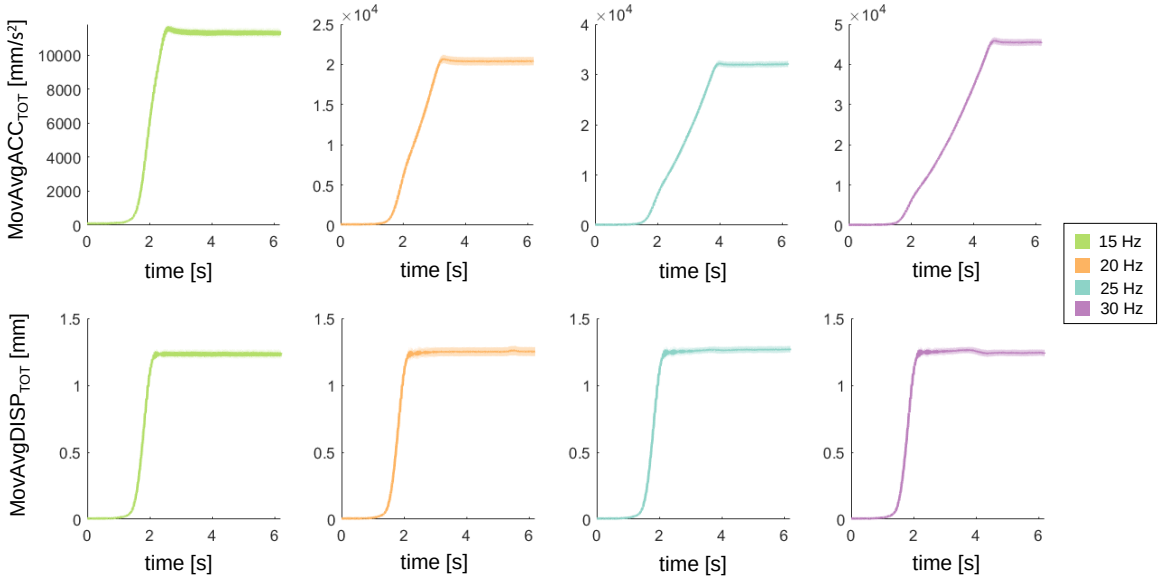

Figure 4. 5: Platform acceleration and displacement during WBVs

The moving average of the acceleration (top row) and displacement (bottom row) measured by the sensor attached to the platform are displaced (mean +/- standard error) during WBVs at different frequencies. The accelerometer data recorded for the same frequency, while the subject held a HS or a FF posture have been pooled together.

4.3.1 Muscle dynamics analysis

Our results confirmed that the muscles dynamics differed significantly depending on the posture and frequency: overall, a larger displacement was observed in HS trials and at lower frequencies. A characteristic mechanical peak was recorded shortly after the start of the

stimulations in both postures, with the only exceptions of TA and SOL muscles when stimulated at 15 Hz. Moreover, although peaks varied among muscles, postures and frequencies, the average displacement showed a similar trend with a successive drop and a further stabilisation some seconds after the peak (Figure 4.6).

More in detail, although peak heights seemed stable across the frequency range, the drop changed significantly among muscles and postures (Figure 4.6). GL displacement after the peak, was significantly smaller at higher frequencies - at 20, 25 and 30 Hz rather than at 15 Hz ($p<.001$) and at 30 Hz rather than at 20 ($p<.001$) (Figure 4.6, a.1) in HS. In FF, a similar trend was recorded: a smaller displacement was found at 30 Hz with respect to 25 Hz ($p<.001$) (Figure 4.6, a.2). At each frequency, the displacement recorded at the GL site after the vibration onset was greater in HS than in FF ($p<.001$).

The average displacement recorded at the SOL site was smaller at 30 Hz than at 15, 20 and 25 Hz ($p<.001$) while in HS (Figure 4.6, b.1). Similarly, in FF, a smaller displacement was recorded at 30 Hz than at 15, 20 and 25 Hz ($p<.001$) and at 25 Hz than at 15 Hz ($p<.001$) (Figure 4.6, b.2). As for the GL, the displacement recorded at the SOL after the vibration onset was significantly bigger in HS than in FF ($p<.001$).

The mechanical response of TA also confirmed the trend observed for the other two muscles. Its displacement was always smaller at higher frequencies ($p<.001$) in HS (see Figure 4.6, c.1) and in FF (see Figure 4.6, c.2). The total displacement of the TA muscle after the vibration onset was greater in HS than in FF ($p<.001$)

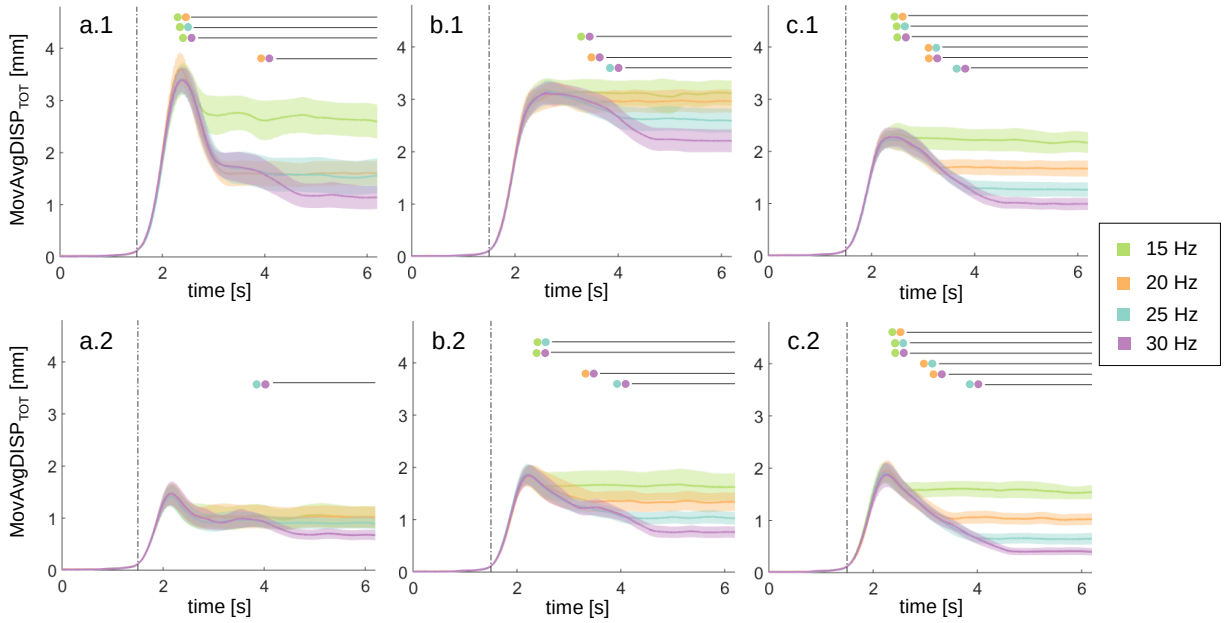

Figure 4. 5: Muscle dynamics during WBVs at different frequencies and postures

Moving average of the total displacement (mean +/- standard error) for each muscle (a=GL, b=SOL, c=TA). The top row (.1) shows the mechanical responses while subjects underwent the WBVs in hack squat; the bottom row (.2) shows the responses while subjects were in forefeet. The results of the cluster-based permutation tests are indicated by the black lines ($p<.003125$) and the conditions considered for each comparison are listed via the colour-wise legend. The vertical dotted line represents the vibration onset

Similar results were obtained from the permutation test run on the relative displacement estimated at each muscle site, further confirming that the differences obtained for the absolute displacement of muscles across conditions were not caused by differences in the stimulus delivered by the platform (see Figure 4.7).

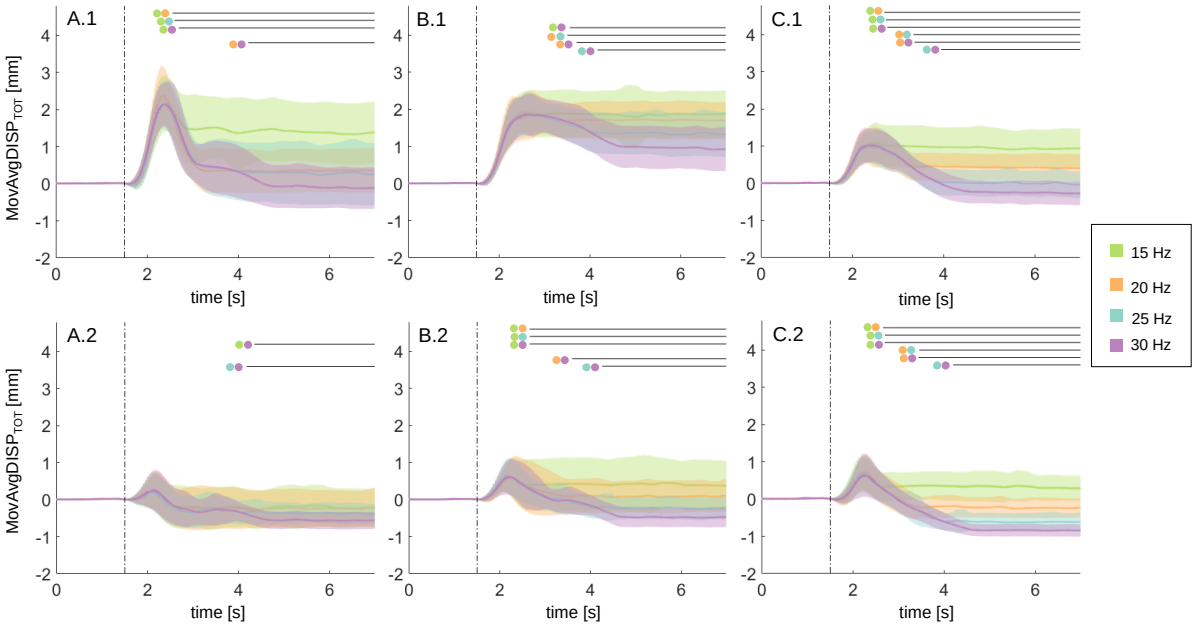

Figure 4. 6: Muscle dynamics normalised by platform displacement

Mean (+/- standard error) of the $MovAvgDISP_{TOT}$ of each muscle (a=GL, b=SOL, c=TA) from which the $MovAvgDISP_{TOT}$ of the platform was subtracted. The top row (.1) shows the normalised mechanical responses while subjects underwent the WBVs in hack squat; the bottom row (.2) shows the responses while subjects were in forefeet. The results of the cluster-based permutation tests are indicated by the black lines (p<.003125) and the conditions considered for each comparison are listed via the colour-wise legend. The vertical dotted line represents the vibration onset

Figure 4.8 shows the three-dimensional components of muscle displacement recorded for a representative subject at t_P and t_A, which was located 4.7 s after the vibration onset since the longest peak duration was of 3.12 s, recorded for the GL in HS_{30}. Overall, two main effects can be highlighted. The first is a reduction of muscle oscillations mainly along the muscle longitudinal direction (x-axis) with some effects also along the y-axis. The second is a change of phase (sometimes a complete inversion) that can be noted as the frequency of the stimulation changes.

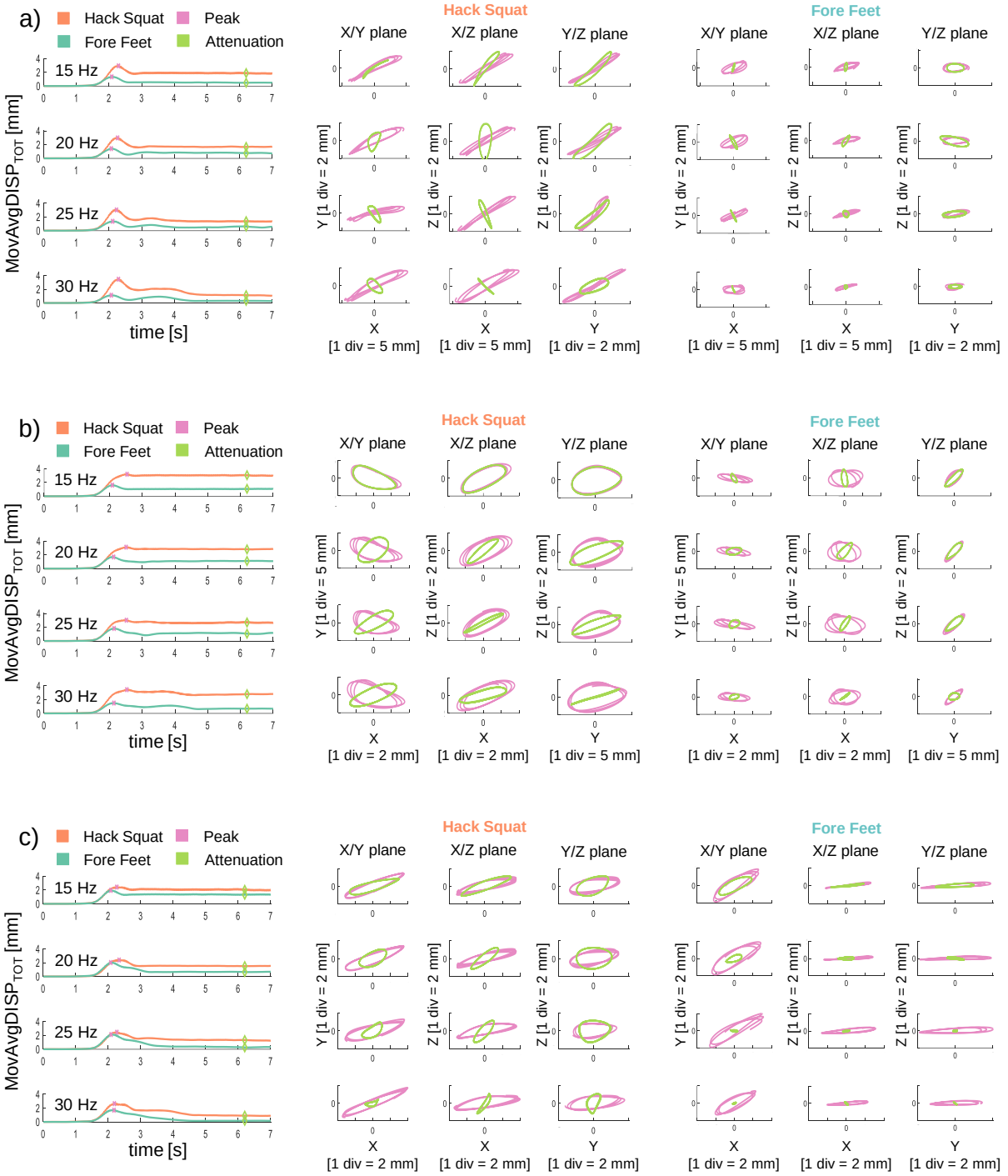

Figure 4. 7: Lissajous figures of GL, SOL and TA undergoing WBVs

Details of the mechanical response of the investigated muscles (a= Gastrocnemius Lateralis, b= Soleus, c= Tibialis Anterior) for a representative subject. For each muscle, graphs on the left depict the moving average of the total displacement observed for the two postures (hack squat, HS, in orange and forefeet, FF, in dark green) at the four WBV frequencies. Each row indicates the stimulation frequency: 15, 20, 25 and 30 Hz, from top to bottom. Peak and attenuation points are also shown with pink and light green markers (cross and diamond, respectively). The relevant 2-D displacement projections (Lissajous figures) are shown in the central and right panel for the HS and FF postures, respectively, computed at t_P (pink curve) and at t_A (light green curve)

4.3.2 Muscle activity analysis

Normality was confirmed for the dependent variables in almost all conditions for all three muscles. $incrementRMS_{WBV}$ was not always normally distributed for TA, but the latter distributions were similarly skewed to those that met normality. Four subjects were removed from the $incrementRMS_{WBV}$ dataset of GL and SOL, and three from that of TA, since represented outlier values. Distribution of $incrementRMS_{WBV}$ values for the different muscles, posture and frequencies is depicted in Figure 4.9.

A significant WBV-induced muscle activation ($incrementRMS_{WBV}$) was observed in all conditions for the GL (p<.05 for HS_{15}; p<.001 for remaining conditions) and in almost all conditions for the SOL (p<.001), apart from HS_{15} (p<.05 for HS_{20} and HS_{25}). Instead, the TA showed a significant response to WBVs only for 15 and 30 Hz (both HS and FF) and FF_{25} (p<.05).

ANOVA analyses showed that although no significant interaction was found for the GL, main effect of stimulation frequency (F(3, 60) = 14.397, p< .001, η^2 = .633) and subject posture were statistically significant (F(1, 20) = 15.433, p= .001, η^2 = .436). Specifically, GL-sEMG activity increased more in in FF than in HS (p=.001) and 30 Hz was the stimulation frequency that evoked the highest muscular activation when compared to 15 Hz (p<.001) and 20 Hz (p=.001). The WBV-induced increment of GL activation was also higher at 25 Hz than at 20 Hz (p<.05). Similarly, no significant interaction was found for the SOL and a similar stimulation frequency (F(1.772, 35.434) = 12.982, p< .001, η^2 = .394) and subject posture (F(1, 20) = 6.357, p<.05, η^2 = .241) main effects were found. The WBV-induced increment of SOL activity was higher in FF than in HS (p=.02) and 30 Hz was the stimulation frequency in which the highest sEMG increment was found when compared to 15 Hz (p<.01), 20 Hz (p<.01) and 25 Hz (p<.05). Moreover, a 25 Hz stimulation led to a higher muscle activation than 20 Hz (p<.01). No significant interaction nor main effect was instead found for the TA.

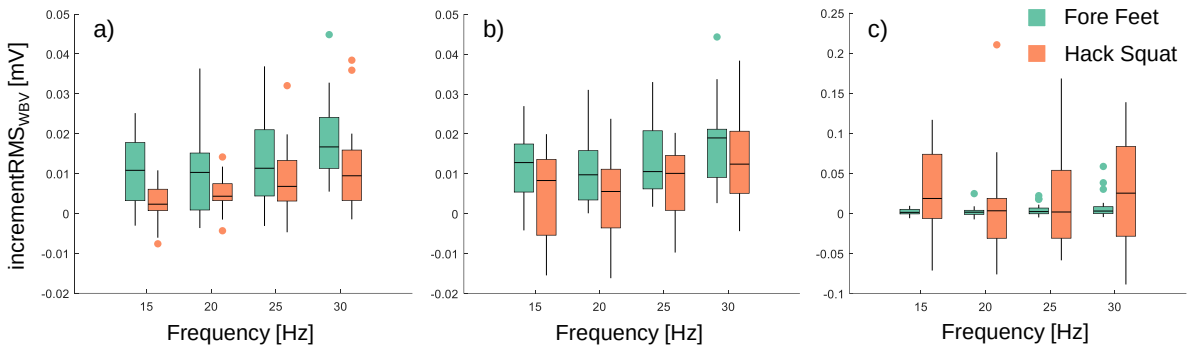

Figure 4. 8: sEMG RMS ANOVA results

Box plots of incrementRMS$_{WBV}$ values at different stimulation frequencies (15-30 Hz) of a=Gastrocnemius Lateralis (N=21), b=Soleus (N=21), and c=Tibialis Anterior (N=22) are shown. Different colours are used to distinguish between the muscle responses in hack squat (orange) and in forefeet (dark green) while the dots represent the outliers retained for the specific population. No significant interactions resulted from the ANOVAs. For significant main effects of stimulation frequency and subject posture refer back to the text. The figure was produced with Gramm (Morel, 2018)

4.3.3 Relation between muscle dynamics and muscle activity

Pearson correlation analyses yielded significant results for the SOL muscle. Specifically, a positive correlation was found between the increase of muscle activity and the amount of displacement attenuation for the following tests: 1) on the pooled data (*rho*=0.2886, *p*<.001, see Figure 4.10, B); 2) on the data collected in FF pooled across frequencies (*rho*= 0.48483, *p*<.001, see Figure 4.11, B) and 3) on the data collected in FF_{20} and FF_{25} (*rho*=.63778, *p*=.0019 and *rho*=.066425, *p*=.001 respectively). No significant correlations were found between the augmented activation of GL and TA and the extent of displacement reduction measured at the respective site (see Figure 4.10, A and C).

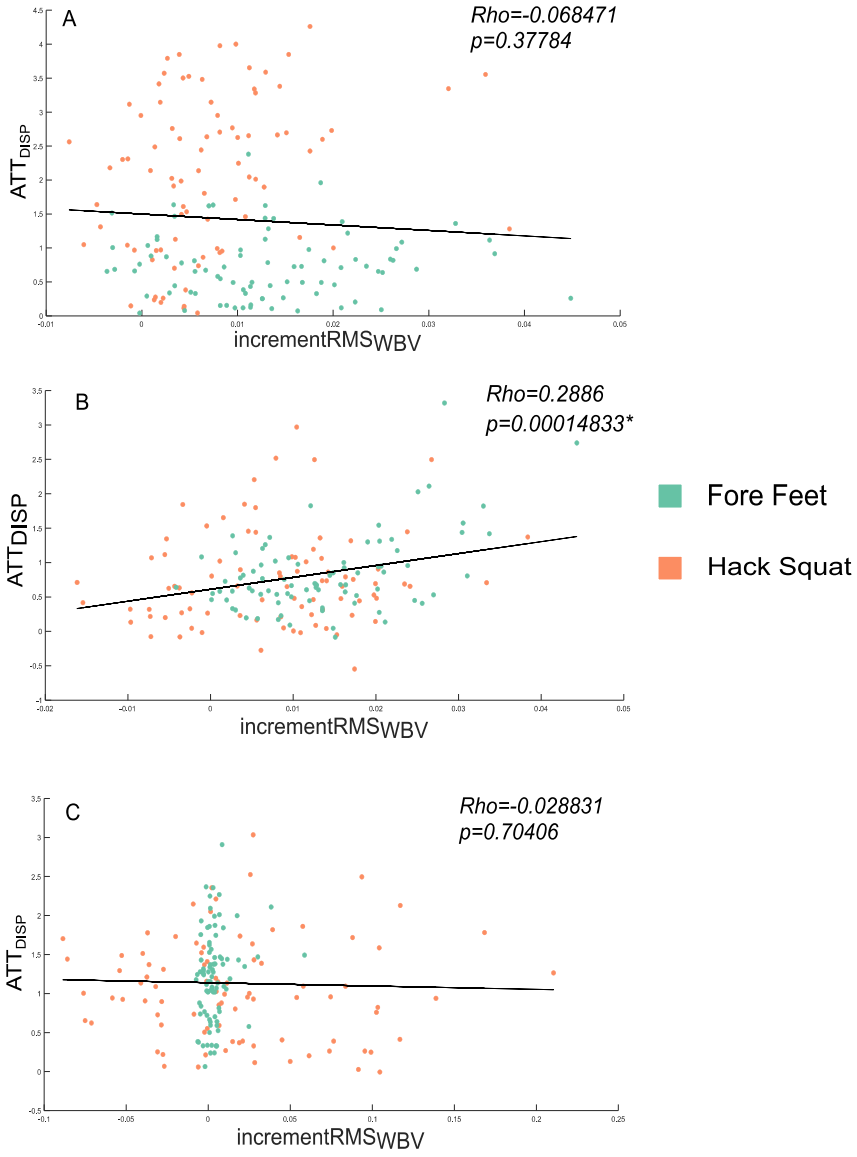

Figure 4. 9: Correlation between muscle activity and displacement attenuation – pooled data

Person correlation analyses were performed between the increase of activation of GL (A), SOL (B) and TA (C) and their respective displacement attenuation (N=168). The asterisk depicts the significant correlation found for the SOL muscle.

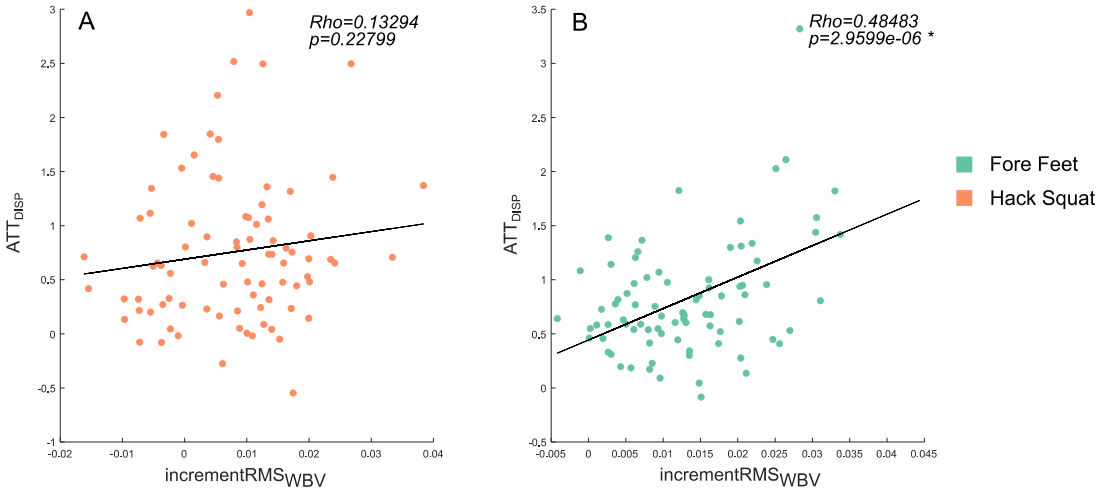

Figure 4. 10: Correlation between SOL activity and displacement attenuation – effect of posture

Results of correlation analyses (N=84) performed between the increase of activation of SOL and the displacement attenuation recorded in hack squat (A) and forefeet (B). The asterisk depicts the significant correlation found for in forefeet.

4.4 Discussions

Although every muscle shows a distinct response to WBVs - significantly determined by subject posture and stimulation frequency - a common mechanical pattern, never highlighted before, can be observed from our results. In response to vibratory stimulations, the extent of oscillations of muscles shows a rising phase, a peak oscillation and a subsequent drop, all of which completed within 4 to 5 seconds after the vibration onset, followed by a sustained stable response (plateau). Neither the stimulation amplitude nor the posture of participants varied during individual tests, hence it was concluded that a neuromuscular response must have been responsible of this phenomenon. However, the platform employed longer times to reach higher vibration frequencies (see figure 4.5, top tow), posing a possible confound effect. Therefore, to further verify that the observed differences in muscle displacement were due to different neuromuscular responses rather than differences in the stimulation, the muscle displacements were normalised by the platform one, using a framework similar to a previously proposed one (Cesarelli et al., 2010). Since changes in muscle length are those responsible for the increased muscle activity observed during WBVs (Cardinale and Bosco, 2003; Cardinale and Wakeling, 2005), the mechanical response of muscle was characterised by the muscle displacement

rather than acceleration. Moreover, we reasoned that as displacement is derived directly from acceleration, significant differences in the latter would reflect in the first. The permutation tests run on the normalised muscle displacements not only confirmed the results from non-normalised data, but were also able to capture a greater deal of differences between responses to different stimulation frequencies, suggesting that the observed muscle responses were indeed to be attributed to a neuromuscular response rather than differences in the stimulation.

The overall displacement recorded in HS for the analysed muscles, both in the peak and in the plateau phases, was always significantly larger than in FF. This could find explanation in the fact that vibrations are transmitted differently through the body according to leg geometry and joint stiffness (Lafortune and Lake, 1996), with higher level of vibration registered at the knee level when the subjects hold a HS position rather than a FF one (Harazin and Grzesik, 1998).

The three-dimensional analysis of the *peak vs plateau* muscle oscillations also revealed two interesting mechanical responses. Firstly, the reduction of the extent of the displacement clearly appeared along the longitudinal direction (x-axis), suggesting activity along the main contraction axis of the muscle. Secondly, the change of phase of the mechanical response, notable in the Lissajous figures as a different angle between the two ellipses, might represent a counter action to produce force during the lengthening phase of the muscle, condition necessary to dissipate vibration power (Wakeling et al., 2002a). In fact, although MUs can synchronize to vibrations in a one-to-one fashion within physiological limitations, their response to WBVs is characterised by the presence of a variable latency jitter, which delays the activation (reflected by the phase shift) but does not de-synchronise it (Romano et al., 2018).

Both these effects require further investigations to confirm such findings; nevertheless, our results align to the muscle tuning theory and are backed by correlation outcomes (discussed later on): the increased muscle activation dampen soft-tissue oscillations in response of impact forces applied to the feet (i.e. during gait and running) (Wakeling et al.,

2003, 2002b; Wakeling and Nigg, 2001b). During WBVs, in fact, vibrations are transferred from the feet to the muscles via the body kinematic chain and produce soft-tissue compartment oscillations around the stimulation frequency, which in our case was in the range of the natural frequencies of calf muscles (Wakeling and Nigg, 2001a). In light of the reported theory, it is therefore reasonable to assume that, if a resulting potential resonance is detected, muscle contraction is increased to avoid damage, creating the characteristic raising and falling curves observed in our recordings. This increase in muscle stiffness in fact, not only dampen the oscillations to a controlled level (observed plateau phase), but in turn shifts the natural frequency of the soft tissue toward higher values (Wakeling and Nigg, 2001a), and away from the WBV one. These dynamic analyses advance the understanding of muscles reaction to WBVs according to stimulation characteristics and, specifically, highlight that only after a period of time, which in this study is around 5 seconds, this reaction can completely settle. This may also explain why static exercises are found to be more effective than the dynamic ones (Abercromby et al., 2007a): during the first, muscles have time to tune to WBVs while during the latter the kinematic chain is continuously altered, leading to continuous changes in muscle contraction and sensitivity to vibrations (Burke et al., 1976a).

WBV-induced muscle activation has also highlighted specific combinations of posture/frequency able to produce maximal results. Recordings have been appropriately filtered for vibration-induced motion artefacts and therefore results were not overestimated (Fratini et al., 2014, 2009a; Romano et al., 2018). As expected, muscles behaved differently: GL activity was significantly enhanced in all WBV combinations, supporting the previously-demonstrated beneficial effects of WBV (Cardinale and Lim, 2003a; Di Giminiani et al., 2013; Krol et al., 2011; Marin et al., 2009; Roelants et al., 2006), while for the SOL and the TA only specific combinations were able to significantly increase muscle activation.

ANOVA results highlighted that undergoing WBV in forefeet led to a higher increase of GL and SOL sEMG activity rather than holding a hack squat position, confirming previous research findings (Ritzmann et al., 2013). This can be explained as contracted muscles are

more responsive (Burke et al., 1976a), being both muscles plantar-flexors and therefore more engaged in FF than HS (Carlsöö, 1961; Okada, 1972). Generally, WBVs delivered at 30 and 25 Hz triggered a greater activation in both muscles rather than 20 and 15 Hz, as similar findings reported (Di Giminiani et al., 2013) and supporting previous proposal of GL natural frequency residing between 25 and 30 Hz (Cesarelli et al., 2010). These conclusions are further confirmed by the observation of the permutation test results. Most differences were appreciable for the plateau phase, rather than the peak, where the displacement of GL and SOL soft-tissue compartments was significantly reduced at 30 Hz than at other WBV frequencies, further supporting the idea that this frequency is the one triggering the largest tuning effect. Moreover, the positive correlation found between the sEMG increase of the SOL muscle and the extent of displacement attenuation further suggest that the reduction of displacement observable in the plateau phase is indeed the manifestation of a neuromuscular response, potentially activated to reduce resonance. Despite these encouraging results, it is important to point out that, although significant, the increase of muscle activation is relatively small, as the reported partial-eta squared values suggest and therefore its impact on the sport and rehabilitative field might be limited. However, these findings are in line with previous studies, even if the direct comparison is not possible because of differences in the data pre-processing and normalisation (Lienhard et al., 2014a; Ritzmann et al., 2013).

No specific trend was instead found for the TA. This results might be explained by (*i*) the stimulation frequencies used in this study that were limited to 30 Hz and not enough close to TA's natural frequency, which ranges up to 50 Hz (Wakeling et al., 2002a); (*ii*) the selected postures that did not lead to an appropriate level of TA engagement, limiting its response to WBVs (Burke et al., 1976a).Combining the above, it can be inferred that 30 Hz-forefeet might be the best combination of stimulation frequency and subject posture when aiming to effectively enhance both GL and SOL muscular responses, which is in agreement with previous studies (Cesarelli et al., 2010; Ritzmann et al., 2013). For the explored combinations, instead, the TA muscle showed that WBVs elicit muscular activity but did not allow to identify

any combination producing a significantly higher response. Therefore, a wider range of frequencies and postures should be explored.

Finally, although some combinations of WBV key variables are more effective in targeting leg muscles, Wilcoxon test results showed that WBV stimulation evoked significantly higher EMG responses even from those muscles that would normally not be contracted in the prescribed posture (i.e. TA in FF, SOL and GL in HS) (Carlsöö, 1961; Okada, 1972), especially if delivered at frequencies close to the natural one of the soft-tissues (Wakeling and Nigg, 2001a). This is in agreement with previous studies reporting increased GL activations while subjects underwent WBV in hack squat at high frequencies (25-30 Hz) (Abercromby et al., 2007a; Di Giminiani et al., 2013; Pollock et al., 2010).

4.5 Limitations

The impossibility of synchronising muscle activation and soft tissue acceleration is among the limitations of this study, as it would have allowed the quantification of the correspondence between the physiological and the mechanical response. Moreover, the synchronisation of the sEMG and accelerometer recordings with the accelerometer attached to the WBV platform would have allowed to monitor the punctual muscular response to the vibrations for each individual subject. However, in regard of the latter, the synchronisation procedure adopted in this chapter allowed for a more accurate synchronisation *between* subjects. Vibrations propagate differently along the body according not only to the level of stiffness of the muscles, but also to the dimensions of the limbs themselves. As all the participants differed in height and body mass, it is reasonable to believe that the mechanical stimulation “travelled” differently along very different bodies. With the procedure here proposed it was possible to align the soft-tissue accelerations depending on the time point where the tissue begins to oscillate, rather than on the platform onset.

4.6 Conclusions

Our results highlighted that WBVs via side-alternating platforms can be optimised for calf muscle training, if aimed at achieving the maximal level of elicited response, and in particular:

- In order to allow muscles to produce a stable contraction, training programmes should only include static exercise on a vibrating platform or, at least, participants should hold the same posture for a minimum of five seconds.

- Calf muscles produce maximal response if participants are standing on the forefeet during stimulations.

- Finally, vibration frequencies in the range of 25-30Hz should be used during WBV training sessions for calf muscles.

The systematic targeting of the plantar flexors via proper selection of stimulation frequency and subject posture represents an opportunity to maximise the ankle strategy outcome and to possibly improve postural control.

5. Characterisation of WBV effect on Postural Control

5.1 Introduction

For a few decades it has been thought that balance was maintained merely by passive local reflexes, as mammals were found to be able to stand still solely by tonic muscle contractions (Magnus, 1925). However, this view has been recently challenged and a new working hypothesis has been proposed suggesting that balancing –as well as any other type of human movement- requires active planning, therefore involving global multisensory integration and processing of a higher level (Casadio et al., 2005; Lakie et al., 2003; Loram et al., 2005b, 2005a; Loram and Lakie, 2002; Morasso and Sanguineti, 2002; Morasso and Schieppati, 1999). According to this perspective, as we stand, inputs from the outer environment are processed online by the central nervous system (CNS) to maintain a stable upright stance (Horak, 2006; Shumway-cook and Horak, 1986). Vestibular, visual, somatosensory and auditory cues are integrated to regulate muscle contraction over time, with the ultimate goal of adjusting the centre of mass position, preventing falls (Forbes et al., 2018; Horak and Macpherson, 1996). Efficient postural control results from an effective interplay between sensory feedbacks integration and cortical drive to the muscles, which allows to *detect*, *react to* and *correct* the perturbations that normally occur while standing upright. Two effective tools are available to investigate the communication occurring between muscles and the brain: intermuscular coherence (IMC) and corticomuscular coherence (CMC) (Boonstra, 2013).

IMC is thought to represent the common neural input that, originating from efferent and afferent pathways, is fed to motor units (MUs) of different muscles (Sears and Stagg, 1976). To facilitate motor control, the CNS is thought to deal with the several degrees of freedom of the musculoskeletal system by coordinating muscle activation, i.e. recruiting muscles in groups (Bernstein, 1967; Farmer, 1998; Turvey, 1990). An innovative way to look at IMC is to study muscle synchrony via complex network analysis, which has largely been employed to understand the organisation of cortical activity (Hassan and Wendling, 2018; Rubinov and Sporns, 2010). Thanks to this technique, the synchronous modulation of muscles across tasks was revealed to be functional, which means that different muscle networks are employed to carry out different “planned” movements (Boonstra et al., 2015; Kerkman et al., 2020).

Similarly, CMC has been historically thought to represent pyramidal neurons signalling to spinal motor neurons, subsequently commanding the corresponding muscle fibres (Halliday et al., 1995). However, recent findings suggest that it also reflects afferent couplings, namely the ascending flow of information that from receptors in the muscles reaches somatosensory areas in the brain (Campfens et al., 2013; J. Liu et al., 2019; Witham et al., 2011). This belief is further supported by the fact that oscillations in beta band (15-30 Hz) are observed both in the motor (M1) and somatosensory (S1) cortex (Witham et al., 2007; Witham and Baker, 2007) and are coherent with the activity recorded from contralateral contracting muscles (Baker et al., 1997; Conway et al., 1995). The presence of activity in beta frequency range has been vastly documented in the human motor system (Grosse et al., 2002; Salmelin and Hrai, 1994; Tiihonen and Kajola, 1989) and is the reason why CMC is mostly investigated in beta band (J. Liu et al., 2019; Witham et al., 2011). Most studies on CMC used experimental designs involving steady-state motor output, such as precision grip and isometric contractions, (Conway et al., 1995; Kilner et al., 2002, 1999; Kristeva et al., 2007, 2002; Omlor et al., 2007; Ushiyama et al., 2017; Watanabe et al., 2020) or dynamic voluntary movements (Andrykiewicz et al., 2007; Petersen et al., 2012; Peterson and Ferris, 2019; Roeder et al., 2020), such as walking. Very few studies evaluated CMC during standing balance (Masakado et al., 2008; Murnaghan et al., 2014) and even less managed to prove the existence of CMC during postural control (Jacobs et al., 2015; Ozdemir et al., 2018; Vecchio et al., 2008), possibly because CMC depends a lot on the task (Kilner et al., 2000, 1999), the functional role and level of specialisation of the chosen muscles (Ushiyama et al., 2012, 2010) and even the individuals themselves (Campfens et al., 2013; Ushiyama et al., 2011).

Although most studies failed to find CMC in beta band during balance tasks, it is sensible to investigate postural control mechanisms by inspecting couplings in such frequency range. Oscillations between 13 and 30 Hz have in fact been linked to the attempt of preserving the ongoing sensorimotor state. More in detail, Engel and Fries suggest that beta band activity (BBA) acts as a facilitator of proprioceptive feedback processing (Engel and Fries, 2010). In the intended attempt of preserving the status quo and regaining balance after a disturbance,

the enhanced activity observed in beta band is thought to promote the handling of proprioceptive signals coming from the periphery, on which we rely for the perception and recalibration of the sensorimotor system (Baker, 2007).

Among all the inputs that we use online to modify our posture, somatosensory ones play perhaps the most important role due to the fact that proprioceptive thresholds are the lowest in detecting centre of pressure (COP) velocity (Fitzpatrick and Mccloskey, 1994; Peterka, 2002; Sturnieks et al., 2008). Receptors in the muscles -muscle spindles- are stretch-sensitive and yield information about the length and contraction of muscles, contributing to the perception of limb and joint position in space (Gandevia, 1996; G M Goodwin et al., 1972; Proske, 2005). As most sensory organs, even muscle spindles lose their sensitivity in time (Miwa et al., 1995; Swash and Fox, 1972) and this is also thought to partially explain the decline in standing balance that is usually observed with ageing (Lord et al., 1994, 1991; Swash and Fox, 1972). Therefore, finding a way to improve proprioceptive sensitivity becomes crucial for any training and rehabilitation programme aiming at improving postural control.

A renowned way to stimulate muscle spindles is to apply mechanical vibrations to muscle bellies and tendons. These have been proven to evoke reflex responses - tonic vibration reflex (TVR)- that result in a MU firing rate increase and, consequently, in a bigger electromyographic (EMG) response (Burke et al., 1976a; Burke and Schiller, 1976; Hagbarth et al., 1976; Homma et al., 1972; Martin and Park, 1997; Person and Kozhina, 1992, 1989). A way to extend muscle spindle stimulation to the lower limbs is to expose every muscle to the mechanical stimulus, which is possible by delivering vibrations to the whole body via an oscillating platform, as it occurs in whole body vibration (WBV) stimulation. The latter has been recently included in training and rehabilitative programmes as a mean to evoke neuromuscular responses from various muscles and therefore enhance muscle contractions (Alam et al., 2018; Cardinale and Bosco, 2003; Delecluse et al., 2003; Osawa et al., 2013; Rittweger, 2010). Because TVR has been appointed as the main mechanism responsible for the enhanced sensitivity of muscle spindles primary endings and for the increased muscle activation

observed during WBVs (Cardinale and Bosco, 2003; Pollock et al., 2012; Ritzmann et al., 2010), the latter represents a reasonable candidate for muscle spindle stimulation.

The goal of this study was to investigate the effect that mechanical vibrations - intended as a way to stimulate muscle spindles - have on postural control mechanisms. Vibrations are delivered in such a way that the targeted muscles –soleus (SOL) and gastrocnemius lateralis (GL)- are those that contribute the most to the primary strategy put into place during undisturbed human standing: the ankle strategy (Horak and Nashner, 1986). The effect that calf-muscle spindle stimulation has on postural control mechanisms is studied via classic analyses of CMC and BBA as well as state-of-the-art IMC network analyses (Boonstra et al., 2015; J. Liu et al., 2019). Balance outcomes are evaluated with typical posturography analyses and muscle activity is analysed with more common root mean square values.

5.2 Materials and Methods

5.2.1 Subjects and experimental design

Eleven females and six males (age: 23.06 ± 2.51 years; height: 167.22 ± 9.74 cm; mass: 61.32 ± 10.69 kg) volunteered in the study after giving written consent. History of neuromuscular or balance disorder and recent injuries to the lower limbs were the exclusion criteria. Among the inclusion criteria, participants were required to do more than 5 hours per week of physical activity. They were also asked to not consume alcoholic beverages and to not assume medication over the 24 hours prior to the experiment. The protocol of the study received approval by the Ethics Committee on Life and Health Sciences of Aston University.

A single-group, repeated-measure design was used and the data were collected at the Aston Laboratory for Immersive Virtual Environments. Electroencephalographic (EEG), COP and surface EMG (sEMG) signals of calf muscles were collected while participants underwent a balance task, performed before and after WBV mechanical stimulation.

5.2.2 Experimental protocol and data recording

A familiarisation session was run for participants to get acquainted with the WBV device before the study began. After the recording equipment was set up, the first part of the study consisted in recording four baseline balance (BB) trials of 60 seconds. Participants were instructed to "stand as still as possible" (Zok et al., 2008) with feet shoulder-width apart and arm along the trunk while fixating their gaze at a tape cross placed on the wall in front of them, at approximately 2.5 meters distance. After the baseline trials were collected, the second part of the study took place: a one-minute vibratory stimulation was delivered with a side-alternating platform (Galileo® Med, Novotec GmbH, Pforzheim, Germany) that operated at 30 Hz, peak-to-peak amplitude of 4 mm. While undergoing the WBVs, participants stood on their forefeet, knees unlocked, keeping contact between heels and a 4 cm tall foam parallelepiped glued to the platform (Ritzmann et al., 2014). This combination of WBV settings (stimulation frequency and subjects' posture) was chosen as it triggers the greatest response of the plantarflexors muscles -SOL and GL- (refer to Chapter 4). The WBV stimulation was followed by the recording of four balance trials of 60 seconds each, which will be referred to as Post-Stimulation balance (PSB) trials. After the WBVs, participants were asked to position themselves on the platform as soon as they felt ready to undergo the postural task. We will refer to BB and PSB as the two conditions tested in this study.

EEG and sEMG data were acquired using EEGO sports ES-232 (ANT neuro, Enschede Netherlands). To collect the electrical brain activity (EEG), a 64-channel Ag/AgCl wet-electrode waveguard cap was used in connection to a portable amplifier fixated on the participants' backs. Data were continuously collected with a standardised 10-20 system montage and were sampled at 1000 Hz. Caps of different sizes were fitted on the head of participants; the correct placement was obtained by checking that Cz was placed at mid-distance between the nasion and inion anatomical points and at mid-distance between the left and right lobes. Muscle signals (sEMG) were collected via bipolar Ag/AgCl electrodes (Arbo Solid Gel, KendallTM, CovidienTM 30 mm x 24 mm, centre-to-centre distance 24 mm) that were connected to the portable amplifier via cascaded bipolar adaptors XS-271.A, XS270.B,

XS-270.C. Electrodes were placed over the tibialis anterior (TA), GL, SOL, rectus femoris (RF) and biceps femoris (BF) muscles of both legs and arranged along the presumed direction of muscle fibres, as recommended by the SENIAM guidelines (Hermens et al., 2000, 1999). The reference electrode was placed over the tuberosity of the right tibia. To reduce inter-electrode resistance, the skin area was shaved and degreased by mean of light abrasion with a disinfectant. To quantify balance, COP trajectories were recorded and sampled at 1000 Hz via an AMTI OR 6-7 force platform (Advanced Mechanical Technology, Watertown, MA, USA) connected to a motion capture system (Vicon Nexus, Vicon Motion Systems Limited, Oxford, UK). A LabJack U3-HV acquisition unit was programmed in Matlab ®R2019a (The Mathworks, Inc., Natick, MA) with a custom-made script to synchronise electrophysiological acquisitions and posturography data. The trigger signal was sent as a 5V TTL signal to the DB25 port of the EEGO sports master amplifier and as a 1.25V TTL signal to the rear of the Vicon Lock unit.

5.2.3 Data synchronisation

Since participants reacted differently to the stimulation, different delays were recorded between the WBV stimulation and the first PSB trial.

To allow a consistent comparison while evaluating the *acute* effect of WBV on balance, the first BB and PSB trials were preprocessed to match the delay between the WBVs and the first PSB across participants. The distribution of the time employed by each participant to reposition on the force platform (delays) was analysed and the subjects whose delay represented an outlier values were removed from the dataset. The recordings (EEG, sEMG and COP) of the retained subjects were then synchronised to those of the subject that scored the greatest delay and were further cropped to match the duration of the shortest recording. The same cropping procedure was applied to the first BB trials, which were cropped at the same time point of the corresponding PSB trial to make the trials collected before and after the WBVs comparable. These preprocessed signals will be hereafter referred to as the *cropped* ones.

The *long-term* effect of WBV stimulation on balance was evaluated by concatenating the four BB trials and the four PSB trials into two 240 second-long epochs, which were then used for analyses. These signals will be hereafter referred to as the *concatenated* ones.

5.2.4 Data preprocessing –EEG and sEMG

The cropped and the concatenated EEG epochs were preprocessed in Matlab ®R2019a (The Mathworks, Inc., Natick, MA) in a semi-automatic fashion, following the steps proposed in the software Cartool (Brunet et al., 2011). The EEG signals were de-trended, mirrored to avoid edge-artefacts (Cohen, 2014), filtered in beta band (13-32 Hz) with a zero-phase FIR filter, cropped and de-trended again. Eye-blinks were removed automatically by subtracting the signals recorded at FP1, FPz and FP2 sites from the remaining 60 EEG channel data, proportionally to their contribution to each channel (Croft and Barry, 2000; Parra et al., 2005; Pedroni et al., 2019). Channels with standard deviation (SD) exceeding the average SD by a factor of 1.7 were replaced by the average of the signals from neighbouring channels (Hassan and Wendling, 2018). The value of the factor was placed at 1.7 after a visual inspection – confirmed also by a second researcher- of the preprocessed channels confirmed that this threshold was not too conservative, leading to the interpolation of channels exceeding the physiological range of ±80 μV (Hassan and Wendling, 2018). Channels were re-referenced to the common average to increase signal-to-noise ratio (SNR) (Mima and Hallett, 1999; Snyder et al., 2015).

The cropped and the concatenated sEMG epochs were preprocessed and analysed in Matlab ®R2019a (The Mathworks, Inc., Natick, MA), using custom-made scripts. The power line noise was occasionally present not only at 50 Hz, but also at superior and inferior harmonics. To suppress such noise, a comb stop-band filter was used at harmonics between 25 and 150 Hz, using a stop band of 1 Hz. The signals were band-pass filtered between 20 and 260 Hz with a zero-phase Butterworth filter (Roeder et al., 2020), after padding was applied to avoid edge-artefacts (Cohen, 2014). Filtered sEMG epochs were then rectified (Halliday et

al., 1995; Halliday and Farmer, 2010; Myers et al., 2003; Sebik et al., 2013) with a Hilbert transform, which provides results similar to a full-wave rectification (Boonstra and Breakspear, 2012; Murnaghan et al., 2014; Myers et al., 2003). The preprocessing was done using Fieldtrip ft_preprocessing function (Oostenveld et al., 2011).

5.2.5 Data analysis

5.2.5.1 CMC

CMC analyses were performed only on those muscles targeted by the vibrations: the lower limb ones (SOL, GL and TA). Coherence estimates were computed between the preprocessed EEG and sEMG signals (both between the cropped epochs and the concatenated ones), for a total of 360 couplings [EEG channels (60) x muscles (6)] per condition. Power spectral densities (PSD) of EEG and sEMG signals were estimated with Welch's averaged periodogram method (Welch, 1967), segmenting the epochs in Hamming windows of one seconds and zero overlap (Jacobs et al., 2015). The CMC between the signal x –EEG- and y –sEMG- was then calculated as:

$$C_{xy}(f) = \frac{\left|P_{xy}(f)\right|^2}{P_{xx}(f)P_{yy}(f)}$$

where P_{xy} is the cross-spectral density between the input signals for a given frequency f, and P_{xx} and P_{yy} are the auto-spectral densities of x and y, respectively. In total, 720 CMC vectors [EEG channels (60) x muscles (6) x condition (2)] were retained for statistical analyses.

5.2.5.2 BBA

To quantify beta band activity changes between before and after the WBVs, the average power in beta frequency range (15-30 Hz) was used as a summary statistic (Omlor et al., 2007). PSDs were estimated with Welch's averaged periodogram (Welch, 1967), using non-overlapping Hamming windows of one second, and were obtained for cropped and concatenated EEG epochs recorded from the sensors overlying the sensorimotor cortex (C3, C4, CP3 and CP4),

(Anderson et al., 1995; Müller et al., 2000; Southgate et al., 2010; Tsuchimoto et al., 2017). For each subject, average power values were then averaged across channels and two summary values ($BetaPower_{BB}$ and $BetaPower_{PSB}$) were retained for statistical analyses.

5.2.5.3 IMC and muscle networks

sEMG signals from *all muscles* were instead used for connectivity analyses. IMC was estimated between all muscle pairs using *mschoere* Matlab function. Forty-five combinations ($C_{n,k}$) resulted from the formula:

$$C_{n,k} = \frac{n!}{k!\,(n-k)!}$$

where $n = 10$ is the total number of muscles (nodes) and $k = 2$ is the number of muscles in each arrangement (pair). Magnitude-squared coherence values were computed over sEMG power spectral density (PSD) using Welch method, with window length of 1 second and overlap of 75% (Boonstra et al., 2015). To break down the connectivity values into different frequency components and to make the coupling strength comparable between conditions, a non-negative matrix factorization (NNMF) algorithm was run on a $N \times [M \times P \times C]$ (frequency bin x [muscle pairs x participants x conditions]) weighted undirected connectivity matrix. *Nnmf* Matlab function was used to decompose the coherence spectra (0-40 Hz) in two matrixes $W_{AllSubj}$ $[N \times K]$) and $H_{AllSubj}$ $[K \times [M \times P \times C]]$, where K equals 6 and is the number of frequency components in which the matrix was factorised. 5000 iterations were used. The two matrixes were then reshaped into subject-specific W $[N \times K]$ and H $[K \times M]$ for both conditions (W_{BB} $[42 \times 6]$ and $H_{BB}[6 \times 45]$; W_{PSB} $[42 \times 6]$ and $H_{PSB}[6 \times 45]$). For every subject, H was reshaped into six weighted undirected connectivity matrixes C, which yielded the connection strengths between nodes (muscles) in every frequency band. C_{BB} and C_{PSB} resulted in 10×10 connectivity matrixes. To conduct a static node-wise analysis, four connectivity metrics were obtained for every node of the subject-specific C_{BB} and C_{PSB} of every frequency component: clustering coefficient (CC), participation coefficient (PC), betweenness centrality (BC) and node strength (STR). The network measures obtained from the same muscle were used for

statistical analysis. To run a static edge-wise analysis, the connection strengths of the 45 muscle pairs yielded by C_{BB} - C_{PSB} were retained for statistical analysis.

5.2.5.4 sEMG

A root mean square (RMS) value was obtained from the preprocessed sEMG epochs of those muscles targeted by the WBVs (SOL, GL and TA) before and after the stimulation. In total, 12 [muscle (6) x condition (2)] RMS values were obtained for each participant and retained for statistical analysis. To quantify the level of muscle fatigue induced by the stimulation, a frequency parameter was extracted from the filtered unrectified sEMG epochs. Specifically, the median frequency (MF_{BB} - MF_{PSB}) of the sEMG power spectrum –computed with the same specifics used for IMC estimation- was identified for each participant and for each muscle as the frequency that divides the spectrum in two parts of equal power (S. H. Liu et al., 2019; Stolen et al., 1981).

5.2.5.5 COP

The cropped COP coordinates and the concatenated ones were analysed in Matlab ®R2019a (The Mathworks, Inc., Natick, MA) with custom-made scripts. The mean of each signal was subtracted from anterior-posterior (AP) and medial-lateral (ML) COP coordinates, which were then low-pass filtered at 12.5 Hz using a 4^{th} order Butterworth filter (Donker et al., 2007). For each condition and each participant, as described in (Prieto et al., 1996), COP mean distance (MD) and COP mean velocity (MV) values were computed for both directions: MD_{AP}, MD_{ML}, MV_{AP} and MV_{ML} . The four stabilometric parameters were normalised by participant's height, weight and age by applying a simultaneous detrending normalisation (Chiari et al., 2002; O'Malley, 1996).

To compute the multiscale sample entropy (MSE), the preprocessed AP and ML time-series were further normalised by their standard deviation values (Donker et al., 2007; Lake et al., 2002; Richman and Moorman, 2000). MSE was obtained with a Matlab File Exchange function and the recommended default values of the pattern length and similarity criterion were used (Costa et al., 2005, 2002; Malik, 2020; Zhou et al., 2016). The complexity index (CI) was

computed as the sum of the individual sample entropies obtained for every time scale in both directions –ML and AP- obtaining CI_{ML} and CI_{AP} respectively (Busa et al., 2016; Busa and van Emmerik, 2016). For the long-term analyses -due to the dimension of the data- the MSE was not computed on the concatenated epochs, but on the individual epochs of one minute. The MSE values obtained from the four epochs preceding (and following) the WBVs were averaged to obtain MSE_{BB} (and MSE_{PSB}) that were used to compute the respective complexity index values.

5.2.6 *Statistical Analysis*

5.2.6.1 CMC

For every muscle, the 60 CMC vectors obtained from BB trials were compared to the respective ones obtained from the PSB trials via mean of a cluster-based permutation test (Maris and Oostenveld, 2007), which was carried out in Fieldtrip using 2000 permutations (Oostenveld et al., 2011). Comparisons were run in the beta frequency range and this procedure was applied to the CMC vectors obtained from both the cropped and concatenated EEG and sEMG epochs.

5.2.6.2 BBA

A one-tailed Wilcoxon test was run to evaluate whether any significant difference was present in BBA in the somatosensory cortex between before and after the vibratory stimulation. The directionality of results from the permutation test was used to infer on the effect of WBVs on BBA.

5.2.6.3 IMC

Since we had no prior information on the effect of WBVs on muscular connectivity during balance, two-tailed Wilcoxon signed rank tests were used to test it. Tests were run for every muscle in every frequency component between the connectivity metric obtained from C_{BB} and C_{PSB}. For the node-wise analysis, 4x10x6 ([metrics X muscles X frequency components]) tests were performed on the connectivity metrics obtained from the balance results. For the edge-wise analysis, 45x6 ([muscle pairs X frequency components]) tests were run on the connection strengths computed from the balance trials, respectively. To correct for the multiple

comparisons, the False Discovery Rate (FDR) (Benjamini and Hochberg, 1995; Groppe et al., 2011; Thissen et al., 2002) procedure was applied for every metric (CC, PC, BC, STR, edge) across muscles, within each frequency band.

5.2.6.4 sEMG

To quantify the differences in muscle activations between the balance trials (before and after WBV stimulation), six two-tailed Wilcoxon signed rank test were run between RMS_{BB} and RMS_{PSB}, one for each muscle. To test the hypothesis that a greater level of muscle fatigue was induced by the WBVs, six one-tailed Wilcoxon signed tests were run between MF_{BB} and MF_{PSB}, one for each muscle.

5.2.6.5 COP

Since we had no a priori expectation on the effect of WBVs on postural stability, a two-tailed Wilcoxon signed rank test was run for every normalised parameter (MD_{AP}, MD_{ML}, MV_{AP} and MV_{ML}). Since two parameters were obtained from each time-series (ML and AP), a Bonferroni correction was applied to the significance level that was therefore set at 0.025. A Spearman correlation coefficient was used to quantify the level of collinearity between the COP parameters and the anthropometrics.

Another two-tailed Wilcoxon signed rank test was used to test for significant differences between complexity indexes measured in moth directions before and after the mechanical vibrations.

5.3 Results

For the main analyses on the acute effect, two subjects were removed from the dataset as the time occurred between the vibratory stimulations and the balance trials -delays- were outlier values (11.6 s and 40.4 s). The alignment of balance recordings resulted in trials of the length of 44.779 s. The average delay occurred between the WBV stimulation and the balance task

was 27.8726 +/-4.1071 s. For the analyses on the longer-term effect, all 17 subjects were retained, and the concatenation of balance trials resulted in two 4-minute long epochs.

5.3.1 CMC results

The permutation test run on 45 s-long epochs found two significant clusters in correspondence of a bigger CMC after the WBVs. Specifically, a stronger coupling was observed around 22 Hz between the right GL and electrodes situated mostly in the contralateral hemisphere (Figure 5.1, a.1). The effect had the same directionality for the right SOL and the same central contralateral electrodes but was centred around 18 Hz (Figure 5.1). No significant difference was identified on the CMC vectors obtained from the concatenated EEG and sEMG epochs.

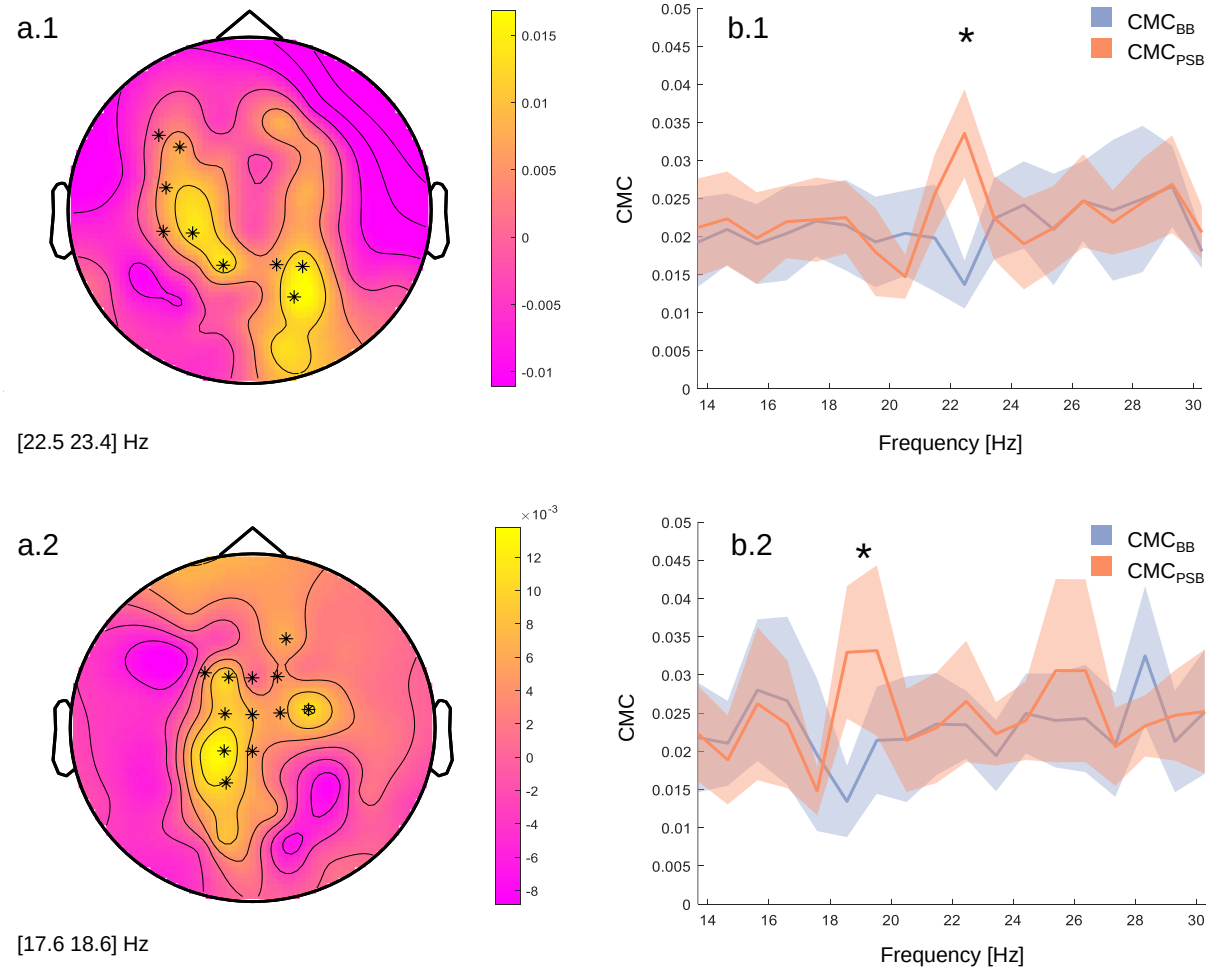

Figure 5. 1: Corticomuscular coherence topographic maps and spectra

On the left-side, voltage topographic maps of the difference between EMG-EEG couplings before and EMG-EEG couplings after the WBVs (CMC_{BB} and CMC_{PSB}, respectively), averaged across subjects, are reported for the right GL (a.1) and the right SOL (a.2). The asterisks depict electrodes that showed a significantly bigger CMC around 23 Hz (a.1) and 19 Hz (a.2). On the right-side, CMC spectra (mean +/- standard error) of EMG-EEG couplings before and after the stimulation are reported for the right GL (b.1) and the right SOL (b.2). The asterisks depict the frequency bin at which the CMC signals differed between conditions, as identified by the cluster-based permutation test. Results are shown for CMC vectors obtained from the 45 second-long baseline (BB) and post-stimulation (PSB) trials.

5.3.2 BBA results

A one-side Wilcoxon test was used to test the hypothesis that S1 BBA after the vibratory stimulation was higher than during the baseline balance trials. The result obtained for $BetaPower_{BB}$ and $BetaPower_{PSB}$ estimated from cropped epochs showed that BBA in S1 increased after the WBVs (p<.01) and are displayed in Figure 5.2. No change was found in the long term, when BBA was estimated from the concatenated epochs.

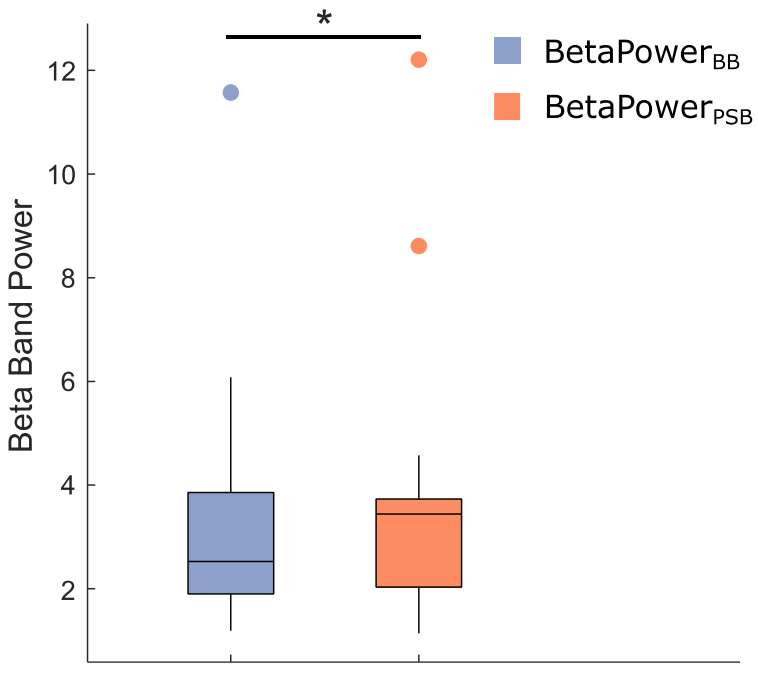

Figure 5. 2: Changes in beta band activity

Box plot of the average power estimated in beta band for EEG epochs recorded at C3, C4, CP3 and CP4 during balance trials before (purple) and after (orange) the vibratory stimulation. Significance (p<.01) is indicated by the asterisk and results are reported for 45-s long epochs.

5.3.3 IMC results

The components obtained from the NNMF of the cross-coherence spectra of 45-s long epochs are displayed in Figure 5.3 and represent the following frequency bands: 0 Hz; 2 Hz; 8 Hz; 14 Hz; broad band peaking around 10, 20 and 30 Hz; general broad band. The node-wise analysis provided significant results only for few components and metrics (Figure 5.4):

- The clustering coefficient (obtained from the muscle network at 2 Hz) of right SOL, left SOL, right GL and left GL decreased significantly after the stimulation (*p<.05, FDR corrected*);

- The strength of the right SOL node (obtained from the muscle network at 2 Hz) decreased after the WBVs (*p<.05, FDR corrected*);

- The betweenness-centrality of the right SOL (obtained from the muscle network peaking around 10,20 and 30 Hz) decreased after the WBVs (*p<.01*);

- The betweenness-centrality of the left BF (obtained from the muscle network peaking around 2 Hz) increased after the WBVs (*p<.01).*

Similarly, few significant results were obtained for the edge-wise analysis (Figure 5.3):

- The connection strength between the two SOL muscles decreased at 2 Hz after the stimulation (*p<.05, FDR corrected*). In addition, the connections between left GL-right SOL and between right SOL-right GL decreased after the WBVs (*p<.01*);

- The connection between left RF and left BF at 8 Hz increased after the stimulation (*p<.05, FDR corrected*);

- The strength of the connection between left RF and the left SOL increased after the WBVs (*p<.05, FDR corrected*), for the broad frequency component peaking at 10, 20 and 30 Hz;

- The connection strength between left GL-right RF and left GL-right BF increased after the WBVs ($p<.01$) in the broad frequency component.

Similar frequency components were obtained from the concatenated epochs. However, although a decrease of CC and STR was measured at 2 Hz for both the left and right soleus, these results did not pass the FDR correction. Similarly, a decrease in the strength connection between left SOL-right SOL and between left SOL-left GL was significant, but did not pass the FDR correction.

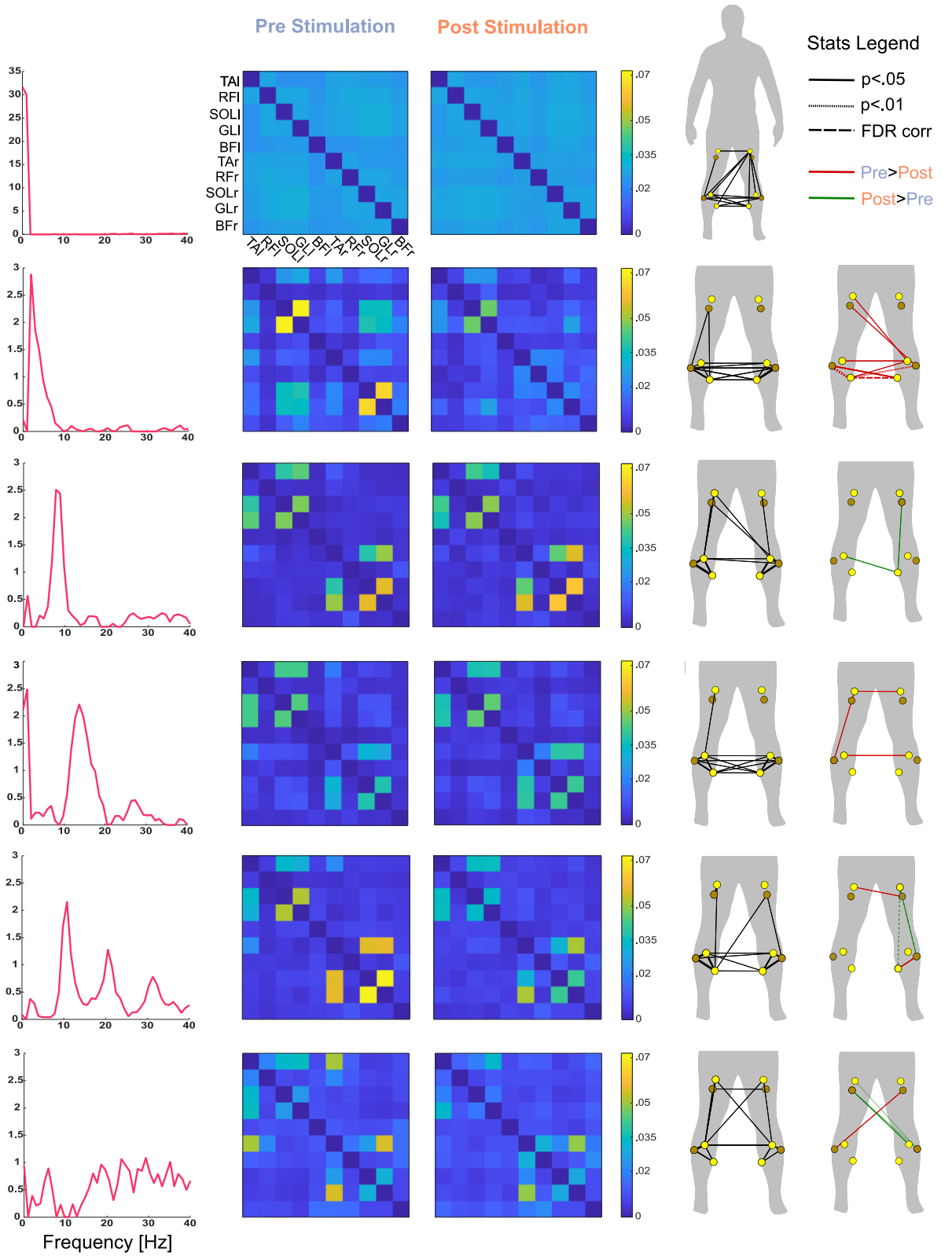

Figure 5. 3: Edge-wise analysis of muscle networks

The left column depicts the six frequency components in which the coherence spectra were decomposed via NNMF (one for each row). The second and third columns show the adjacency matrixes, averaged across subjects, obtained for each frequency component from the 45-s long trials before and after the stimulation, respectively. These matrixes give the connection strengths, at different frequencies, between the 10 muscles (nodes of the network). The fourth column depicts the muscle

networks averaged across subjects and conditions: the weight of the edges is obtained by averaging the two adjacency matrixes (pre and post stimulation) for each frequency component. The widths of the edges in column 4 reflect the strength of the connection. The fifth column depicts the statistical results of the edge-wise analysis. For each frequency component, only those edges that were significantly different (p<.05) between conditions (pre vs post) are depicted. Comparisons that resulted particularly significant (p<.01) are depicted via a dotted line; comparisons that resulted significant after FDR correction are depicted via a dashed line. The colours of the edges reflect the direction of the effect, with red lines indicating that the connection strength decreased after the stimulation and green lines indicating an increase after the stimulation. The width of green and red lines indicates the size of the effect.

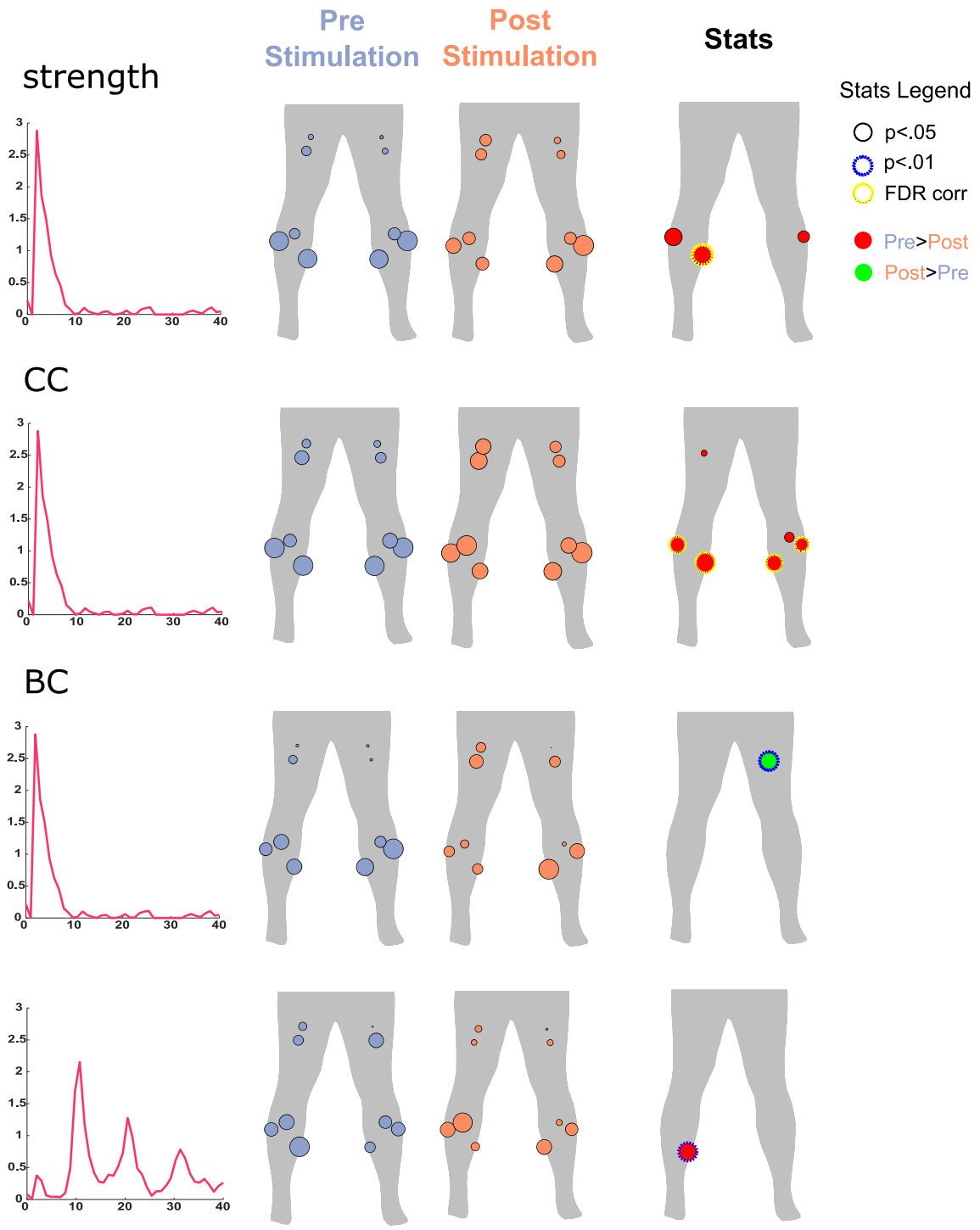

Figure 5. 4: Node-wise analyses of muscle networks

Results are reported only for those network metrics and frequency components where at least one node changed significantly (p<.01) between conditions: strength, clustering coefficients and betweenness-centrality. The left column depicts the frequency component of interest. The second and third columns show the network metric values, obtained for the specific frequency band, for each node before and after the stimulation, respectively. The fourth column represents the statistical results of the node-wise analysis. For each frequency component and metric, only those nodes that were significantly different (p<.05) between conditions (pre vs post) are depicted. Node that changed significantly (p<.01) are contoured by a blue line and those that survived FDR correction are contoured by a yellow line. The colours of the nodes reflect the direction of the effect, with red nodes indicating that the specific metric

decreased after the stimulation and green lines indicating an increase after the stimulation. The size of the nodes indicates the size of the effect.

5.3.4 sEMG results

The acute-term analyses revealed that muscular activation increased especially among the right muscles, which represented the dominant ones for most subjects (11 out of 15): GL ($p<.01$) and SOL ($p<.01$) measured a bigger contraction after the vibrations were delivered. Similarly, a RMS_{PSB} bigger than RMS_{BB} was found also for the left GL ($p<.05$) (Figure 5.5). The right GL and SOL –dominant muscles for 12 out of 17 subjects- showed an increased RMS_{PSB} even across the 4 minutes following the WBVs ($p<.05$). The MF of the left GL decreased significantly after the WBVs when computed over the 45 second-long sEMG signals and on the 4 minute-long ones ($p<.05$). The PSD of the other muscles did not shift towards lower frequencies after the stimulation.

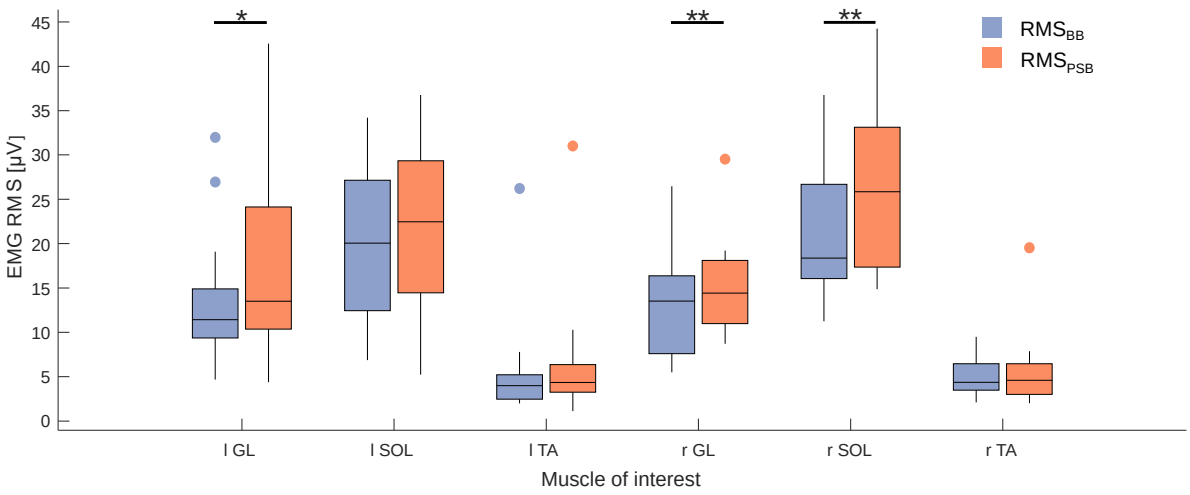

Figure 5. 5: sEMG RMS before and after the WBVs

RMS values of lower limb muscles and their difference between the 45 second-long baseline (BB) and post-stimulation (PSB) trials: (*) and (**) indicate p<.05 and p<.01, respectively.

5.3.5 COP results

The COP parameters (MD_{AP}, MD_{ML}, MV_{AP} and MV_{ML}) were all weakly dependent on the anthropometric measures, with low not-significant Spearman correlation coefficients (ρ<0.5 and $p>.05$). Wilcoxon tests run on 45-second long trials revealed that MD_{ML}, MV_{ML} and MV_{AP}

increased immediately after the WBV (*p<.001, p<.01, p<.001* respectively), while the mean distance covered by the COP in the anterior-posterior direction was not affected by the WBV stimulation (*p*>.025). Moreover, CI_{ML} decreased significantly in the minute following the mechanical vibrations (see Table 5.1 for numerical values and Figure 5.6 for visual representation). When the analyses were run on 4-minute long trials, the postural control in the ML direction appeared recovered and the only significant results concerned metrics in the AP direction, registering a significant increase in MV_{AP} and CI_{AP} after the WBVs (*p<.001* and *p<.05* respectively).

	Acute effect			Long-term effect		
	Before WBV	After WBV	Sig.	Before WBV	After WBV	Sig
MD_{ML} [mm]	1.2048 (0.58993)	2.035 (1.0358)	***<.001***	1.8664 (0.5833)	2.0752 (0.84663)	*n.s.*
MD_{AP} [mm]	3.8638 (1.8355)	4.2152 (2.0284)	*n.s.*	4.4109 (1.8188)	4.7835 (2.4278)	*n.s.*
MV_{ML} [mm/s]	3.1203 (1.2576)	4.1649 (1.9881)	***<.01***	3.7458 (1.0435)	4.0312 (1.5435)	*n.s.*
MV_{AP} [mm/s]	5.8089 (2.7194)	7.0018 (3.2175)	***<.001***	6.4842 (2.7002)	7.8529 (3.6153)	***<.001***
CI_{ML} []	29.0177 (9.6788)	24.2097 (12.4752)	***<.05***	38.7976 (11.0532)	37.5236 (14.3219)	*n.s*
CI_{AP} []	18.9068 (10.073(	21.0632 (11.6938)	n.s.	33.0845+- 14.7674	37.0358 (18.9514)	***<.05***

Table 5. 1: Static posturography results

Mean (SD) values are reported for the static and dynamic stabilometric analysis, during both balance tasks, both before and after the stimulation. The respective significances resulted from the Wilcoxon test are reported as well.

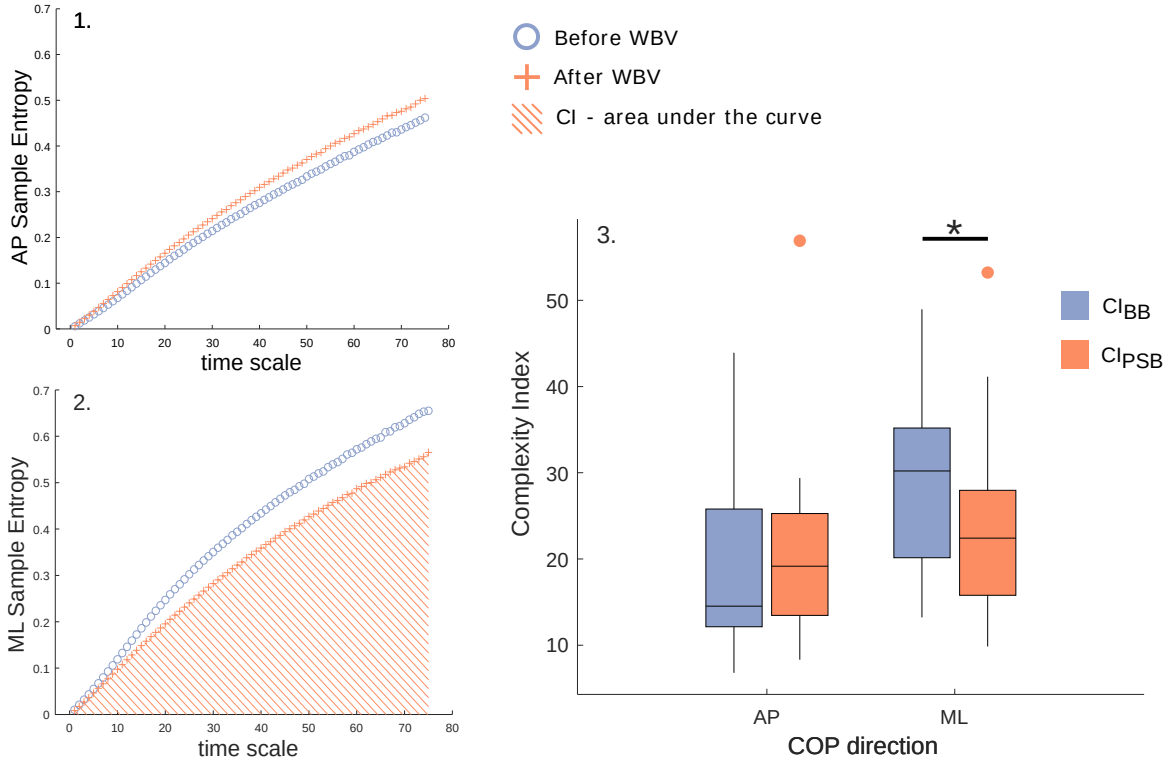

Figure 5. 6: Multiscale sample entropy and complexity index

Plots of sample entropy averaged across subjects in the anterior-posterior (1.) and in the medial-lateral direction (2.) before and after the WBVS (round and cross marker, respectively). In (2.), the area under the curve is displayed to represent the calculation of the CI for the ML direction, post stimulation. In (3.) boxplots of the complexity index are displayed for the ML and AP direction (CI_{ML} and CI_{AP}) and significant differences are depicted by the asterisk (p<.05)).

5.4 Discussions

Based on the results of our previous study (see Chapter 4) and a large body of literature (Alam et al., 2018; Cardinale and Bosco, 2003; Delecluse et al., 2003; Osawa et al., 2013; Rittweger, 2010), we can confidently assume that the sensitivity of soleus and gastrocnemius lateralis muscles spindles was enhanced during the WBVs.

Interestingly, while it is renowned that during WBVs, muscle contraction is boosted, this is the first study that demonstrates that an increased muscle activation persists even after the stimulation itself during upright standing. This increased activity –measured as a bigger RMS sEMG across both GL and the right SOL- is likely to be consequential to an enhancement in the sensitivity of muscles spindles of the related muscles (Cardinale and Bosco, 2003).

However, since this is not a direct measurement of muscle spindle activity, we also tested the hypothesis that the increase of RMS sEMG was caused by fatigue. Since muscle fatigue relates to a diminished capacity to generate force, it should be quantified via mean of MVC-derived or power-derived measures (Vøllestad, 1997). However, when such measures are not available and the EMG recordings are the only one accessible, the median frequency of the EMG power spectrum is the measure that is the least sensitive to noise, and therefore, the recommended one (Stolen et al., 1981). After the WBVs, a reduction of the latter was found only for the left GL, indicating that the increased activity of the sole non-dominant muscle that showed a significant increase after the WBVs is more likely to reflect muscle fatigue than an increased muscle spindle sensitivity (Vøllestad, 1997). However, the MF of the dominant GL and SOL did not shift towards lower frequencies, indicating that, for the dominant plantar flexors, the sEMG increase registered after the WBVs does indeed reflect that their muscle spindles, whose sensitivity was boosted during the WBVs, remain more sensitive even once the stimulation is off. It could also be argued that the observed increase of plantarflexor activation is to be attributed to a substantially different postural stance acquired by participants as a results of vibration-caused illusionary kinaesthetic (Guy M. Goodwin et al., 1972). Illusionary limb displacement –or ‘’aftereffect’’- has in fact been registered after vibrations (Ribot-Ciscar et al., 1998) and would explain an illusionary shift of the COP towards the anterior direction, which would in turn explain the increased activity of both plantarflexors. However, it would not be straightforward to justify why only the dominant plantarflexors showed an enhanced activation, since contraction of both the right and the left ones is needed to stabilise a system that is falling forward. Because the position taken by the participants on the force platform at the beginning of the postural task was not consistent across trials, it is not possible to test this hypothesis. However, the fact that only the dominant plantarflexors showed an increased activation after WBVs suggest that it is more likely for the latter to reflect muscle spindle sensitivity rather than the counteraction to a shift in postural stance.

This inference relates well to our results on corticomuscular coherence, which support the idea that a greater exchange of information between the muscles and the cortex occurred

after the WBVs (J. Liu et al., 2019). Since CMC has been historically utilised to describe the cortical drive to the muscles (Halliday et al., 1995), while recent findings support the idea that it also reflects afferent couplings from the periphery to the cortex itself (Campfens et al., 2013; Witham et al., 2011), the findings of this study can be interpreted in two ways. If read in the first perspective, our results indicate that a bigger cortical drive to the targeted muscles occurred after the stimulation. Using the more recent approach, we may suggest that more sensitive muscle spindles translated into a more abundant flux of proprioceptive feedbacks from the relevant muscles –right SOL and GL. Either way, the increased CMC measured after the WBVs indicates an overall greater interplay between afferent and efferent signals that from the periphery reached the brain -and vice versa- with the purpose of detecting perturbations and correcting them via muscle modulation.

Building on this train of thoughts, the enhanced activity observed after the stimulation in beta band falls well in support of this hypothesis. An increased BBA in the somatosensory areas of the brain –measured as a greater spectral power over C3, CP3, C4 and CP4 (Anderson et al., 1995; Müller et al., 2000) - indicates a greater attempt of the sensorimotor system to preserve the *status quo* (Engel and Fries, 2010; Spitzer and Haegens, 2017). More specifically, a bigger BBA allows the system to more efficiently process proprioceptive signals from the periphery with the ultimate goal of '*recalibrating'* the sensorimotor set or, in our case, adjusting the COP position after an unexpected loss of balance (Engel and Fries, 2010).

The increased need for recalibration and the increased CMC observed after the WBVs are well justified by the fact that, in our participants, the ability of balancing declined immediately after the stimulation. In fact we observe a clear degradation of stability in the medial-lateral direction after the mechanical stimulation, as shown by a larger COP displacement and velocity in the ML plane (Geurts et al., 1993; Palmieri-Smith et al., 2002). In addition to these unambiguous results, a reduced complexity of postural sway in the ML direction further confirms the reduction of the ability to maintain balance and the increased attempt of the system to maintain an upright stance. A smaller CI does in fact indicate a bigger

regularity of COP paths, which is positively correlated to the attention needed to balance and reflects a less automatic postural control (Busa and van Emmerik, 2016; Donker et al., 2007). From our results it could therefore be inferred that, being the ML COP trajectories more regular after the WBVs, participants employed a greater amount of effort to maintain the same upright stance, which is in line with BBA results. The observed balance disruption in the ML direction is reasonable as this is the one that is mostly affected by the WBVs. In the AP direction instead, we observe only an increased COP velocity, which –if not associated with a bigger COP displacement- is not recognised as a sign of worsening balance (Davids et al., 1999; Palmieri-Smith et al., 2002). To link these behavioural results with the physiological ones, when the postural instability grows, lager COP movements lead to greater uncertainty in the periphery, which triggers a bigger demand for oscillatory recalibration (Baker, 2007).

The increased need for cortical recalibration is reflected in the modified muscular networks that are observed after the WBVs. As shown by our results, the weights of the muscle networks are modified –or *recalibrated*- across different frequency ranges after the WBVs. Specifically, the greatest changes are observed in correspondence of those muscles from which the affluence of afferent information increased, namely the soleus and gastrocnemius lateralis. Changes in connection strength are observable across these muscles –bilaterally- especially at very low frequencies (< 5 Hz), which resemble the frequency ranges reported by previous studies on intermuscular coherence during balance (Boonstra et al., 2015, 2008; Mochizuki et al., 2006; Peterson and Ferris, 2019). Moreover, significant differences are detectable for the network metrics at the same frequency. The clustering coefficient of bilateral SOL and GL was significantly reduced after the stimulation, as well as the strength of the right SOL. This could lead to the speculation -well aligned to the current literature (see next paragraph)- that these muscles were less synchronised with the rest of the network and therefore modulated more individually.

It was in fact suggested that IMC at frequencies below 6 Hz reflects subcortical inputs or reflexes, while IMC at higher frequencies reflects cortical ones (Nandi et al., 2019). In details,

the first backs stiffness control while the second supports direction specific muscle control via synergy formation. In our case, the reduced STR and CC found for the plantarflexors indicate a reduction of synchronisation of the latter with other muscles –or reduced IMC- for frequencies below 5 Hz. This might suggest that subcortical inputs (spinal reflexes) were less employed for the modulation of the plantarflexors after the WBVs. Because the plantarflexors were clearly more active after the stimulation, but less spinal modulation was present, it could be that more cortical control was employed for these muscles. However, this conclusion is valid only if IMC at low frequencies reflects modulation via subcortical inputs. To this regard, different views are present in the literature. Loram et al. do in fact suggest that the changes in plantarflexors length observed around 2 Hz during unperturbed balance are the result of active modulation of muscle activity, rather than simple reflex responses to modulate stiffness (Loram et al., 2005b, 2005a). Besides the differentiation of the strategies put into place (SLAT, MLAT or LLAT), the network reconfiguration observed after the WBVs suggest that a *change in the modulation* of muscle activation is likely to have occurred after the stimulation while a cortical-muscular loop might have played an important role in this *recalibration*.

As for the analyses conducted on the four minutes before and after the WBVs, significant results are found only for the sEMG and COP data. The first ones indicate that an enhanced muscle activation of dominant GL and SOL -triggered by the mechanical vibrations- persisted even once the stimulation was off (Merletti and Farina, 2016). The posturography results are instead more complicated to interpret. When computed across the four minutes after the WBVs, the COP parameters seem to stabilise in the ML plane and only an increase of COP velocity in the AP direction is found, which, if not associated with an increase of COP displacement, is more complicated to interpret (Palmieri-Smith et al., 2002). Davids et al.(1999) did in fact report a smaller mean COP velocity in participants who had an anterior cruciate ligament complete rupture than in the control group (Davids et al., 1999), contradicting the common belief that a higher velocity reflects a worse ability of controlling posture (Palmieri-Smith et al., 2002).

The simultaneous recording of a significant increase of mean velocity and no significant change of COP distance might suggest that the average amount of time necessary to cover a fixed distance decreases after vibrations are applied. Although not straightforward, it is reasonable to infer that the decrease of time between one COP position and the next one might be linked to an increased muscle's ability to adjust their length to counterbalance a body sway. This interpretation, although questionable, is in line with a more efficient postural control as the increased AP complexity index –measured over the four minutes after the stimulation- suggests (Donker et al., 2007).

5.5 Limitations

The small sample size is to be listed among the limitations of the current study as a bigger sample size would have allowed more powerful analyses. However, the sample size used here is in line with previous published studies (Airaksinen et al., 2015; Boonstra et al., 2015).

5.6 Conclusions

Our results indicate that WBVs (delivered via a side-alternating Galileo platform) disrupt balance in the ML direction (increment of COP measures) and therefore a bigger effort is necessary for controlling the upright stance (decrement of COP complexity index). At the same time, an increased activation is measured across the targeted muscles, which is thought to reflect an increase of muscle spindle sensitivity that in turn translates into a bigger influx of proprioceptive feedbacks to the cortex (partially explained by CMC increase). A greater cortical control is then employed to recalibrate the sensorimotor system and more reliance is put on proprioceptive feedbacks (BBA increase). The increased oscillatory recalibration translates into the employment of a different muscle modulation (muscle network reconfiguration), needed to readjust the COP position online. In summary, *muscle spindle stimulation led to a recalibration of postural control mechanisms in the acute term*.

Altogether, our results suggest that, while balance is highly disrupted in the first place, the system may be able to recover from such disruption and regain control of postural mechanisms over a period of four minutes.

6. General Discussions

The work presented in this thesis verges around the understanding of how mechanical vibrations -delivered to the whole body via an oscillating platform- can affect the postural responses employed to maintain balance during undisturbed upright standing.

The reason that drove our research towards this direction is the fact that, although the processing of sensory inputs is the backbone of our postural control, the final outcome of bringing the COM back within the base of support is ultimately implemented via the modulation of muscle contraction (Peterka, 2002). Therefore, the stimulation of the musculoskeletal system was central to our design in order to target directly the actuation of postural strategies. A simple way to trigger a muscle contraction and therefore train the muscle to some extent is to evoke a reflex response via mean of mechanical vibrations (Cardinale and Bosco, 2003). The latter do in fact induce muscle fibres to continuously shorten and lengthen: this change in muscle length is detected by sensory organs such as muscle spindles that synchronise the firing rate of *Ia* and *II* afferent fibres with the vibratory cycle, initiating a reflex response –the TVR. The enhanced inflow of afferent signals leads the motor unit (MU) firing rate to not only to increase but also synchronise with the vibratory cycle -within its physiological limits- resulting in an enhanced muscle contraction that is measurable with sEMG.

Among the different means of stimulating skeletal muscles, WBVs was chosen as it represents a safe and easy way to trigger muscle response. Moreover, as it does not require extreme effort by the person receiving it, it is suitable for those groups of people for whom performing intense physical activity could be challenging. In this perspective, WBV stimulation represents a viable training mean for both healthy subpopulations such as athletes and older adults (Mahieu et al., 2006; Osugi et al., 2014; S. M. Verschueren et al., 2004), and more vulnerable ones like children with cerebral palsy (Saquetto et al., 2015) and patients with Parkinson’s disease (Turbanski et al., 2005).

Moreover, this mean of stimulation offered the possibility to not only train the muscular response (via the enhancement of the muscular contraction), but also stimulate the muscle

spindles (via the TVR) (Cardinale and Bosco, 2003) that play a fundamental role in detecting internal and external perturbations during balance (Forbes et al., 2018). In other words, mechanical stimulation via WBVs allowed us to stimulate not only the musculoskeletal system but also the proprioceptive one that dominates in shaping the postural responses. In this perspective, we hypothesised the WBVs had a double effect on upright standing balance. On one side, it had the potential to target the muscle spindles (the *detectors*), affecting the flow of afferent signals that help detecting and reacting to perturbations. On the other side, it affected the skeletal muscles, the *actuators* of the postural response.

The first objective of this thesis was to enhance the sensitivity of the spindles of those muscles that most contribute to the actuation of the ankle strategy: plantarflexors and dorsiflexors. This strategy was specifically targeted because it is the mechanism that dominates during undisturbed upright stance (Blenkinsop et al., 2017; Gatev et al., 1999). In fact, due to our body mass distribution, the human COM is positioned slightly in front of the ankle and, in order not to topple forward because of gravity, the plantarflexors exert a force that pulls the COM backward (Horak and Nashner, 1986; Winter, 1995). Since it is impossible to produce the correct amount of force, the dorsiflexors also act to bring the body forward again and so on in a continuous cycle that manifests as an oscillatory motion around the ankle joint that is well described by the inverted-pendulum model.

6.1 Effect of subject's posture and stimulation frequency on muscles during WBV

As mentioned above, the first goal of this thesis was to define the combination of stimulation frequency and subject posture that triggered the biggest response from the muscles involved in the ankle strategy mechanism. Among the plantarflexors, the gastrocnemius lateralis (GL) and soleus (SOL) were chosen and among the dorsiflexors, the tibialis anterior (TA) was selected. The choice fell on these muscles for three reasons. 1) They are superficial muscles, meaning that sEMG is suitable for the quantification of their activation. 2) Detailed and approved guidelines are available for the placement of the sEMG sensors (Hermens et al.,

2000, 1999). 3) They are relatively distant from each other, reducing the possibility of cross-talk artefacts (Merletti and Farina, 2016).

We hypothesised that a single combination of WBV parameters could result optimal for the three muscles. However, a stimulation that triggered muscle response the most was found only for GL and SOL. For the TA, no WBV stimulation seemed to work particularly better than the others, which is probably because its natural frequency might be located at higher frequencies than those tested (Wakeling et al., 2002a). This partial result may be justified by the fact that during WBVs, two mechanisms are thought to explain the increased muscle activity: TVR on one side and muscle tuning on the other (Cardinale and Bosco, 2003; Cardinale and Wakeling, 2005). While, according to the TVR paradigm, the motor unit firing rate synchronises with every stimulation cycle –as long as it is physiologically feasible-, in the muscle tuning paradigm muscular activation patterns depend on the stimulation frequency. In regard of the latter mechanism, the biggest muscle activation –associated with the greatest level of vibration dampening- is found when the frequency of the impact force is close to the natural frequency of the muscle itself (Wakeling et al., 2002a). Since the natural frequency depends not only on the mass but also on the muscle force produced, the same muscle can have different resonant frequencies depending on its level of contraction (Wakeling and Nigg, 2001a). One simple way to modulate the engagement level of a muscle is by acquiring a specific *static* posture (Carlsöö, 1961; Okada, 1972), which also allows to keep joint kinematics constant, leaving muscle activity the only option for the body through which to dissipate mechanical energy. Muscles such as the Rectus Femoris and the Tibialis Anterior are for example more engaged when a hack squat posture is kept, while the Gastrocnemius and the Soleus are more contracted when a person goes on forefeet (Carlsöö, 1961; Okada, 1972).

We therefore asked our participants to undergo WBV stimulation at different frequencies while holding two static postures: a hack squat and a forefeet one. To investigate the dynamic reaction of each muscle to the mechanical stimulation, an accelerometer was placed on the skin in correspondence of the underlying muscle belly. Moreover, to better

understand the meaning of the change of the muscle oscillations in time and to relate it to its physiological counterpart, the electromyographic activity of each muscle was recorded as well.

Results on muscle dynamics highlighted a pattern that, to the author's knowledge, had never been shown before. The displacements estimated from the accelerations recorded in correspondence of the muscle bellies do in fact peak at first and then stabilise around a constant value for the rest of the trial. However, neither the acceleration of the platform nor the displacement estimated from it showed a similar behaviour. The graphs obtained for both these parameters show a linear increase with a successive stabilisation (plateau) and no "peak phase". Specifically, while the platform displacement values are constant across frequencies, the acceleration maximum value -around which the signal stabilises- increase for increasing frequencies, as expected (Figure 4.5). Because the platform did transmit vibrations in a linear fashion, it can be concluded that the peak-plateau pattern observed from the skin-mounted accelerometers reflects some kind of neuromuscular reaction. Interestingly, the amplitude and duration of the peak depend on both the posture held by the subject and the frequency of the stimulation received, and differ across muscles. Our findings suggest that muscles are characterised by specific reaction times during which the oscillation recorded at the skin level peaks and is then reduced, reaching a steady-state. This behaviour is in line with the muscle tuning paradigm and is likely to reflect the muscle reaction to avoid resonance by increasing its stiffness. Moreover, it further confirms the importance of WBV parameters such as the posture held by the person receiving it and the frequency of the stimulation.

Overall, all muscles presented some common patterns. In the first place, smaller plateau values were observed for higher frequencies. Considering that the amplitude of the platform oscillation did not change across frequencies, it was concluded that higher frequencies were dampened more than lower ones. Since the natural frequencies of the triceps surae muscles are similar and GL one was found to be around 30 Hz (Cesarelli et al., 2010), this result is in line with the muscle tuning paradigm according to which a greater dampening occurs when the stimulation frequency is close to the natural frequency of the tissue (Wakeling

et al., 2002a). This interpretation is supported also by the physiological measures, as the obtained results indicate that both posture and frequency have a significant main effect on GL and SOL WBV-induced activation. More in detail, the RMS-increase of both muscles was significantly bigger in forefeet (FF) than in hack squat (HS). Although it is renowned that the activation of plantarflexors is greater in FF than in HS (Carlsöö, 1961; Okada, 1972), this results indicate that the WBVs trigger a greater response in these muscles when they are more activated, in line with the fact that vibrations are more effective on contracted muscles than on relaxed ones (Burke et al., 1976a). As for the frequency, 25 and 30 Hz evoked greater responses than 15 and 20 Hz, results that are in agreement with the conclusions drawn from the mechanical dynamics. Similarly for the TA, smaller plateau values were found in correspondence of higher frequencies, with 30 Hz leading to the greatest drop after the peak. Although this outcome might suggest that higher frequencies may trigger greatest muscle response, it is important to notice that the physiological counterpart does not support such conclusion. In fact, no significant differences were found neither across frequencies nor posture, which led to conclude that perhaps higher frequencies are necessary to evoke a significant response. This conclusion is sensible because the TA is a small muscle with a small mass and, considering that smaller masses correspond to bigger natural frequencies (Wakeling and Nigg, 2001a), its resonant frequency might be located above 30 Hz (Wakeling et al., 2002a). On a further note, it is important to highlight that the filtering procedure applied to sEMG RMS did allow to avoid the overestimation of muscle activity during WBVs and to correct for the different proportions of signal that were removed for different frequencies.

The second common pattern observable from the soft tissue displacement is that bigger oscillations occurred during HS rather than during FF, both in the peak –reaction- phase and in the plateau –attenuation- one. Because maintaining different postures means forming different kinematic chains, it is reasonable to assume that vibrations propagated differently along the body accordingly to leg geometry and joint stiffness (Lafortune and Lake, 1996). Moreover, our results confirm previous findings showing that the same stimulation led to higher

level of vibrations at the knee level in HS rather than in FF (Harazin and Grzesik, 1998), further confirming the importance of investigating the effect of the posture kept.

The third and last common pattern is observable from the three-dimensional plots of the accelerometer oscillations. As Figure 4.6 shows, the greatest reduction of displacement between the peak and plateau phase (across muscles, frequencies and postures) occurs along the longitudinal direction of the muscle, suggesting activity along the main contraction axis. Moreover, the change of phase of the mechanical response may represent the evidence of a synchronised counter action enabled to dissipate vibration power (Wakeling et al., 2002a).

Altogether, these findings allowed us to draw some general guidelines that might be of use to training professionals and practitioners who are currently using WBVs or are considering it for future applications. 1) It is important to select the WBV parameters in the best possible way since not all WBV stimulations actually induce a significant muscular enhancement (as shown by the TA RMS). 2) Muscles are characterised by specific reaction times –that in our case spanned from four to five seconds- to react to the stimulation and initiate the response that is the actual goal of the stimulation itself. 3) Therefore, dynamic exercises might be less efficacious than static ones because the body kinematic chain is in constant change together with the level of muscle contraction, on which depend muscle sensitivity to vibrations.

More importantly for the scope of this thesis, the reported results indicate that a high frequency stimulation –delivered to a person standing on the forefeet- is more efficacious in triggering a muscular response from the plantarflexors (GL and SOL). As for the analysed dorsiflexor muscle (TA), our inconclusive findings suggest that the best stimulation frequency might not reside within the range tested. Therefore, it was concluded that, in order to evoke the greatest response from the plantarflexors muscles (which play a fundamental role for balancing during upright standing) with the device available in the laboratory, *a stimulation of 30 Hz* delivered to a person undergoing a training *in forefeet* would have represented the best choice.

6.2 Effect of WBV on postural control

To test whether the stimulation of plantarflexors muscle spindles affected postural control mechanisms, trials of undisturbed upright stance were recorded before and after the WBVs. The balance task was kept to its simplest as the goal was to investigate natural balance. Moreover, in order to isolate the proprioceptive response, the other systems involved in the maintenance of a stable posture –vestibular and visual- were not specifically stimulated during the balance tasks.

Most studies involving WBVs and balance assessment actually investigate the long-term effect of intense stimulation. In healthy adults, for example, balance control was assessed two days before and two days after a WBV training of four weeks (tree sessions per week, with sets of 3 to 20 minutes WBs) (Ritzmann et al., 2014). Similarly, interventions of eight and six weeks (static HS posture and vibrations of 30 Hz for the first one, dynamic exercises and variable stimulation frequency and amplitude for the second one) were evaluated in term of postural control, yielding discording outcomes (Dallas et al., 2017; Mahieu et al., 2006). Results from the time-up-and-go (TUG) test and the tandem standing time suggested that, with older adults, training routines of six weeks and six months of static WBV exercises were beneficial for balance (Bautmans et al., 2005; Osugi et al., 2014).

A different approach was instead used in our study as we investigated the acute effect of WBV stimulation on postural control rather than the effect of a long-term intervention. To quantify such effect, physiological measures were collected on top of behavioural ones, to provide insights about the mechanisms producing the latter, namely the COP displacement observable from the posturography. To our knowledge, this is the first time the WBV effect on corticomuscular coherence and intermuscular coherence is investigated.

Among the several results reported in this thesis, the increased muscle activation registered during the balance task *after* the WBVs –quantified as sEMG RMS- is probably the most interesting finding of all. In fact, on one side, the RMS is a variable wildly used to quantify

the extent of muscle activation (Merletti and Farina, 2016), making it reliable and of simple interpretation; on the other side, the sEMG was collected during a static task so it is not compromised by motion artefacts that are instead more common during WBVs. The enhanced muscle activity that was registered *after the stimulation* predominantly for the dominant SOL and GL suggests that a greater amount of MUs were firing after the WBVs rather than before (Merletti and Farina, 2016), although the balance task was unaltered. If read in the perspective of “muscle spindle stimulation”, this result is likely to reflect a larger sensitivity of the spindles of the plantarflexors that were targeted by the stimulation (Cardinale and Bosco, 2003). Moreover, the bigger GL and SOL activation did not occur only in the first trial following the vibrations, but persisted throughout the four minutes after the stimulation, revealing the extent of WBVs effect on the neuromuscular system. This result suggests that muscle spindles, which were stimulated during the WBVs, remain more sensitive even once the stimulation is off. However, this outcome alone does not necessarily relate to how postural control strategies might have been affected by WBVs. An insight on this can be offered by the results obtained from the corticomuscular and intermuscular coherence (CMC and IMC) analyses, if read jointly with the quantification of cortical activity in beta band.

CMC analyses indicate that –after the stimulation- a significantly bigger corticomuscular coherence is observable between the dominant plantarflexors and the contralateral EEG activity around 20 Hz. Although it is true that very few studies found CMC during undisturbed upright standing, it is important to highlight that the CMC coherence values resulted from our study are in line with the order of magnitude of those of previous studies (Jacobs et al., 2015; Murnaghan et al., 2014; Vecchio et al., 2008). Moreover, while during sustained contraction the coherence spectra show a single broad peak across the whole frequency range 15-30 Hz (Andrykiewicz et al., 2007; Murnaghan et al., 2014; Ushiyama et al., 2017; Witham et al., 2011), during balance tasks, lower peaks are visible at different frequencies in the same beta band (Jacobs et al., 2015). Once more, our results are in line with the literature since we observe different peaks in the range 15-30 Hz. It is possible that differences between the conditions are appreciable *only because* the sensorimotor system

was stimulated by the WBVs which triggered a greater exchange of information between the periphery and the nervous system. In fact, CMC is thought to represent both afferent and efferent signals from the proprioceptive organs to the CNS and vice versa (J. Liu et al., 2019). Therefore, the increased CMC observed for the dominant GL and SOL, at 23 and 19 Hz respectively, might reflect either a greater influx of proprioceptive feedback from the spindles -that are more sensitive and possibly more responsive after the vibrations- or a larger cortical drive to the muscles, needed after the vibrations to maintain a steady motor output.

The cortical activity in beta band was quantified as the average power between 15 and 30 Hz of the signals recorded from the electrodes overlying the sensorimotor cortex. In this thesis, we did not reconstruct the EEG sources because, since neither the participant-specific electrode positions nor the structural MRI scan were available, the accuracy of the reconstructed source locations would have been limited (Michel et al., 2004). Therefore, we analysed the scalp EEG signals measured by the electrodes C3, C4, CP3 and CP4, which are employed in the literature for analysing the sensorimotor cortex activation (Müller et al., 2000; Southgate et al., 2010; Tsuchimoto et al., 2017). BBA was found to be significantly bigger after the WBVs, suggesting a bigger extent of the sensorimotor system to maintain the status quo (Engel and Fries, 2010). If read in the perspective of “postural control following muscle spindle stimulation”, this finding indicates a greater effort to preserve a stable posture and possibly a greater processing of proprioceptive feedbacks for the recalibration of the sensorimotor set (Baker, 2007).

The behavioural results obtained from the COP trajectories are helpful to understand the reason behind the greater need for sensorimotor recalibration that seems to characterise balance after the WBVs. Among the many variables available to quantify balance, the mean COP distance (MD) and the mean COP velocity (MV) were chosen as the first one is associated with the postural control effectiveness, while the second one with the regulatory activity put into place during postural control (Kim et al., 2012; Prieto et al., 1996). Moreover, both of them were proven to be reliable measures for double-legged stance trials (Le Clair and

Riach, 1996; Murray et al., 1975). Since a simultaneous increase of both COP MD and MV suggests a decreased ability to maintain balance (Palmieri-Smith et al., 2002), it was quite straightforward to conclude that the ability to maintain an upright stance was compromised by the WBVs in the acute term, especially in the frontal plane. This result is sensible as the stimulation occurred mainly in the medial-lateral direction and is further confirmed by a decrease of the complexity of the COP trajectory registered in this plane. The smaller complexity index (CI) registered in the first minute after the stimulation does in fact suggest a reduced automaticity and efficacy of the postural control strategies that was also measured for pathological subjects when compared to healthy ones (Busa et al., 2016; Busa and van Emmerik, 2016). In other words, our results suggest that the mechanical stimulation destabilised the postural control especially in the ML direction to the point that a greater effort was needed to balance, which well correlates with the increased cortical activity in beta band (Busa and van Emmerik, 2016; Donker et al., 2007).

Last but not least, the results obtained from the analyses on intermuscular coherence are in support of the fact that, after the WBVs, balance was destabilised and a greater effort was necessary to keep an upright posture, triggering a greater need for sensorimotor recalibration (Baker, 2007). The muscle network estimated in the first balance trial after the stimulation did in fact differ from the one before, suggesting that different activation patterns were employed after the muscle spindles were stimulated. Specifically and most interestingly, the greatest differences between conditions are appreciable for the dominant SOL and GL, that are the muscles targeted by the WBVs. Moreover, the biggest changes occur at low frequencies, which are the frequencies at which stronger IMC values are reported in the literature (Boonstra et al., 2015, 2008; Mochizuki et al., 2006; Peterson and Ferris, 2019). These network alterations are likely to reflect the recalibration of the sensorimotor system that occurred in response of a compromised balance. Although it could be speculated that lower clustering coefficients of SOL and GL found after the WBVs might indicate that the recruitment of these muscles occurred in a more “individual” and less synchronised fashion, we do not want to push this interpretation too far as the physiological interpretation of muscle network

metrics is still quite limited in the literature. Moreover, different interpretations of the physiological counterpart of low-frequency IMC are available too (Loram et al., 2005a; Nandi et al., 2019) and we believe future studies are necessary to prove whether WBVs are capable of altering the *type* of postural responses employed during balance (short, medium and long latencies).

Altogether, these results suggest that medial-lateral stability is compromised by the WBVs in the acute term and that a greater effort is therefore needed to maintain an undisturbed upright stance *after* the stimulation than *before*. On top of this and since our findings suggest that muscle spindles remain more sensitive even *after* the stimulation, our results might indicate that the stimulation evoked a more substantial interplay between the periphery and the CNS, ultimately leading to sensorimotor recalibration.

It is important to highlight that the above interpretation applies to the understanding of the *immediate effect* of WBVs on postural control. In fact, these results subsist only in the first minute after the WBVs and tend to fade away with time, which suggests that the increased communication between muscles and the brain –induced by the mechanical stimulation- might have a short lifespan. Differently from neural markers, COP and EMG markers persist even when computed on a longer time scale (four minutes). More comprehensive paradigms are needed to test this hypothesis, but it could be speculated that, after the acute response, balance seems not only to return to pre-stimulation levels, but also to improve after the WBVs. The argument in support of this statement is twofold. On one side, a greater COP velocity is observed in the AP direction after the stimulation but, contrarily to what is usually reported in the literature (Palmieri-Smith et al., 2002), it is not associated with bigger COP fluctuations. Since the same distance was covered over a shorter time after the WBVs (same COP displacement but bigger COP velocity), this may reflect the ability of the system to recruit muscles faster and therefore be more prompt to react to unexpected perturbations (Loram et al., 2005a). On the other side, the complexity of the AP COP trajectory increases significantly in the long-term, suggesting a re-appropriation of a more autonomous and spontaneous

postural control. Moreover, reading this result jointly with the fact that no alteration in the AP COP displacement was recorded after the WBVs, it could be speculated that the postural control employed after the vibrations was not only more spontaneous, but also –possibly- more efficient (Donker et al., 2007).

6.3 Thesis key findings

To summarise, the major findings of this thesis are related to 1) the customisation of WBV stimulation for the enhancement of calf muscles activation and 2) the effect of calf muscle stimulation via WBVs on postural control. Our findings demonstrate that, by selecting the appropriate (static) posture and stimulation frequency it is possible to target specific muscles and therefore to maximise their response to the stimulation. Specifically, a 30 Hz stimulus delivered to a person standing on the forefeet via a side-oscillating platform evokes the greatest response from the plantarflexors. When investigating the effect of the latter stimulation on postural control, our results suggest that the muscle spindle sensitivity, which is boosted by the mechanical stimuli, remain enhanced even after the WBVs. On the behavioural side, the WBVs compromise balance in the acute term, but not in the long one. On the physiological side, the stimulation of the proprioceptive system boosts the interplay between the periphery and the central nervous system, favouring the processing of proprioceptive feedbacks for the maintenance of balance, ultimately leading to sensorimotor recalibration.

6.4 Future works

Starting from the drawbacks of the study designs, a potential future work is suggested for the continuation of this line of research.

Beside the fact that synchronised sEMG signals and accelerations were not available for the first study, another issue that hinders the potential of this design is the determination of the natural frequency of the specific muscles for each subject. According to Wakeling et al. (2002), the natural frequency of a specific muscle corresponds to the peak of the PSD obtained from the relevant sEMG signal recorded in response to white-noise stimulation (Wakeling et

al., 2002a). Since the platform available in the laboratory was not controllable remotely but could work just at predefined frequencies, the response of muscles to a white-noise driven displacement could not be measured. However, the definition of subject- and muscle-specific natural frequencies would not only help interpret the physiological and mechanical outcomes, but also determine the most effective combination of WBV parameters at an individual level.

The rational continuation of our research would be to investigate whether the *type* of postural responses employed by the participants change after muscle spindles are stimulated. In other words, the next step would be to research whether the modulation of postural response shifts from subcortical to cortical -or vice versa- after the stimulation of muscle spindles.

Because postural response latencies are measured as the time between the onset perturbation (i.e. surface translation) and the first measurable increase of EMG activity (Huisinga and Horak, 2014), they are measurable only in response to a known disturbance, artificially triggered by the experimenter. Since they cannot be quantified during undisturbed balance, we are not able to discern short latency responses from medium and long ones, and therefore could not draw any conclusions on whether or not cortical-loops were the preferred ones after the WBVs.

Since it is suggested that a decrease in response latencies reflects a switch to (shorter) spinal reflex pathway (Ackermann et al., 1991), it would be reasonable to measure whether the latencies of the postural responses increase or decrease after the WBV. An example of a study design that would allow to not only measure the latencies but also increase the reliability of the results includes the recording of several WBV stimulations and the respective post-stimuli balance trials. More in details, four one-minute balance trials can be collected at the beginning of the experiment (baseline) and after the different WBV stimulations. During the balance tasks, sudden translations of the platform would constitute the external artificial perturbation. To increase the SNR, several WBV stimulations would be delivered with the specific outlined in the first experimental chapter. Averaging the response times before and after the WBVs would also allow to compare acute responses and long term ones, while

increasing the reliability of the results. Postural responses with shorter latencies after the WBVs could reflect a shift in the control from cortical to spinal and vice versa for longer ones.

A deeper understanding of the extent to which mechanical vibrations boost muscle spindle sensitivity and whether this leads to a change in the postural strategies preferred by the CNS could result useful for the implementation of rehabilitation protocols for different subpopulations, including older adults.

Besides the applicability of these results, it is important to remember that WBVs –other than having the ability to stimulate muscle spindle sensitivity- led to a clear disruption of balance in the minute after the stimulation. While this might be a natural and unavoidable consequence of the substantial shake to which the body is exposed in the sagittal plane, it would be worth exploring whether delivering vibrations in alternative ways could impact postural control while not disrupting balance in the acute term (which might not be viable for the elderly). Promising results come from a study delivering light vibrations to the sole of the foot (Zhou et al., 2016), which are found to boost postural control, as shown by the increment of complexity of the posturography. Different delivery methods should therefore be explored via the joint analyses of behavioural measures and physiological ones as it was proposed here. In this way, it will be possible to understand not only *whether* vibrations-induced muscle spindle stimulation actually improves postural control but also *where* the increased postural control originates, namely from a shift in control strategy, higher influx of proprioceptive inputs or system recalibration.

References

Abercromby, A., Amonette, W., Layne, C., Mcfarlin, B., Hinman, M., Paloski, W., 2007a. Variation in neuromuscular responses during acute whole-body vibration exercise. Med. Sci. Sports Exerc. 39, 1642–1650. https://doi.org/10.1249/mss.0b013e318093f551

Abercromby, A., Amonette, W., Layne, C., Mcfarlin, B., Hinman, M., Paloski, W., 2007b. Vibration exposure and biodynamic responses during whole-body vibration training. Med. Sci. Sports Exerc. 39, 1794–1800. https://doi.org/10.1249/mss.0b013e3181238a0f

Ackermann, H., Dichgans, J., Guschlbauer, B., 1991. Influence of an acoustic preparatory signal on postural reflexes of the distal leg muscles in humans. Neurosci. Lett. 127, 242–246. https://doi.org/10.1016/0304-3940(91)90803-2

Airaksinen, K., Lehti, T., Nurminen, J., Luoma, J., Helle, L., 2015. Cortico-muscular coherence parallels coherence of postural tremor and MEG during static muscle contraction. Neurosci. Lett. 602, 22–26. https://doi.org/10.1016/j.neulet.2015.06.034

Alam, M.M., Khan, A.A., Farooq, M., 2018. Effect of whole-body vibration on neuromuscular performance: A literature review. Work 59, 571–583. https://doi.org/10.3233/WOR-182699

Anderson, C.W., Devulapalli, S., Stopz, E.A., 1995. EEG Signal Classification with Different Signal Representations, in: Proceedings of 1995 IEEE Workshop on Neural Networks for Signal Processing. pp. 475–483. https://doi.org/doi: 10.1109/NNSP.1995.51492

Androulidakis, A.G., Doyle, L.M.F., Gilbertson, T.P., Brown, P., 2006. Corrective movements in response to displacements in visual feedback are more effective during periods of 13-35 Hz oscillatory synchrony in the human corticospinal system. Eur. J. Neurosci. 24, 3299–3304. https://doi.org/10.1111/j.1460-9568.2006.05201.x

Androulidakis, A.G., Doyle, L.M.F., Yarrow, K., Litvak, V., Gilbertson, T.P., Brown, P., 2007. Anticipatory changes in beta synchrony in the human corticospinal system and associated improvements in task performance. Eur. J. Neurosci. 25, 3758–3765. https://doi.org/10.1111/j.1460-9568.2007.05620.x

Andrykiewicz, A., Patino, L., Naranjo, J.R., Witte, M., Hepp-Reymond, M.C., Kristeva, R., 2007. Corticomuscular synchronization with small and large dynamic force output. BMC Neurosci. 8, 1–12. https://doi.org/10.1186/1471-2202-8-101

AX3 OMGUI Configuration and Analysis Tool, v38, GitHub, 2015.

Baker, S.N., 2007. Oscillatory interactions between sensorimotor cortex and the periphery. Curr. Opin. Neurobiol. 17, 649–655. https://doi.org/10.1016/j.conb.2008.01.007

Baker, S.N., Olivier, E., Lemon, R.N., 1997. Coherent oscillations in monkey motor cortex and hand muscle EMG show task-dependent modulation. J. Physiol. 501, 225–241.

Barrat, A., Barthélemy, M., Pastor-Satorras, R., Vespignani, A., 2004. The architecture of complex weighted networks. Proc. Natl. Acad. Sci. U. S. A. 101, 3747–3752. https://doi.org/10.1073/pnas.0400087101

Barroso, F.O., Torricelli, D., Moreno, J.C., Taylor, J., Gomez-Soriano, J., Bravo-Esteban, E., Piazza, S., Santos, C., Pons, J.L., 2014. Shared muscle synergies in human walking and cycling. J. Neurophysiol. 112, 1984–1998. https://doi.org/10.1152/jn.00220.2014

Basmajian, J. V., 1978. Muscle Alive: Their functions revealed by electromyography, 4th editio. ed. Baltimore: Williams & Wilkins.

Bautmans, I., Van Hees, E., Lemper, J.C., Mets, T., 2005. The feasibility of whole body vibration in institutionalised elderly persons and its influence on muscle performance, balance and mobility: A randomised controlled trial [ISRCTN62535013]. BMC Geriatr. 5, 1–8. https://doi.org/10.1186/1471-2318-5-17

Benjamini, Y., Hochberg, Y., 1995. Controlling the False Discovery Rate: A Practical and Powerful Approach to Multiple Testing. J. R. Stat. Soc. 57, 289–300. https://doi.org/10.2307/2346101

Berger, H., Gloor, P., 1969. On the Electroencephalogram of Man: the Fourteen Original Reports on the Human Electroencephalogram, Translated. ed. Elsevier.

Bernstein, N., 1967. The Co-ordination and Regulation of Movements,. Pergamon.

Bifulco, P., Cesarelli, M., Romano, M., Fratini, A., 2013. Comments on the article '"Rectification of SEMG as a tool to demonstrate synchronous motor unit activity during vibration."' J. Electromyogr. Kinesiol. 23, 1250–1251. https://doi.org/10.1016/j.jelekin.2012.09.009

Biggs, N., Lloyd, E.K., 1999. Graph Theory 1736-1936. New York: Oxford University Press.

Blenkinsop, G.M., Pain, M.T.G., Hiley, M.J., 2017. Balance control strategies during perturbed and unperturbed balance in standing and handstand. R. Soc. Open Sci. 4. https://doi.org/10.1098/rsos.161018

Bogaerts, A., Verschueren, S., Delecluse, C., Claessens, A.L., Boonen, S., 2007. Effects of whole body vibration training on postural control in older individuals: A 1 year randomized controlled trial. Gait Posture 26, 309–316. https://doi.org/10.1016/j.gaitpost.2006.09.078

Bongiovanni, B.Y.L.G., Hagbartht, K., Stjernbergt, L., 1990. Prolonged muscle vibration reducing motor output in maximal voluntary contractions in man. J. Physiol. 423, 15–26.

Bongiovanni, L.G., Hagbarth, K.E., 1990. Tonic vibration reflexes elicited during fatigue from maximal voluntary contractions in man. J. Physiol. 423, 1–14. https://doi.org/10.1113/jphysiol.1990.sp018007

Boonstra, T.W., 2013. The potential of corticomuscular and intermuscular coherence for research on human motor control. Frontiers (Boulder). 7, 907–915. https://doi.org/10.1038/nn1309

Boonstra, T.W., Breakspear, M., 2012. Neural mechanisms of intermuscular coherence: implications for the rectification of surface electromyography. J. Neurophysiol. 107, 796–807. https://doi.org/10.1152/jn.00066.2011

Boonstra, T.W., Danna-Dos-Santos, A., Xie, H.B., Roerdink, M., Stins, J.F., Breakspear, M., 2015. Muscle networks: Connectivity analysis of EMG activity during postural control. Sci. Rep. 5, 1–14. https://doi.org/10.1038/srep17830

Boonstra, T.W., Roerdink, M., Daffertshofer, A., Van Vugt, B., Van Werven, G., Beek, P.J., 2008. Low-alcohol doses reduce common 10- to 15-Hz input to bilateral leg muscles during quiet standing. J. Neurophysiol. 100, 2158–2164. https://doi.org/10.1152/jn.90474.2008

Bosco, C., Colli, R., Introini, E., Cardinale, M., Tsarpela, O., Madella, a, Tihanyi, J., Viru, a, 1999. Adaptive responses of human skeletal muscle to vibration exposure. Clin. Physiol. 19, 183–187. https://doi.org/10.1046/j.1365-2281.1999.00155.x

Bronstein, A.M., 1986. Suppression of visually evoked postural responses. Exp. Brain Res. 63, 655–658. https://doi.org/10.1007/BF00237488

Brunet, D., Murray, M.M., Michel, C.M., 2011. Spatiotemporal analysis of multichannel EEG: CARTOOL. Comput. Intell. Neurosci. 2011. https://doi.org/10.1155/2011/813870

Bryant, E.C., Trew, M.E., Bruce, A.M., Kuisma, R.M.E., Smith, A.W., 2005. Gender differences in balance performance at the time of retirement. Clin. Biomech. 20, 330–335. https://doi.org/10.1016/j.clinbiomech.2004.11.006

Bullmore, E., Sporns, O., 2009. Complex brain networks: Graph theoretical analysis of structural and functional systems. Nat. Rev. Neurosci. 10, 186–198. https://doi.org/10.1038/nrn2575

Burden, A., 2010. How should we normalize electromyograms obtained from healthy participants? What we have learned from over 25years of research. J. Electromyogr. Kinesiol. 20, 1023–1035. https://doi.org/10.1016/j.jelekin.2010.07.004

Burke, D., Hagbarth, K.E., Lofstedt, L., Wallin, B.G., 1976a. The responses of human muscle spindle endings to vibration during isometric contraction. J. Physiol. 261, 695–711. https://doi.org/10.1113/jphysiol.1976.sp011581

Burke, D., Hagbarth, K.E., Löfstedt, L., Wallin, B.G., 1976b. The responses of human muscle spindle endings to vibration during non-contracting muscles. J. Physiol. 261, 695–711. https://doi.org/10.1113/jphysiol.1976.sp011581

Burke, D., Schiller, H.H., 1976. Discharge pattern of single motor units in the tonic vibration

reflex of human triceps surae. J. Neurol. Neurosurg. Psychiatry 39, 729–741. https://doi.org/10.1136/jnnp.39.8.729

Busa, M.A., Jones, S.L., Hamill, J., van Emmerik, R.E.A., 2016. Multiscale entropy identifies differences in complexity in postural control in women with multiple sclerosis. Gait Posture 45, 7–11. https://doi.org/10.1016/j.gaitpost.2015.12.007

Busa, M.A., van Emmerik, R.E.A., 2016. Multiscale entropy: A tool for understanding the complexity of postural control. J. Sport Heal. Sci. 5, 44–51. https://doi.org/10.1016/j.jshs.2016.01.018

Campfens, S.F., Schouten, A.C., Putten, M.J.A.M. Van, Kooij, H. Van Der, 2013. Quantifying connectivity via efferent and afferent pathways in motor control using coherence measures and joint position perturbations. Exp. Brain Res. 228, 141–153. https://doi.org/10.1007/s00221-013-3545-x

Cardinale, M., Bosco, C., 2003. The use of vibration as an exercise intervention. Exerc. Sport Sci. Rev. 31, 3–7.

Cardinale, M., Lim, J., 2003a. Electromyography activity of vastus lateralis muscle during whole-body vibrations of different frequencies. J. Strength Cond. Res. 17, 621–624. https://doi.org/10.1519/1533-4287(2003)017<0621:EAOVLM>2.0.CO;2

Cardinale, M., Lim, J., 2003b. The acute effects of two different whole body vibration frequencies on vertical jump performance. Med Sport 56, 287–292.

Cardinale, M., Wakeling, J., 2005. Whole body vibration exercise: Are vibrations good for you?

Br. J. Sports Med. 39, 585–589. https://doi.org/10.1136/bjsm.2005.016857

Carlsöö, S., 1961. The static muscle load in different work positions: An electromyographic study. Ergonomics 4, 193–211. https://doi.org/10.1080/00140136108930520

Casadio, M., Morasso, P.G., Sanguineti, V., 2005. Direct measurement of ankle stiffness during quiet standing: Implications for control modelling and clinical application. Gait Posture 21, 410–424. https://doi.org/10.1016/j.gaitpost.2004.05.005

Caton, R., 1875. The Electric Currents of the Brain. Br. Med. J. 2, 278. https://doi.org/10.1080/00029238.1970.11080764

Cesarelli, M., Fratini, A., Bifulco, P., La Gatta, A., Romano, M., Pasquariello, G., 2010. Analysis and modelling of muscles motion during whole body vibration. EURASIP J. Adv. Signal Process. 2010, 26–28. https://doi.org/10.1155/2010/972353

Chang, C.J., Yang, T.F., Yang, S.W., Chern, J.S., 2016. Cortical modulation of motor control biofeedback among the elderly with high fall risk during a posture perturbation task with augmented reality. Front. Aging Neurosci. 8, 1–13. https://doi.org/10.3389/fnagi.2016.00080

Chiari, L., Rocchi, L., Cappello, A., 2002. Stabilometric parameters are affected by anthropometry and foot placement. Clin. Biomech. 17, 666–677. https://doi.org/10.1016/S0268-0033(02)00107-9

Cochrane, D.J., Sartor, F., Winwood, K., Stannard, S.R., Narici, M. V., Rittweger, J., 2008. A Comparison of the Physiologic Effects of Acute Whole-Body Vibration Exercise in Young

and Older People. Arch. Phys. Med. Rehabil. 89, 815–821. https://doi.org/10.1016/j.apmr.2007.09.055

Cochrane, D. J., Stannard, S.R., Sargeant, A.J., Rittweger, J., 2008. The rate of muscle temperature increase during acute whole-body vibration exercise. Eur. J. Appl. Physiol. 103, 441–448. https://doi.org/10.1007/s00421-008-0736-4

Cohen, M.X., 2014. Analyzing Neural Time Series Data. MIT Press; 1 edition.

Conway, B.A., Halliday, D.M., Farmer, S.F., Shahani, U., Maas, P., Weir, A.I., Rosenberg, J.R., 1995. Synchronization between motor cortex and spinal motoneuronal pool during the performance of a maintained motor task in man. J. Physiol. 489, 917–924.

Costa, M., Goldberger, A.L., Peng, C.K., 2005. Multiscale entropy analysis of biological signals. Phys. Rev. E - Stat. Nonlinear, Soft Matter Phys. 71, 1–18. https://doi.org/10.1103/PhysRevE.71.021906

Costa, M., Goldberger, A.L., Peng, C.K., 2002. Multiscale Entropy Analysis of Complex Physiologic Time Series. Phys. Rev. Lett. 89, 6–9. https://doi.org/10.1103/PhysRevLett.89.068102

Croft, R.J., Barry, R.J., 2000. EOG correction: Which regression should we use? Psychophysiology 37, 123–125. https://doi.org/10.1017/S0048577200001633

Dallas, G., Mavvidis, A., Kirialanis, P., Papouliakos, S., 2017. The effect of 8 weeks of whole body vibration training on static balance and explosive strength of lower limbs in physical education students. Acta Gymnica. https://doi.org/10.5507/ag.2017.018

Davids, K., Kingsbury, D., George, K., O'Connell, M., Stock, D., 1999. Interacting constraints and the emergence of postural behavior in acl-deficient subjects. J. Mot. Behav. 31, 358–366. https://doi.org/10.1080/00222899909601000

Day, B.L., Séverac Cauquil, A., Bartolomei, L., Pastor, M.A., Lyon, I.N., 1997. Human body-segment tilts induced by galvanic stimulation: A vestibularly driven balance protection mechanism. J. Physiol. 500, 661–672. https://doi.org/10.1113/jphysiol.1997.sp022051

De Gail, P., Lance, J.W., Neilson, P.D., 1966. Differential effects on tonic and phasic reflex mechanisms produced by vibration of muscles in man. J. Neurol. Neurosurg. Psychiatry 29, 1–11. https://doi.org/10.1136/jnnp.29.1.1

Delecluse, C., Roelants, M., Diels, R., Koninckx, E., Verschueren, S., 2005. Effects of Whole Body Vibration Training on Muscle Strength and Sprint Performance in Sprint-Trained Athletes. Int. J. Sports Med. 26, 1662–668. https://doi.org/10.1016/S0162-0908(08)70351-9

Delecluse, C., Roelants, M., Verschueren, S., 2003. Strength increase after whole-body vibration compared with resistance training. Med. Sci. Sports Exerc. 35, 1033–1041. https://doi.org/10.1249/01.MSS.0000069752.96438.B0

Di Giminiani, R., Masedu, F., Padulo, J., Tihanyi, J., Valenti, M., 2015. The EMG activity-acceleration relationship to quantify the optimal vibration load when applying synchronous whole-body vibration. J. Electromyogr. Kinesiol. 25, 853–859. https://doi.org/10.1016/j.jelekin.2015.09.004

Di Giminiani, R., Masedu, F., Tihanyi, J., Scrimaglio, R., Valenti, M., 2013. The interaction between body position and vibration frequency on acute response to whole body

vibration. J. Electromyogr. Kinesiol. 23, 245–251. https://doi.org/10.1016/j.jelekin.2012.08.018

Dijkstra, T.M.H., Schoner, G., Gielen, C.C.A.M., 1994. Temporal stability of the action-perception cycle for postural control in a moving visual environment T.M.H. Exp. Brain Res. 97, 477–486.

Dolny, D.G., Reyes, F.C.G., 2008. Whole body vibration exercise: Training and benefits. Curr. Sports Med. Rep. 7, 152–157. https://doi.org/10.1097/01.CSMR.0000319708.18052.a1

Donker, S.F., Roerdink, M., Greven, A.J., Beek, P.J., 2007. Regularity of center-of-pressure trajectories depends on the amount of attention invested in postural control. Exp. Brain Res. 181, 1–11. https://doi.org/10.1007/s00221-007-0905-4

Ebersbach, G., Edler, D., Kaufhold, O., Wissel, J., 2008. Whole Body Vibration Versus Conventional Physiotherapy to Improve Balance and Gait in Parkinson's Disease. Arch. Phys. Med. Rehabil. 89, 399–403. https://doi.org/10.1016/j.apmr.2007.09.031

Engel, A.K., Fries, P., 2010. Beta-band oscillations-signalling the status quo? Curr. Opin. Neurobiol. 20, 156–165. https://doi.org/10.1016/j.conb.2010.02.015

Fagnani, F., Giombini, A., Di Cesare, A., Pigozzi, F., Di Salvo, V., 2006. The effects of a whole-body vibration program on muscle performance and flexibility in female athletes. Am. J. Phys. Med. Rehabil. 85, 956–962. https://doi.org/10.1097/01.phm.0000247652.94486.92

Farmer, S.F., 1998. Rhythmicity, synchronization and binding in human and primate motor systems. J. Physiol. 509, 3–14. https://doi.org/10.1111/j.1469-7793.1998.003bo.x

Field, A., 2013. Discovering Statistics using IBM SPSS statistics, 4th ed. SAGE Publication Ltd.

Fitzpatrick, R., Mccloskey, D.I., 1994. Proprioceptive , visual and vestibular thresholds for the perception of sway during standing in humans 173–186.

Fitzpatrick, R.C., Gorman, R.B., Burke, D., Gandevia, S.C., 1992. Postural proprioceptive reflexes in standing human subjects: bandwidth of response and transmission characteristics. J. Physiol. 458, 69–83.

Forbes, P.A., Chen, A., Blouin, J.S., 2018. Sensorimotor control of standing balance. Handb. Clin. Neurol. 159, 61–83. https://doi.org/10.1016/B978-0-444-63916-5.00004-5

Fratini, A., Bifulco, P., Romano, M., Clemente, F., Cesarelli, M., 2014. Simulation of surface EMG for the analysis of muscle activity during whole body vibratory stimulation. Comput. Methods Programs Biomed. 113, 314–322. https://doi.org/10.1016/j.cmpb.2013.10.009

Fratini, A., Bonci, T., Bull, A., 2016. Whole body vibration treatments in postmenopausal women can improve bone mineral density: Results of a stimulus focussed meta-analysis. PLoS One 11, 1–16. https://doi.org/10.1371/journal.pone.0166774

Fratini, A., Cesarelli, M., Bifulco, P., Romano, M., 2009a. Relevance of motion artifact in electromyography recordings during vibration treatment. J. Electromyogr. Kinesiol. 19, 710–718. https://doi.org/10.1016/j.jelekin.2008.04.005

Fratini, A., La Gatta, A., Bifulco, P., Romano, M., Cesarelli, M., 2009b. Muscle motion and EMG activity in vibration treatment. Med. Eng. Phys. 31, 1166–1172.

https://doi.org/10.1016/j.medengphy.2009.07.014

Fratini, A., La Gatta, A., Cesarelli, M., Bifulco, P., 2009c. Whole Body Vibration training: analysis and characterization. 2009 9th Int. Conf. Inf. Technol. Appl. Biomed. 1–4. https://doi.org/10.1109/ITAB.2009.5394317

Fung, J., Macpherson, J.M., 1999. Attributes of quiet stance in the chronic spinal cat. J. Neurophysiol. 82, 3056–3065. https://doi.org/10.1152/jn.1999.82.6.3056

Gandevia, S.C., 1996. Kinesthesia : roles for afferent signals and motor commands, in: Rowell, L., JT, S. (Eds.), Handbook of Physiology, Exercise: Regulation and Integration of Multiple Systems. Oxford University Press, New York, pp. 128–172.

Garatachea, N., Jimenez, A., Bresciani, G., Marino, N.A., Gonzalez-Gallego, J., De Paz, J.A., 2007. The effects of movement velocity during squatting on energy expenditure and substrate utilization in whole body vibration. J. Strength Cond. Res. 21, 594–598.

Gatev, P., Thomas, S., Kepple, T., Hallett, M., 1999. Feedforward ankle strategy of balance during quiet stance in adults. J. Physiol. 514, 915–928. https://doi.org/10.1111/j.1469-7793.1999.915ad.x

Gerber, E.M., 2020. permutest [WWW Document]. URL https://uk.mathworks.com/matlabcentral/fileexchange/71737-permutest (accessed 5.20.20).

Geurts, a C., Nienhuis, B., Mulder, T.W., 1993. Intrasubject variability of selected force-platform parameters in the quantification of postural control. Arch. Phys. Med. Rehabil.

74, 1144–1150.

Gilbertson, T., Lalo, E., Doyle, L., Di Lazzaro, V., Cioni, B., Brown, P., 2005. Existing motor state is favored at the expense of new movement during 13-35 Hz oscillatory synchrony in the human corticospinal system. J. Neurosci. 25, 7771–7779. https://doi.org/10.1523/JNEUROSCI.1762-05.2005

Goodwin, G M, Mccloskey, D.I., Matthews, P.B.C., 1972. The contribution of muscle afferents to kinesthesia shown by vibration induced illusions of movement and by the effects of paralysing joint afferents. Brain 95, 705–748.

Goodwin, Guy M., Mccloskey, D.I., Matthews, P.B.C., 1972. Proprioceptive illusions induced by muscle vibration: Contribution by muscle spindles to perception? Science (80-.). 175, 1382–1384. https://doi.org/10.1126/science.175.4028.1382

Granit, R., Steg, G., 1956. Tonic and Phasic Ventral Horn Cells Differentiated by Post-Tetanic Potentiation in Cat Extensors. Acta Physiol Scand 37, 114–126.

Groppe, D.M., Urbach, T.P., Kutas, M., 2011. Mass univariate analysis of event-related brain potentials/fields I: A critical tutorial review. Psychophysiology 48, 1711–1725. https://doi.org/10.1111/j.1469-8986.2011.01273.x

Gross, T.S., Nelson, R.C., 1988. The shock attenuation role of the ankle during landing from a vertical jump. Med. Sci. Sports Exerc. 20, 506–514.

Grosse, P., Cassidy, M.J., Brown, P., 2002. EEG – EMG , MEG – EMG and EMG – EMG frequency analysis : physiological principles and clinical applications. Clin. Neurophysiol.

113, 1523–1531.

Guimerà, R., Nunes Amaral, L.A., 2005. Functional cartography of complex metabolic networks. Nature 433, 895–900. https://doi.org/10.1038/nature03288

Hagbarth, K.E., Hellsing, G., Löfstedt, L., 1976. TVR and vibration-induced timing of motor impulses in the human jaw elevator muscles. J. Neurol. Neurosurg. Psychiatry 39, 719–728. https://doi.org/10.1136/jnnp.39.8.719

Halliday, D.M., Farmer, S.F., 2010. On the need for rectification of surface EMG. J. Neurophysiol. 103, 3547. https://doi.org/10.1152/jn.00222.2010

Halliday, D.M., Rosenberg, J.R., Amjad, A.M., Breeze, P., Conway, B.A., Farmer, S.F., 1995. A framework for the analysis of mixed time series/point process data-theory and application to the study of physiological tremor, single motor unit discharges and electromyograms. Prog. Biophys. Mol. Biol. 64, 237–278.

Harazin, B., Grzesik, J., 1998. The transmission of vertical whole-body vibration to the body segments of standing subjects. J. Sound Vib. 215, 775–787. https://doi.org/10.1006/jsvi.1998.1675

Hari, H., Puce, S., 2017. MEG-EEG Primer. Oxford University Press, Madison Avenue.

Hassan, M., Wendling, F., 2018. Electroencephalography Source Connectivity. IEEE Signal Process. Mag. 81–96. https://doi.org/10.1109/MSP.2017.2777518

Hayes, K.C., 1982. Biomechanics of Postural Control. Exerc. Sport Sci. Rev. 10, 363–391.

Hermens, H.J., Bart, F., Catherine, D.-K., Gunter, R., 2000. Development of recommendations for SEMG sensors and sensor placement procedures. J. Electromyogr. Kinesiol. 10, 361–374.

Hermens, H.J., Freriks, B., Merletti, R., Stegeman, D., Blok, J., Rau, G., Disselhorst-Klug, C., Hägg, G., 1999. European Recommendations for Surface ElectroMyoGraphy, Results of the SENIAM project. Roessingh Res. Dev. 8th ed, 8–11. https://doi.org/10.1016/S1050-6411(00)00027-4

Hirayama, K., Homma, S., Mizote, M., Nakajima, Y., Watanabe, S., 1974. Separation of the contributions of voluntary and vibratory activation of motor units in man by cross-correlograms. Jpn. J. Physiol. 24, 293–304.

Hlavacka, F., Njiokiktjien, C., 1985. Postural Responses Evoked by Sinusoidal Galvanic Stimulation of the Labyrinths. Acta Otolaryngol 99, 107– 112.

Homma, S., Kanda, K., Watanabe, S., 1972. Preferred spike intervals in the vibration reflex. Jpn. J. Physiol. 22, 421–432.

Horak, F.B., 2006. Postural orientation and equilibrium : what do we need to know about neural control of balance to prevent falls. Age Ageing 35, 7–11. https://doi.org/10.1093/ageing/afl077

Horak, F.B., Jacobs, J. V., 2007. Cortical control of postural responses. J. Neural Transm. 114, 1339–1348. https://doi.org/10.1007/s00702-007-0657-0.Cortical

Horak, F.B., Macpherson, J.M., 1996. 7 . Postural orientation and equilibrium, in: Rowell LB,

S.J. (Ed.), Handbook of Physiology, Exercise: Regulation and Integration of Multiple Systems. Oxford University Press, New York, pp. 255–92.

Horak, F.B., Nashner, L.M., 1986. Central programming of postural movements: Adaptation to altered support-surface configurations. J. Neurophysiol. 55, 1369–1381. https://doi.org/10.1152/jn.1986.55.6.1369

Horak, F.B., Sharon, S.M., Shumway-Cook, A., 1997. Postural Pertubations: New Insights for Treatment of Balance Disorders. Phys. Ther. 77, 517–533.

Horak, F.B., Shupert, C.L., Dietz, V., Horstmann, G., 1994. Vestibular and somatosensory contributions to responses to head and body displacements in stance. Exp. Brain Res. 100, 93–106. https://doi.org/10.1007/BF00227282

Howell, D.C., 2010. Statistical methods for psychology, 7th ed., I. ed. Belmont, CA: Wadsworth, Cengage Learning.

Huisinga, J., Horak, B., 2014. Postural response latencies are related to balance control during standing and walking in patients with multiple sclerosis. Arch Phys Med Rehabil 95, 1390–1397. https://doi.org/10.1016/j.apmr.2014.01.004.Postural

Hülsdünker, T., Mierau, A., Neeb, C., Kleinöder, H., Strüder, H.K., 2015. Cortical processes associated with continuous balance control as revealed by EEG spectral power. Neurosci. Lett. 592, 1–5. https://doi.org/10.1016/j.neulet.2015.02.049

Hülsdünker, T., Mierau, A., Strüder, H.K., 2016. Higher balance task demands are associated with an increase in individual alpha peak frequency. Front. Hum. Neurosci. 9, 1–12.

https://doi.org/10.3389/fnhum.2015.00695

Inglis, J.T., Horak, F.B., Shupert, C.L., Jones-Rycewicz, C., 1994. The importance of somatosensory information in triggering and scaling automatic postural responses in humans. Exp. Brain Res. 101, 159–164. https://doi.org/10.1007/BF00243226

Ivanenko, Y., Gurfinkel, V.S., 2018. Human postural control. Front. Neurosci. 12, 1–9. https://doi.org/10.3389/fnins.2018.00171

Jacobs, J. V., Wu, G., Kelly, K.M., 2015. Evidence for beta corticomuscular coherence during human standing balance: Effects of stance width, vision, and support surface. Neuroscience 298, 1–11. https://doi.org/10.1016/j.neuroscience.2015.04.009

Kanda, K., 1972. Contribution of polysynaptic pathways to the tonic vibration reflex. Jpn. J. Physiol. 22, 367–377.

Kerkman, J.N., Bekius, A., Boonstra, T.W., Daffertshofer, A., Dominici, N., 2020. Muscle synergies and coherence networks reflect different modes of coordination during walking. Front. Physiol. 11, 1–13. https://doi.org/10.3389/fphys.2020.00751

Kerschan-Schindl, K., Grampp, S., Henk, C., Resch, H., Preisinger, E., Fialka-Moser, V., Imhof, H., 2001. Whole-body vibration exercise leads to alterations in muscle blood volume. Clin. Physiol. 21, 377–82. https://doi.org/10.1046/j.1365-2281.2001.00335.x

Kilner, J.M., Baker, S.N., Salenius, S., Hari, R., Lemon, R.N., 2000. Human cortical muscle coherence is directly related to specific motor parameters. J. Neurosci. 20, 8838–8845. https://doi.org/10.1523/jneurosci.20-23-08838.2000

Kilner, J.M., Baker, S.N., Salenius, S., Jousm, V., Hari, R., Lemon, R.N., 1999. Task-dependent modulation of 15 — 30 Hz coherence between rectified EMGs from human hand and forearm muscles. J. Physiol. 516, 559–570.

Kilner, J.M., Fisher, R., Lemon, R.N., 2002. Modulation of synchrony between single motor units during precision grip tasks in humans. J. Physiol. 541, 937–948. https://doi.org/10.1113/jphysiol.2001.013305

Kim, J., Kwon, Y., Chung, H.Y., Kim, C.S., Eom, G.M., Jun, J.H., Park, B.K., 2012. Relationship between body factors and postural sway during natural standing. Int. J. Precis. Eng. Manuf. 13, 963–968. https://doi.org/10.1007/s12541-012-0125-0

Kristeva, R., Fritsch, C., Timmer, J., Lu, C., 2002. Effects of attention and precision of exerted force on beta range EEG- EMG synchronization during a maintained motor contraction task. Clin. Neurophysiol. 113, 124–131.

Kristeva, R., Patino, L., Omlor, W., 2007. Beta-range cortical motor spectral power and corticomuscular coherence as a mechanism for effective corticospinal interaction during steady-state motor output. Neuroimage 36, 785–792. https://doi.org/10.1016/j.neuroimage.2007.03.025

Krol, P., Piecha, M., Slomka, K., Sobota, G., Polak, A., Juras, G., 2011. The effect of whole-body vibration frequency and amplitude on the myoelectric activity of vastus medialis and vastus lateralis. J. Sport. Sci. Med. 10, 169–174.

Kvorning, T., Bagger, M., Caserotti, P., Madsen, K., 2006. Effects of vibration and resistance training on neuromuscular and hormonal measures. Eur. J. Appl. Physiol. 96, 615–625. https://doi.org/10.1007/s00421-006-0139-3

Lafortune, M.A., Lake, M.J., 1996. Dominant Role of Interface Over Knee Angle for Cushioning Impact Loading and Regulating Initial Leg Stiffness. J. Biomech. 29, 1523–1529.

Lafortune, M.A., Lake, M.J., Hennig, E.M., 1996. Differential shock transmission response of the human body to impact severity and lower limb posture. J. Biomech. 29, 1531–1537. https://doi.org/10.1016/S0021-9290(96)80004-2

Lake, D.E., Richman, J.S., Pamela Griffin, M., Randall Moorman, J., 2002. Sample entropy analysis of neonatal heart rate variability. Am. J. Physiol. - Regul. Integr. Comp. Physiol. 283, 789–797. https://doi.org/10.1152/ajpregu.00069.2002

Lakie, M., Caplan, N., Loram, I.D., 2003. Human balancing of an inverted pendulum with a compliant linkage: Neural control by anticipatory intermittent bias. J. Physiol. 551, 357–370. https://doi.org/10.1113/jphysiol.2002.036939

Lam, F.M.H., Lau, R.W.K., Chung, R.C.K., Pang, M.Y.C., 2012. The effect of whole body vibration on balance, mobility and falls in older adults: A systematic review and meta-analysis. Maturitas 72, 206–213. https://doi.org/10.1016/j.maturitas.2012.04.009

Le Clair, K., Riach, C., 1996. Postural stability measures: What to measure and for how long. Clin. Biomech. 11, 176–178. https://doi.org/10.1016/0268-0033(95)00027-5

Lebedev, M., Polyakov, A., 1992. Analysis of surface EMG of human soleus muscle subjected to vibration. J. Electromyogr. Kinesiol. 2, 26–35.

Lebedev, M.A., Polyakov, A. V., 1991. Analysis of the interference electromyogram of the human soleus muscle under vibrational stimulation. Neurophysiology 23, 47–54.

https://doi.org/10.1007/BF01052289

Lee, D.D., Seung, H.S., 1999. Learning the parts of objects by non-negative matrix factorization 401, 788–791.

Lienhard, K., Cabasson, A., Meste, O., Colson, S.S., 2015. Comparison of sEMG processing methods during whole-body vibration exercise. J. Electromyogr. Kinesiol. 25, 833–840. https://doi.org/10.1016/j.jelekin.2015.10.005

Lienhard, K., Cabasson, A., Meste, O., Colson, S.S., 2014a. Determination of the optimal parameters maximizing muscle activity of the lower limbs during vertical synchronous whole-body vibration. Eur. J. Appl. Physiol. 114, 1493–1501. https://doi.org/10.1007/s00421-014-2874-1

Lienhard, K., Cabasson, A., Meste, O., Colson, S.S., 2014b. sEMG during whole-body vibration contains motion artifacts and reflex activity. J. Sport. Sci. Med. 14, 54–61.

Liu, J., Sheng, Y., Liu, H., 2019. Corticomuscular coherence and its applications: A review. Front. Hum. Neurosci. 13, 1–16. https://doi.org/10.3389/fnhum.2019.00100

Liu, S.H., Lin, C.B., Chen, Y., Chen, W., Huang, T.S., Hsu, C.Y., 2019. An EMG patch for the real-time monitoring of muscle-fatigue conditions during exercise. Sensors (Switzerland) 19. https://doi.org/10.3390/s19143108

Lohman, E.B., Petrofsky, J.S., Maloney-Hinds, C., Betts-Schwab, H., Thorpe, D., 2007. The effect of whole body vibration on lower extremity skin blood flow in normal subjects. Med. Sci. Monit. 13, CR71-6.

Loram, I.D., Lakie, M., 2002. Direct measurement of human ankle stiffness during quiet standing: The intrinsic mechanical stiffness is insufficient for stability. J. Physiol. 545, 1041–1053. https://doi.org/10.1113/jphysiol.2002.025049

Loram, I.D., Maganaris, C.N., Lakie, M., 2005a. Human postural sway results from frequent, ballistic bias impulses by soleus and gastrocnemius. J. Physiol. 564, 295–311. https://doi.org/10.1113/jphysiol.2004.076307

Loram, I.D., Maganaris, C.N., Lakie, M., 2005b. Active, non-spring-like muscle movements in human postural sway: How might paradoxical changes in muscle length be produced? J. Physiol. 564, 281–293. https://doi.org/10.1113/jphysiol.2004.073437

Lord, S.R., Clark, R.D., Webster, I.W., 1991. Postural Stability and Associated Physiological Factors in a Population of Aged Persons. J. Gerontol. 46, 69–76.

Lord, S.R., Ward, J.A., Williams, P., Anstey, K., 1994. Physiological Factors Associated with Falls in Older Community-Dwelling Women. J. Am. Geriatr. Soc. 42, 1110–1117.

Lowry, R., 2015. Concepts and Applications of Inferential Statistics [WWW Document]. Electron. Ed. URL http://vassarstats.net/textbook/ (accessed 11.12.20).

Magnus, R., 1925. The Croonian Lecture: animal posture. Proc. R. Soc. B 98, 339–353.

Mahieu, N.N., Witvrouw, E., Van De Voorde, D., Michilsens, D., Arbyn, V., Van Den Broecke, W., 2006. Improving strength and postural control in young skiers: Whole-body vibration versus equivalent resistance training. J. Athl. Train. 41, 286–293.

Maki, B.E., McIlroy, W.E., 2007. Cognitive demands and cortical control of human balance-recovery reactions. J. Neural Transm. 114, 1279–1296. https://doi.org/10.1007/s00702-007-0764-y

Malik, J., 2020. Multiscale Sample Entropy (https://www.mathworks.com/matlabcentral/fileexchange/62706-multiscale-sample-entropy), MATLAB Central File Exchange. Retrieved June 18, 2020. [WWW Document].

Marin, P., Bunker, D., Rhea, M., Ayllon, F., 2009. Neuromuscular Activity During Whole Body Vibration of Different Amplitudes and Footwear Conditions: Implications for Prescription of Vibratory Stimulation. J. Strength Cond. Res. 23, 2311–2316.

Marin, P.J., Rhea, M.R., 2010a. Effects of Vibration Training on Muscle Power: A Meta-Analysis. J. Strength Cond. Res. 24, 871–878.

Marin, P.J., Rhea, M.R., 2010b. Effects of Vibration Training on Muscle Strength: A Meta-Analysis. J. Strength Cond. Res. 24, 548–556.

Maris, E., 2012. Statistical testing in electrophysiological studies. Psychophysiology 49, 549–565. https://doi.org/10.1111/j.1469-8986.2011.01320.x

Maris, E., Oostenveld, R., 2007. Nonparametric statistical testing of EEG- and MEG-data. J. Neurosci. Methods 164, 177–190. https://doi.org/10.1016/j.jneumeth.2007.03.024

Marsden, C.D., Meadows, J.C., Hodgson, H.J., 1969. Observations on the reflex response to muscle vibration in man and its voluntary control. Brain 92, 829–846.

Martin, B.J., Park, H.S., 1997. Analysis of the tonic vibration reflex: Influence of vibration variables on motor unit synchronization and fatigue. Eur. J. Appl. Physiol. 75, 504–511. https://doi.org/10.1007/s004210050196

Masakado, Y., Ushiba, J., Tsutsumi, N., Takahashi, Y., Tomita, Y., Kimura, A., Liu, M., 2008. EEG-EMG coherence changes in postural tasks. Electromyogr. Clin. Neurophysiol. 48, 27–33.

Massion, J., 1998. Postural control systems in developmental perspective. Neurosci. Biobehav. Rev. 22, 465–472. https://doi.org/10.1016/S0149-7634(97)00031-6

Maurer, Peterka, 2005. A new interpretation of spontaneous sway measures based on a simple model of human postural control. J. Neurohysiology 93, 189–200. https://doi.org/10.1152/jn.00221.2004.

McBride, J.M., Nuzzo, J.L., Dayne, A.M., Israetel, M.A., Nieman, D.C., Triplett, N.T., 2010. Effect of an Acute Bout of Whole Body Vibration Excercise on Muscle Force Output and Motor Neuron Excitability. J. Strength Cond. Res. 24, 184–189. https://doi.org/10.1519/JSC.0b013e31819b79cf

Merletti, R., Farina, D., 2016. Surface Electromyography. Wiley.

Michel, C.M., Murray, M.M., Lantz, G., Gonzalez, S., Spinelli, L., Grave De Peralta, R., 2004. EEG source imaging. Clin. Neurophysiol. 115, 2195–2222. https://doi.org/10.1016/j.clinph.2004.06.001

Mierau, A., Pester, B., Hülsdünker, T., Schiecke, K., Strüder, H.K., Witte, H., 2017. Cortical

Correlates of Human Balance Control. Brain Topogr. 30, 434–446. https://doi.org/10.1007/s10548-017-0567-x

Mima, T., Hallet, M., 1999. Corticomuscular Coherence : A Review. J. Clin. Neurophysiol. 16, 501–511.

Mima, T., Hallett, M., 1999. Electroencephalographic analysis of cortico-muscular coherence: reference effect, volume conduction and generator mechanism. Clin. Neurophysiol. 110, 1892–1899. https://doi.org/10.1016/S1388-2457(99)00238-2

Miwa, T., Miwa, Y., Kanda, K., 1995. Dynamic and static sensitivities of muscle spindle primary endings in aged rats to ramp stretch. Neurosci. Lett. 201, 8–11.

Mochizuki, G., Semmler, J.G., Ivanova, T.D., Garland, S.J., 2006. Low-frequency common modulation of soleus motor unit discharge is enhanced during postural control in humans. Exp. Brain Res. 175, 584–595. https://doi.org/10.1007/s00221-006-0575-7

Mohd Razali, N., Bee Wah, Y., 2011. Power comparisons of Shapiro-Wilk, Kolmogorov-Smirnov, Lilliefors and Anderson-Darling tests. J. Stat. Model. Anal. 2, 21–33.

Morasso, P.G., Sanguineti, V., 2002. Ankle muscle stiffness alone cannot stabilize balance during quiet standing. J. Neurophysiol. 88, 2157–2162. https://doi.org/10.1152/jn.2002.88.4.2157

Morasso, P.G., Schieppati, M., 1999. Can muscle stiffness alone stabilize upright standing? J. Neurophysiol. 82, 1622–1626. https://doi.org/10.1152/jn.1999.82.3.1622

Morel, P., 2018. Gramm: grammar of graphics plotting in Matlab. J. Open Source Softw. 3, 568. https://doi.org/10.21105/joss.00568

Müller, T., Ball, T., Kristeva-Feige, R., Mergner, T., Timmer, J., 2000. Selecting relevant electrode positions for classification tasks based on the electro-encephalogram. Med. Biol. Eng. Comput. 38, 62–67. https://doi.org/10.1007/BF02344690

Murnaghan, C.D., Squair, J.W., Chua, R., Inglis, J.T., Carpenter, M.G., 2014. Cortical contributions to control of posture during unrestricted and restricted stance. J. Neurophysiol. 111, 1920–1926. https://doi.org/10.1152/jn.00853.2012

Murray, M., Seireg, A., Sepic, S., 1975. Normal Postural Stability and Steadiness: Quantitative Assessment. J. Bone Jt. Surg. 57, 510–516. https://doi.org/10.1017/CBO9781107415324.004

Myers, L.J., Lowery, M., O'Malley, M., Vaughan, C.L., Heneghan, C., St. Clair Gibson, A., Harley, Y.X.R., Sreenivasan, R., 2003. Rectification and non-linear pre-processing of EMG signals for cortico-muscular analysis. J. Neurosci. Methods 124, 157–165. https://doi.org/10.1016/S0165-0270(03)00004-9

Nandi, T., Hortobágyi, T., van Keeken, H.G., Salem, G.J., Lamoth, C.J.C., 2019. Standing task difficulty related increase in agonist-agonist and agonist-antagonist common inputs are driven by corticospinal and subcortical inputs respectively. Sci. Rep. 9, 1–12. https://doi.org/10.1038/s41598-019-39197-z

Nigg, B., Wakeling, J., 2001. Impact forces and muscle tuning: A new paradigm. Exerc. Sport Sci. Rev. 29, 37–41. https://doi.org/10.1097/00003677-200101000-00008

Nowak, D.A., Rosenkranz, K., Hermsdörfer, J., Rothwell, J., 2004. Memory for fingertip forces: Passive hand muscle vibration interferes with predictive grip force scaling. Exp. Brain Res. 156, 444–450. https://doi.org/10.1007/s00221-003-1801-1

O'Malley, M.J., 1996. Normalization of temporal-distance parameters in pediatric gait. J. Biomech. 29, 619–625. https://doi.org/10.1016/0021-9290(95)00088-7

Okada, M., 1972. An electromyographic estimation of the relative muscular load in different human postures. J. Hum. Ergol. (Tokyo). 1, 75–93. https://doi.org/10.11183/jhe1972.1.75

Omlor, W., Patino, L., Hepp-Reymond, M.C., Kristeva, R., 2007. Gamma-range corticomuscular coherence during dynamic force output. Neuroimage 34, 1191–1198. https://doi.org/10.1016/j.neuroimage.2006.10.018

Oostenveld, R., Fries, P., Maris, E., Schoffelen, J.M., 2011. FieldTrip: Open source software for advanced analysis of MEG, EEG, and invasive electrophysiological data. Comput. Intell. Neurosci. 2011. https://doi.org/10.1155/2011/156869

Osawa, Y., Oguma, Y., Ishii, N., 2013. The effects of whole-body vibration on muscle strength and power: A meta-analysis. J. Musculoskelet. Neuronal Interact. 13, 342–352.

Osugi, T., Iwamoto, J., Yamazaki, M., Takakuwa, M., 2014. Effect of a combination of whole body vibration exercise and squat training on body balance, muscle power, and walking ability in the elderly. Ther. Clin. Risk Manag. 10, 131–138. https://doi.org/10.2147/TCRM.S57806

Ozdemir, R.A., Contreras-Vidal, J.L., Paloski, W.H., 2018. Cortical control of upright stance in

elderly. Mech. Ageing Dev. 169, 19–31. https://doi.org/10.1016/j.mad.2017.12.004

Palmieri-Smith, R.M., Ingersoll, C.D., Stone, M.B., Krause, B.A., 2002. Center-of-Pressure Parameters Used in the Assessment of Postural Control. J. Sport Rehabil. 11, 51–66.

Parra, L.C., Spence, C.D., Gerson, A.D., Sajda, P., 2005. Recipes for the linear analysis of EEG. Neuroimage 28, 326–341. https://doi.org/10.1016/j.neuroimage.2005.05.032

Pedroni, A., Bahreini, A., Langer, N., 2019. Automagic: Standardized preprocessing of big EEG data. Neuroimage 200, 460–473. https://doi.org/10.1016/j.neuroimage.2019.06.046

Person, R., Kozhina, G., 1992. Tonic vibration reflex of human limb muscles: Discharge pattern of motor units. J. Electromyogr. Kinesiol. 2, 1–9. https://doi.org/10.1016/1050-6411(92)90002-Z

Person, R.S., Kozhina, G.V., 1989. Study of Firing Pattern in Human Soleus Motor Units in Tonic Vibration Reflex. Neurophysiology 21, 540–546.

Peterka, R.J., 2002. Sensorimotor integration in human postural control. J. Neurophysiol. 88, 1097–1118. https://doi.org/10.1152/jn.2002.88.3.1097

Petersen, T.H., Conway, B.A., Nielsen, J.B., 2012. The motor cortex drives the muscles during walking in human subjects. J. Physiol. 590, 2443–2452. https://doi.org/10.1113/jphysiol.2012.227397

Peterson, S.M., Ferris, D.P., 2019. Group-level cortical and muscular connectivity during perturbations to walking and standing balance. Neuroimage 198, 93–103.

https://doi.org/10.1016/j.neuroimage.2019.05.038

Petrofsky, J.S., Khowailed, I.A., 2014. Postural sway and motor control in trans-tibial amputees as assessed by electroencephalography during eight balance training tasks. Med. Sci. Monit. 20, 2695–2704. https://doi.org/10.12659/MSM.891361

Pollock, R.D., Woledge, R.C., Martin, F.C., Newham, D.J., 2012. Effects of whole body vibration on motor unit recruitment and threshold. J. Appl. Physiol. 112, 388–395. https://doi.org/10.1152/japplphysiol.01223.2010

Pollock, R.D., Woledge, R.C., Mills, K.R., Martin, F.C., Newham, D.J., 2010. Muscle activity and acceleration during whole body vibration: Effect of frequency and amplitude. Clin. Biomech. 25, 840–846. https://doi.org/10.1016/j.clinbiomech.2010.05.004

Prieto, T.E., Myklebust, J.B., Hoffmann, R.G., Lovett, E.G., Myklebust, B.M., 1996. Measures of postural steadiness: Differences between healthy young and elderly adults. IEEE Trans. Biomed. Eng. 43, 956–966. https://doi.org/10.1109/10.532130

Proske, U., 2005. What is the role of muscle receptors in proprioception ? Muscle Nerve 31, 780–787. https://doi.org/10.1002/mus.20330

Ribot-Ciscar, E., Rossi-Durand, C., Roll, J.P., 1998. Muscle spindle activity following muscle tendon vibration in man. Neurosci. Lett. 258, 147–150. https://doi.org/10.1016/S0304-3940(98)00732-0

Richman, J.S., Moorman, J.R., 2000. Physiological time-series analysis using approximate entropy and sample entropy. Am. J. Physiol. Hear. Circ. Physiol. 278, 2039–2049.

Rittweger, J., 2010. Vibration as an exercise modality: How it may work, and what its potential might be. Eur. J. Appl. Physiol. 108, 877–904. https://doi.org/10.1007/s00421-009-1303-3

Rittweger, J., Beller, G., Felsenberg, D., 2000. Acute physiological effects of exhaustive whole-body vibration exercise in man. Clin. Physiol. 20, 134–142. https://doi.org/10.1046/j.1365-2281.2000.00238.x

Rittweger, J., Schiessl, H., Felsenberg, D., 2001. Oxygen uptake during whole-body vibration exercise: Comparison with squatting as a slow voluntary movement. Eur. J. Appl. Physiol. 86, 169–173. https://doi.org/10.1007/s004210100511

Ritzmann, R., Gollhofer, A., Kramer, A., 2013. The influence of vibration type, frequency, body position and additional load on the neuromuscular activity during whole body vibration. Eur. J. Appl. Physiol. 113, 1–11. https://doi.org/10.1007/s00421-012-2402-0

Ritzmann, R., Kramer, A., Bernhardt, S., Gollhofer, A., 2014. Whole body vibration training - Improving balance control and muscle endurance. PLoS One 9. https://doi.org/10.1371/journal.pone.0089905

Ritzmann, R., Kramer, A., Gruber, M., Gollhofer, A., Taube, W., 2010. EMG activity during whole body vibration: Motion artifacts or stretch reflexes? Eur. J. Appl. Physiol. 110, 143–151. https://doi.org/10.1007/s00421-010-1483-x

Roeder, L., Boonstra, T.W., Kerr, G.K., 2020. Corticomuscular control of walking in older people and people with Parkinson's disease. Sci. Rep. 10. https://doi.org/10.1038/s41598-020-59810-w

Roelants, M., Verschueren, S.M.P., Delecluse, C., Levin, O., Stijnen, V., 2006. Whole-body-vibration-induced increase in leg muscle activity during different squat exercises. J. Strength Cond. Res. 20, 124–129. https://doi.org/10.1519/R-16674.1

Rogan, S., Hilfiker, R., Herren, K., Radlinger, L., De Bruin, E.D., 2011. Effects of whole-body vibration on postural control in elderly: A systematic review and meta-analysis. BMC Geriatr. 11. https://doi.org/10.1186/1471-2318-11-72

Romano, M., Fratini, A., Gargiulo, G.D., Cesarelli, M., Iuppariello, L., Bifulco, P., 2018. On the Power Spectrum of Motor Unit Action Potential Trains Synchronized With Mechanical Vibration. IEEE Trans. Neural Syst. Rehabil. Eng. 26, 646–653.

Ruan, X.-Y., Jin, F.-Y., Liu, Y.-L., Peng, Z.-L., Sun, Y.-G., 2008. Effects of vibration therapy on bone mineral density in postmenopausal women with osteoporosis. Chin. Med. J. (Engl). 121, 1155–1158.

Rubinov, M., Sporns, O., 2010. Complex network measures of brain connectivity: Uses and interpretations. Neuroimage 52, 1059–1069. https://doi.org/10.1016/j.neuroimage.2009.10.003

Salmelin, R., Hrai, R., 1994. Spatiotemporal Characteristics of sensorimotor neuromagnetic rhythms related to thumb movement. Neuroscience 60, 537–550.

Saquetto, M., Carvalho, V., Silva, C., Conceição, C., Gomes-Neto, M., 2015. The effects of whole body vibration on mobility and balance in children with cerebral palsy: A systematic review with meta-analysis. J. Musculoskelet. Neuronal Interact. 15, 137–144.

Sears, B.Y.T.A., Stagg, D., 1976. Short-Term Synchronization of Intercostal Motorneurone Activity. J. Physiol. 263, 357–381.

Sebik, O., Karacan, I., Cidem, M., Türker, K.S., 2013. Rectification of SEMG as a tool to demonstrate synchronous motor unit activity during vibration. J. Electromyogr. Kinesiol. 23, 275–284. https://doi.org/10.1016/j.jelekin.2012.09.009

Shinohara, M., 2005. Effects of prolonged vibration on motor unit activity and motor performance. Med. Sci. Sports Exerc. 37, 2120–2125. https://doi.org/10.1249/01.mss.0000178106.68569.7e

Shumway-cook, A., Horak, F.A.Y.B., 1986. Assessing the Influence of Sensory Interaction on Balance Suggestion from the Field. Phys. Ther. 66, 1548–1550.

Slatkovska, L., Alibhai, S.M.H., Beyene, J., Cheung, A.M., 2010. Effect of whole-body vibration on BMD: A systematic review and meta-analysis. Osteoporos. Int. 21, 1969–1980. https://doi.org/10.1007/s00198-010-1228-z

Slobounov, S., Cao, C., Jaiswal, N., Newell, K.M., 2009. Neural basis of postural instability identified by VTC and EEG. Exp. Brain Res. 199, 1–16. https://doi.org/10.1007/s00221-009-1956-5

Slobounov, S., Hallett, M., Cao, C., Newell, K., 2008. Modulation of cortical activity as a result of voluntary postural sway direction: An EEG study. Neurosci. Lett. 442, 309–313. https://doi.org/10.1016/j.neulet.2008.07.021

Slobounov, S., Hallett, M., Stanhope, S., Shibasaki, H., 2005. Role of cerebral cortex in human

postural control: An EEG study. Clin. Neurophysiol. 116, 315–323. https://doi.org/10.1016/j.clinph.2004.09.007

Slobounov, S.M., Teel, E., Newell, K.M., 2013. Modulation of cortical activity in response to visually induced postural perturbation: combined VR and EEG study. Neurosci. Lett. 547, 6–9. https://doi.org/10.1016/j.neulet.2013.05.001

Snyder, K.L., Kline, J.E., Huang, H.J., Ferris, D.P., 2015. Independent component analysis of gait-related movement artifact recorded using EEG electrodes during treadmill walking. Front. Hum. Neurosci. 9, 1–13. https://doi.org/10.3389/fnhum.2015.00639

Solis-Escalante, T., van der Cruijsen, J., de Kam, D., van Kordelaar, J., Weerdesteyn, V., Schouten, A.C., 2019. Cortical dynamics during preparation and execution of reactive balance responses with distinct postural demands. Neuroimage 188, 557–571. https://doi.org/10.1016/j.neuroimage.2018.12.045

Southgate, V., Johnson, M.H., Karoui, I. El, Csibra, G., 2010. Motor System Activation Reveals Infants ' On-Line Prediction of Others ' Goals. Psychol. Sci. 21, 355–359. https://doi.org/10.1177/0956797610362058

Spitzer, B., Haegens, S., 2017. Beyond the status quo: A role for beta oscillations in endogenous content (RE)activation. eNeuro 4. https://doi.org/10.1523/ENEURO.0170-17.2017

Sporns, O., Honey, C.J., Kotter, R., 2007. Identification and Classification of Hubs in Brain Networks. PLoS One 2, e1049. https://doi.org/10.1371/Citation

Stolen, F.B., De Luca, C.J., De Luca, C.J., 1981. Frequency Parameters of the Myoelectric Signal as a Measure of Muscle Conduction Velocity. IEEE Trans. Biomed. Eng. BME-28, 515–523. https://doi.org/10.1109/TBME.1981.324738

Sturnieks, D.L., George, R.S., Lord, S.R., 2008. Balance disorders in the elderly Troubles de l ' équilibre chez les personnes âgées. https://doi.org/10.1016/j.neucli.2008.09.001

Sucuoglu, H.M., Tuzun, S., Akbaba, Y.A., Uludag, M., Gokpinar, H.H., 2015. Effect of whole-body vibration on balance using posturography and balance tests in postmenopausal women. Am. J. Phys. Med. Rehabil. 94. https://doi.org/10.1097/PHM.0000000000000325

Swash, M., Fox, K., 1972. The Effect of Age on Human Skeletal Muscle. J. Neurol. Sci. 16, 417–432.

Tankisheva, E., Bogaerts, A., Boonen, S., Delecluse, C., Janses, P., S.M.P., V., 2015. Effects of a Six-Month Local Vibration Training on Bone Density, Muscle Strength, Muscle Mass, and Physical Performance in Postmenopausal Women. J. Strength Cond. Res. 29, 2613–2622.

Thissen, D., Steinberg, L., Kuang, D., 2002. Quick and easy implementation of the Benjamini-Hochberg procedure for controlling the false positive rate in multiple comparisons. J. Educ. Behav. Stat. 27, 77–83. https://doi.org/10.3102/10769986027001077

Thoroughman, K.A., Fine, M.S., Taylor, J.A., 2007. Trial-by-trial motor adaptation: a window into elemental neural computation. Prog. Brain Res. 165, 373–382. https://doi.org/10.1016/S0079-6123(06)65023-1

Tiihonen, J., Kajola, M., 1989. Magnetic mu rhythm in man. Neuroscience 32, 793–800.

Ting, L.H., Kautz, S.A., Brown, D.A., Zajac, F.E., 1999. Phase reversal of biomechanical functions and muscle activity in backward pedaling. J. Neurophysiol. 81, 544–551. https://doi.org/10.1152/jn.1999.81.2.544

Ting, L.H., Macpherson, J.M., 2005. A limited set of muscle synergies for force control during a postural task. J. Neurophysiol. 93, 609–613. https://doi.org/10.1152/jn.00681.2004

Ting, L.H., McKay, J.L., 2007. Neuromechanics of muscle synergies for posture and movement. Curr. Opin. Neurobiol. 17, 622–628. https://doi.org/10.1016/j.conb.2008.01.002

Torres-Oviedo, G., Macpherson, J.M., Ting, L.H., 2006. Muscle synergy organization is robust across a variety of postural perturbations. J. Neurophysiol. 96, 1530–1546. https://doi.org/10.1152/jn.00810.2005

Torres-Oviedo, G., Ting, L.H., 2007. Muscle synergies characterizing human postural responses. J. Neurophysiol. 98, 2144–2156. https://doi.org/10.1152/jn.01360.2006

Torvinen, S., Kannus, P., Sievanen, H., Jarvinen, T.A.H., Pasanen, M., Kontulainen, S., Jarvinen, T., Jarvinen, M., Oja, P., Vuori, I., 2002a. Effect of four-month vertical whole body vibration on performance and balance. Med Sci. Sport. Exerc. 34, 1523–1528. https://doi.org/10.1249/01.MSS.0000027713.51345.AE

Torvinen, S., Kannus, P., Sievänen, H., Järvinen, T.A.H., Pasanen, M., Kontulainen, S., Järvinen, T.L.N., Järvinen, M., Oja, P., Vuori, I., 2002b. Effect of a vibration exposure on

muscular performance and body balance. Randomized cross-over study. Clin. Physiol. Funct. Imaging 22, 145–152. https://doi.org/10.1046/j.1365-2281.2002.00410.x

Torvinen, S., Kannus, P., Sievanen, H., Vuori, I., Paakkala, T., Ilkka, V., Al., E., 2003. Effect of 8-month vertical whole body vibration on bone, muscle performance, and body balance: a randomized controlled study. J. Bone Miner. Res. 18, 876–884.

Torvinen, S., Sievanen, H., Jarvinen, T.A.H., Pasanen, M., Kontulainen, S., Kannus, P., 2002c. Effect of 4-min vertical whole body vibration on muscle performance and body balance: A randomized cross-over study. Int. J. Sports Med. 23, 374–379. https://doi.org/10.1055/s-2002-33148

Tse, Y.Y.F., Petrofsky, J.S., Berk, L., Daher, N., Lohman, E., Laymon, M.S., Cavalcanti, P., 2013. Postural sway and Rhythmic Electroencephalography analysis of cortical activation during eight balance training tasks. Med. Sci. Monit. 19, 175–186. https://doi.org/10.12659/MSM.883824

Tsuchimoto, S., Shibusawa, S., Mizuguchi, N., Kato, K., Ebata, H., Liu, M., Hanakawa, T., Ushiba, J., 2017. Resting-state fluctuations of EEG sensorimotor rhythm reflect BOLD activities in the pericentral areas: A simultaneous EEG-fMRI study. Front. Hum. Neurosci. 11, 1–10. https://doi.org/10.3389/fnhum.2017.00356

Turbanski, S., Haas, C.T., Schmidtbleicher, D., Friedrich, A., Duisberg, P., 2005. Effects of random whole-body vibration on postural control in Parkinson's disease. Res. Sport. Med. 13, 243–256. https://doi.org/10.1080/15438620500222588

Turvey, M.T., 1990. Coordination. Am. Psychol. 45, 938–953.

Ushiyama, J., Masakado, Y., Fujiwara, T., Tsuji, T., Hase, K., Kimura, A., Liu, M., Ushiba, J., 2012. Contraction level-related modulation of corticomuscular coherence differs between the tibialis anterior and soleus muscles in humans. J. Appl. Physiol. 112, 1258–1267. https://doi.org/10.1152/japplphysiol.01291.2011

Ushiyama, J., Suzuki, T., Masakado, Y., Hase, K., Kimura, A., Liu, M., Ushiba, J., 2011. Between-subject variance in the magnitude of corticomuscular coherence during tonic isometric contraction of the tibialis anterior muscle in healthy young adults. J. Neurohysiology 106, 1379–1388. https://doi.org/10.1152/jn.00193.2011.

Ushiyama, J., Takahashi, Y., Ushiba, J., 2010. Muscle dependency of corticomuscular coherence in upper and lower limb muscles and training-related alterations in ballet dancers and weightlifters. J. Appl. Physiol. 109, 1086–1095. https://doi.org/10.1152/japplphysiol.00869.2009.

Ushiyama, J., Yamada, J., Liu, M., Ushiba, J., 2017. Individual difference in β-band corticomuscular coherence and its relation to force steadiness during isometric voluntary ankle dorsiflexion in healthy humans. Clin. Neurophysiol. 128, 303–311. https://doi.org/10.1016/j.clinph.2016.11.025

van Nes, I.;, Geurts, A.;, Hendricks, H.T.., Duysens, J., 2004. Short-Term Effects of Whole-Body Vibration on Postural Control in Unilateral Chronic Stroke Patients: Preliminary Evidence. Am. J. Phys. Med. Rehabil. 83, 867–873.

Vecchio, F., Percio, C. Del, Marzano, N., Fiore, A., Toran, G., Aschieri, P., Gallamini, M., Cabras, J., Rossini, P.M., Babiloni, C., Eusebi, F., 2008. Functional Cortico-Muscular Coupling During Upright Standing in Athletes and Nonathletes: A Coherence Electroencephalographic-Electromyographic Study. Behav. Neurosci. 122, 917–927.

https://doi.org/10.1037/0735-7044.122.4.917

Verschueren, S.M., Brumagne, S., Roelants, M., Delecluse, C., Suy, E., Swinnen, S.P., 2004. The Effects of 24 Weeks Whole Body Vibration Training On Postural Control In The Elderly. Int. J. Sports Med.

Verschueren, S.M.P., Roelants, M., Delecluse, C., Swinnen, S., Vanderschueren, D., Boonen, S., 2004. Effect of 6-month whole body vibration training on hip density, muscle strength, and postural control in postmenopausal women: A randomized controlled pilot study. J. Bone Miner. Res. 19, 352–359. https://doi.org/10.1359/JBMR.0301245

Vøllestad, N.K., 1997. Measurement of human muscle fatigue. J. Neurosci. Methods 74, 219–227. https://doi.org/10.1016/S0165-0270(97)02251-6

Wakeling, J., Liphardt, A., 2006. Task-specific recruitment of motor units for vibration damping. J. Biomech. 39, 1342–1346. https://doi.org/10.1016/j.jbiomech.2005.03.009

Wakeling, J., Liphardt, A.M., Nigg, B., 2003. Muscle activity reduces soft-tissue resonance at heel-strike during walking. J. Biomech. 36, 1761–1769. https://doi.org/10.1016/S0021-9290(03)00216-1

Wakeling, J., Nigg, B., 2001a. Modification of soft tissue vibrations in the leg by muscular activity. J Appl Physiol 90, 412–420. https://doi.org/10.1152/jappl.2001.90.2.412

Wakeling, J., Nigg, B., 2001b. Soft-tissue vibrations in the quadriceps measured with skin mounted transducers. J. Biomech. 34, 539–543.

Wakeling, J., Nigg, B., Rozitis, A., 2002a. Muscle activity damps the soft tissue resonance that occurs in response to pulsed and continuous vibrations. J. Appl. Physiol. 93, 1093–1103. https://doi.org/10.1152/japplphysiol.00142.2002

Wakeling, J., Pascual, S., Nigg, B., 2002b. Altering muscle activity in the lower extremities by running with different shoes. Med. Sci. Sport. Exerc. 34, 1529–1532. https://doi.org/10.1249/01.MSS.0000027714.70099.08

Wakeling, J., Von Tscharner, V., Nigg, B., Stergiou, P., 2001. Muscle activity in the leg is tuned in response to ground reaction forces. J. Appl. Physiol. 91, 1307–1317.

Watanabe, T., Nojima, I., Mima, T., Sugiura, H., Kirimoto, H., 2020. Magnification of visual feedback modulates corticomuscular and intermuscular coherences differently in young and elderly adults. Neuroimage 220, 117089. https://doi.org/10.1016/j.neuroimage.2020.117089

Watts, D.J., Strogatz, S.H., 1998. Collectivedynamics of ‘small-world’ networks. Nature 393, 440–442.

Welch, P.D., 1967. The Use of Fast Fourier Transform for the Estimation of Power Spectra: A Method Based on Time Averaging Over Short, Modified Periodograms. IEEE Trans. Audio Electroacoust. 15, 70–73. https://doi.org/10.1109/TAU.1967.1161901

Wilcoxon, F., 1945. Individual Comparisons by Ranking Methods. Biometrics Bull. 1, 80–83.

Winter, D.A.., 1995. Human balance and posture control during standing and walking. Gait Posture 3, 193–214. https://doi.org/10.1016/0014-5793(86)80927-9

Winter, D.A., 1990. Biomechanics and Motor Control of Human Movement: Fourth Edition, Biomechanics and Motor Control of Human Movement: Fourth Edition. Wiley. https://doi.org/10.1002/9780470549148

Winter, D.A., Patla, A.E., Prince, F., Ishac, M., Gielo-Perczak, K., 1998. Stiffness Control of Balance in Quiet Standing. J. Neurophysiol. 80, 1211–1221. https://doi.org/10.1152/jn.1998.80.3.1211

Witham, C.L., Baker, S.N., 2007. Network oscillations and intrinsic spiking rhythmicity do not covary in monkey sensorimotor areas. J. Physiol. 580, 801–814. https://doi.org/10.1113/jphysiol.2006.124503

Witham, C.L., Riddle, C.N., Baker, M.R., Baker, S.N., 2011. Contributions of descending and ascending pathways to corticomuscular coherence in humans. J. Physiol. 15, 3789–3800. https://doi.org/10.1113/jphysiol.2011.211045

Witham, C.L., Wang, M., Baker, S.N., 2007. Cells in somatosensory areas show synchrony with beta oscillations in monkey motor cortex. Eur. J. Neurosci. 26, 2677–2686. https://doi.org/10.1111/j.1460-9568.2007.05890.x

Wittenberg, E., Thompson, J., Nam, C.S., Franz, J.R., 2017. Neuroimaging of human balance control: A systematic review. Front. Hum. Neurosci. 11, 1–25. https://doi.org/10.3389/fnhum.2017.00170

Wuensch, K.L., 2012. Pairwise Comparisons [WWW Document]. URL http://core.ecu.edu/psyc/wuenschk/StatHelp/Pairwise.htm

Wyon, M., Guinan, D., Hawkey, A., 2010. Whole-Body vibration training increases vertical jump height in a dance population. J. Strength Cond. Res. 24, 866–870.

Wysocki, A., Butler, M., Shamliyan, T., Kane, R.L., 2011. Review Annals of Internal Medicine Whole-Body Vibration Therapy for Osteoporosis : State of the Science. Ann. Intern. Med. 155, 680–686. https://doi.org/10.7326/0003-4819-155-10-201111150-00006

Xu, L., Rabotti, C., Mischi, M., 2015. On the nature of the electromyographic signals recorded during vibration exercise. Eur. J. Appl. Physiol. 115, 1095–1106. https://doi.org/10.1007/s00421-014-3091-7

Yang, X., Wang, P., Liu, C., He, C., Reinhardt, J.D., 2015. The effect of whole body vibration on balance, gait performance and mobility in people with stroke: A systematic review and meta-analysis. Clin. Rehabil. 29, 627–638. https://doi.org/10.1177/0269215514552829

Yao, B., Salenius, S., Yue, G.H., Brown, R.W., Liu, J.Z., 2007. Effects of surface EMG rectification on power and coherence analyses: An EEG and MEG study. J. Neurosci. Methods 159, 215–223. https://doi.org/10.1016/j.jneumeth.2006.07.008

Zhou, J., Lipsitz, L., Habtemariam, D., Manor, B., 2016. Sub-sensory vibratory noise augments the physiologic complexity of postural control in older adults. J. Neuroeng. Rehabil. 13, 1–8. https://doi.org/10.1186/s12984-016-0152-7

Zok, M., Mazzà, C., Cappozzo, A., 2008. Should the instructions issued to the subject in traditional static posturography be standardised? Med. Eng. Phys. 30, 913–916. https://doi.org/10.1016/j.medengphy.2007.12.002

Zuo, X.N., Ehmke, R., Mennes, M., Imperati, D., Castellanos, F.X., Sporns, O., Milham, M.P., 2012. Network centrality in the human functional connectome. Cereb. Cortex 22, 1862–1875. https://doi.org/10.1093/cercor/bhr269